KINETICS OF POLYMER ADSORPTION, DESORPTION AND EXCHANGE

Promotor: dr. G.J. Fleer,
hoogleraar in de fysische en kolloïdchemie.
Co-promotor: dr. M.A. Cohen Stuart, universitair hoofddocent
bij de vakgroep Fysische en Kolloïdchemie.

Jacob Cornelis Dijt

KINETICS OF POLYMER ADSORPTION, DESORPTION AND EXCHANGE

Proefschrift
ter verkrijging van de graad van doctor
in de landbouw- en milieuwetenschappen
op gezag van de rector magnificus,
dr. H.C. van der Plas
in het openbaar te verdedigen
op maandag 28 juni 1993
des namiddags te vier uur in de Aula
van de Landbouwuniversiteit te Wageningen.

CIP-DATA KONINKLIJKE BIBLIOTHEEK, DEN HAAG

Dijt, Jacob Cornelis

Kinetics of polymer adsorption, desorption and exchange /
Jacob Cornelis Dijt. - [S.I. : s.n.]
Thesis Wageningen. - With ref. - With summary in Dutch.
ISBN 90-5485-135-X
Subject headings: polymer adsorption / colloid chemistry

Cover design: Ernst van Cleef
Printing: Grafisch Service Centrum, LUW

The investigations were supported by the Netherlands Foundation for Chemical Research (SON) with financial aid from the Netherlands Organisation for Scientific Research (NWO).

Chapter 3 reprinted from Colloids and Surfaces 51 (1990) 141.
Chapter 4 published in Macromolecules 25 (1992) 5416.

Stellingen

1. Desorptie van polymeer verloopt uiterst traag, zelfs wanneer er nabij het oppervlak een snelle evenwichtsinstelling is tussen vrije en geadsorbeerde ketens.

   Dit proefschrift, hoofdstuk 4.

2. De geadsorbeerde hoeveelheid van diblokcopolymeren stijgt met toenemende kromming van het oppervlak. Deze stijging is vooral zeer uitgesproken bij die bloklengteverhouding waarbij de geadsorbeerde hoeveelheid maximaal is.

   C.M. Wijmans, proefschrift (in voorbereiding).

3. De experimenten van Friedman et al. sluiten in tegenstelling tot de bewering van de auteurs niet uit dat een dunne laag siloxeen op het oppervlak verantwoordelijk is voor de luminescentie van poreus silicium.

   S.L. Friedman, M.A. Marcus, D.L. Adler, Y.-H. Xie, T.D. Harris, and P.H. Citrin, *Appl. Phys. Lett.*, **1993**, *62*, 1934.

4. Veel producten voor de slanke lijn bevatten verdikkingsmiddelen ter vervanging van vet.

5. Glaswerk gereinigd met een zeepoplossing is verre van brandschoon.

6. De rugtitel van Franse en Duitse boeken staat in de regel op z'n kop wanneer het boek met z'n voorkant boven ligt. Ter bevordering van regelmaat en overzicht is het goed deze boeken ondersteboven in de boekenkast te plaatsen.

7. Uit de opmerking "hij doet niets, hoor" blijkt dat angstaanjagend blaffen en grommen voor vele hondebezitters gelijk staat aan niets doen; "iets doen" moet waarschijnlijk worden opgevat als het door bijten toebrengen van (ernstige) verwondingen.

8. Om politici te dwingen zich meer tot het publiek te richten zou het aantal kamerleden evenredig met het percentage wegblijvers bij de verkiezingen verminderd moeten worden.

Stellingen

behorende bij het proefschrift 'The kinetics of polymer adsorption, desorption and exchange' van J.C. Dijt, Landbouwuniversiteit Wageningen, 28 juni 1993.

1 INTRODUCTION

1.1 General

The equilibrium state of adsorbed polymer layers has received much attention in the last decades, both experimentally and theoretically[1,2]. However, the *rate* at which equilibrium is attained has hardly been studied. Some of the results seem to indicate that the equilibration of an adsorbed polymer layer may be rather slow, taking hours or even days. Other results suggest more rapid relaxations. The underlying adsorption mechanism and the factors affecting it are, however, hardly understood. The aim of the study in this thesis was to gain more insight into the kinetics of polymer adsorption. To this end the adsorption kinetics of some well-characterised polymers has been systematically investigated, using two techniques that are especially suitable for kinetic measurements: reflectometry in a stagnation point flow and a streaming potential method in capillary flow.

Polymer adsorption plays an important role in many products and processes where stabilisation or flocculation of colloidal dispersions is required[3]. For example, polymers act as stabilisers in paints, in pharmaceutical and cosmetical ointments and creams, in lubricants used in the oil industry, and in the production of magnetic tapes, fluorescent lamps and television screens. The flocculating capability of polymers is important in applications like paper-making, waste-water treatment, and the production of metals from ores.

1.2 Polymer adsorption

Polymers consist of chain molecules that are built up of a large number of repeating units, called monomers or segments. The chains may be linear, branched, or, in some cases, star-like or ring-shaped. If all the segments in a molecule are identical the polymer is a homopolymer. A chain with more than one type of segment is called a copolymer, and one with charged segments is a polyelectrolyte. In this study only linear, uncharged homopolymers were considered.

In solution, linear polymer molecules behave as flexible chains that can be described by a random coil. The conformation changes dynamically and continually due to rotation around bonds in the backbone of the molecule. The chain dimension in solution depends on the solvent quality and on characteristics of the chain like its stiffness and the number and the

chemical type of the segments.

At the interface between a solid surface and solution a polymer may adsorb (accumulate). This happens when the exchange of solvent in contact with the surface by segments of the polymer chain leads to an increase of the adsorption energy. In order for adsorption to take place this gain of adsorption energy must be high enough to compensate for the loss of conformational entropy of the chain, which is due to the binding of the molecule to the surface. In addition, the gain of adsorption energy is partly counteracted by a repulsive osmotic pressure in the adsorbed layer which is caused by the higher concentration of polymer segments near the surface as compared to the bulk solution.

As long as enough free surface sites are available the adsorption energy contribution dominates, leading to a rather flat polymer conformation with a low entropy and a high fraction of adsorbed segments (fig. 1.1.a). At higher coverage, the chain has more conformational freedom and a lower fraction of adsorbed segments due to the limited availability of free surface sites (fig. 1.1.b). Within the adsorbed chain commonly three conformational states are distinguished, as indicated in fig. 1.1.c. A *train* is a sequence of segments that are all adsorbed, a *loop* is a section of the chain between two trains, and a *tail* is a non-adsorbed, dangling end of the chain.

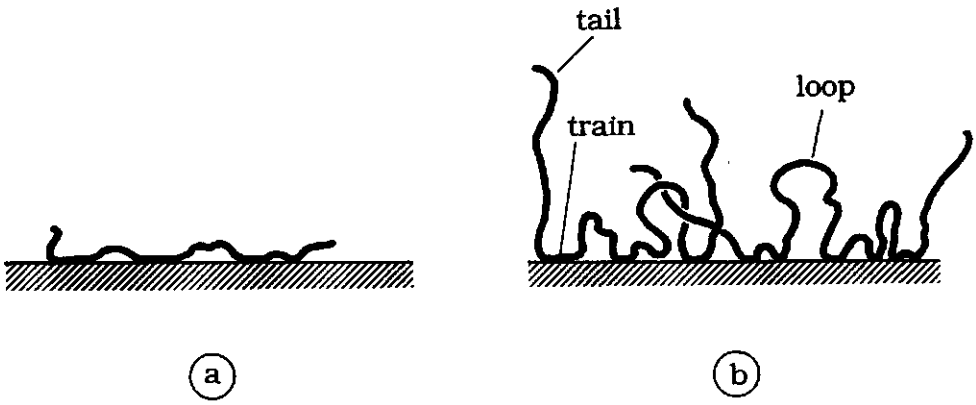

Figure 1.1 Adsorbed layer of a flexible polymer at low surface coverage (**a**), and at high coverage (**b**).

For uncharged polymers, the adsorption energy *per segment* is usually rather small, comparable to the energy of thermal motions (kT). Since a polymer chain is attached to the surface by many segments, the adsorption energy *per chain* can be very high. Therefore, the equilibrium between free and adsorbed chains is usually highly biased towards the

surface side, with a saturated surface layer even if the solution concentration is very low.

It is likely that adsorption reduces the mobility of a polymer chain. Since in most cases the segmental adsorption energy is rather low, by thermal motions the segment-surface contacts are continually broken and reformed. However, movements of the whole chain require desorption of many segments, which is a much less likely event. Therefore, we might expect that chain movements are rather slow.

1.3 Kinetics of polymer adsorption

The kinetics of polymer adsorption is concerned with the rate of adsorption and the elucidation of the adsorption mechanism. In the kinetic process of polymer adsorption one may distinguish at least three contributions: (i) transport of polymer molecules from the bulk solution towards the surface, (ii) attachment to the surface, and (iii) unfolding of the polymer chain. The adsorption rate may be affected by either of these steps, and it could depend on factors like the hydrodynamic conditions, the type, molar mass and concentration of the polymer, the surface coverage, the binding strength, and the solvent quality. For example, Pefferkorn et al.[4] observed that the adsorption rate of polystyrene (PS) from carbon tetrachloride onto silica is proportional to the solution concentration, and that it decreases gradually with increasing coverage. In two other studies, Pefferkorn and co-workers[5,6] found some indications that unfolding of adsorbed polyelectrolytes is a slow process.

In studying the adsorption mechanism a first step might be to separate the transport and surface processes. If the adsorption takes place under well-defined hydrodynamic conditions, the transport through solution (diffusion and convection) can be calculated rather accurately, and it therefore becomes possible to separate unambiguously the mass transfer from the surface processes (attachment and reconformation). In order to achieve this separation, we used a stagnation point flow whereby the adsorbed layer was monitored by reflectometry. With this method a direct and continuous determination of the adsorbed amount (mass/area) is obtained under well-defined hydrodynamic conditions.

Methods that measure only the adsorbed amount, like reflectometry, at best provide indirect information on surface processes like attachment and reconformation. Ideally, one would like to monitor directly the conformations of individual adsorbed chains. Unfortunately, this is not (yet) possible. Some methods are in a rather indirect way sensitive to the

(average) conformation of adsorbed chains. For example, train segments can sometimes be detected by spectroscopic techniques (infrared absorption, NMR) because by virtue of their interaction with the surface train segments may have different spectroscopic properties as compared to segments in loops and tails. Segments in loops and tails have a relatively strong hydrodynamic interaction with the solvent, which, e.g., might be detected by dynamic light scattering or electrokinetic methods.

1.4 Desorption and exchange of polymers

The kinetics of adsorbed polymer layers can also be studied during desorption into solvent. Alternatively, the exchange rate between free and adsorbed chains might be investigated. In both cases, the desorption rate could be indicative of the rate of surface (rearrangement) processes.

Because of the high adsorption energy of long chains the desorbed amounts in solvent are expected to be very low. Indeed, this expectation is confirmed in several studies[7-9]. At high shear rates, Lee and Fuller[10] observed a considerable desorption of PS from chrome into cyclohexane, especially for very long chains. The authors assumed that desorption occurs if the hydrodynamic force on the chain becomes greater than the (total) binding strength of the polymer to the surface. The latter depends on the number of train segments, and therefore flow-enhanced desorption could be used as an indirect measure for the bound fraction.

At low shear rates when there is no flow-enhanced desorption, the desorbed amounts are expected to be very low. Therefore, a quantity should be measured that is sensitive to small changes in the adsorbed amount. For long chains near saturation, small changes in the adsorbed amount strongly influence the extension of the tails, and thereby the hydrodynamic interaction of the adsorbed layer with the solution. The hydrodynamic layer thickness is to a large extent determined by this interaction, and it is therefore a suitable parameter. For adsorption of uncharged polymers from aqueous solution the hydrodynamic thickness can be obtained from the streaming potential. We decided to apply the streaming potential method because it is especially suitable for kinetic studies. With this technique a direct and continuous observation of the adsorbed layer is possible under well-defined hydrodynamic conditions (e.g., in capillary flow), so that the mass transfer can be calculated and thereby separated from the surface processes.

During polymeric exchange, free chains in solution adsorb on a surface

covered with a polymer layer. This adsorption (eventually) leads to desorption of the initially adsorbed molecules. Therefore, the adsorbing polymer is often called a (polymeric) displacer. In case of chemically different polymers, exchange occurs if the chains in solution have a higher adsorption energy *per segment* than the adsorbed molecules. This preference on the basis of a different segmental adsorption energy is usually so strong that always exchange is expected, irrespective of the chain lengths of the displacer and the displaced component. In case of chemically identical polymers of different length, short chains are exchanged by longer ones because this exchange leads to an increase of translational entropy in solution. This entropy gain is rather small, and the chains should differ by at least a factor two in order to expect complete exchange[11].

In practice, polymer samples always contain a distribution of chain lengths, so that exchange occurs, leading to preferential adsorption of the longer chains in the sample over the shorter ones. If the molar mass distribution is broad, then the sample is called polydisperse. In studying the adsorption kinetics, we mainly used "monodisperse" polymers with a narrow chain length distribution, in order to avoid exchange between molecules with a different length.

For the study of the exchange kinetics several methods have been applied. For example, Pefferkorn et al.[7] measured the exchange between radio-active and non-labelled samples of the same polymer (polyacrylamide). These authors observed that the exchange was rather slow, proceeding over several hours, and that it was proportional to the solution concentration of the polymeric displacer. The latter feature is an indication that the attachment of a chain to the surface was limiting the rate of exchange. Frantz and Granick[12] studied the exchange of protonated PS (p-PS) by deuterated PS (d-PS) by directly monitoring the infrared absorption of the adsorbed polymers, which is different for p-PS and d-PS. The adsorption took place from cyclohexane on oxidised silicon. First p-PS was adsorbed, and then, after a waiting period, d-PS was brought into contact with the surface. It was observed that the exchange rate decreases systematically with increasing ageing time, which suggests that during ageing slow reconformations occur within the pre-adsorbed layer.

In this study we used reflectometry to monitor the exchange kinetics. Since the reflectivity of an adsorbed layer contains contributions of all adsorbed species, it is with this technique not possible to distinguish directly between the different components on the surface. In case of

exchange between polymers that differ in length only, reflectometry can be applied to measure the change in the total adsorbed amount. For an accurate measurement therefore usually a large chain length difference is needed. The sensitivity of reflectometry is proportional to the refractive index increment dn/dc of the polymer in solution. The increment dn/dc depends on the type of polymer and solvent. For a study of the exchange between different polymers a large difference of dn/dc is desirable, because then the exchange leads to a pronounced change in the reflectivity of the surface.

1.5 Outline of this study

For this study two techniques were used: reflectometry in a stagnation point flow (chapters 2,3 and 5-7) and a streaming potential method (chapter 4).

Chapter 2 deals with the principles of the measurement of adsorption by reflectometry. Using the results of an optical model we discuss the possibilities of the method for adsorption from dilute solution on a thin film that lays on top of a silicon substrate. For a wide variety of solvents and film materials reflectometry appears to be a suitable method for direct and continuous determination of the adsorbed amount.

In *chapter 3* first the mass transfer in a stagnation point flow is described, and then the kinetics of adsorption of PEO from water onto oxidised silicon is investigated by systematic variation of the flow rate, and of the concentration and the chain length of the polymer. From a comparison of the observed adsorption rate with the calculated rate of mass transfer to the surface it is concluded that the mass transfer is limiting the rate of adsorption nearly up to saturation of the polymer layer.

In *chapter 4* a model is discussed for the desorption rate of polymers into a flow of pure solvent. The model is based on a local equilibrium, i.e., on the assumption that near the surface there is a rapid equilibration between free and adsorbed molecules, and that transport away from the surface is limiting the rate of desorption. With the streaming potential method the equilibrium thickness isotherms, and the kinetics of adsorption and desorption of PEO from aqueous solution onto glass are investigated. The results are found to be in excellent agreement with the predictions of the theoretical model.

In *chapter 5* the adsorption and desorption kinetics of PS from decalin on oxidised silicon are studied by reflectometry. We investigate the influence of the polymer concentration and chain length, and the effect of

an addition of a non-solvent and a displacer of low molar mass. It is found that with increasing coverage the attachment of a chain to the surface becomes gradually slower, and that the rate of attachment is determined by energetical and entropical factors. In this chapter we also examine the adsorption kinetics of PS with a strongly adsorbing end-group.

Chapter 6 deals with the exchange kinetics of polymers that differ in chain length only. Both for PEO and PS we investigate the displacement of adsorbed short chains by longer chains of the same polymer. It is found that the exchange kinetics of PEO is unmistakably faster than that of PS, and that the desorption rate of the displaced PS is determined by a slow surface process.

In *chapter 7* we study the exchange kinetics between three chemically different polymers: polystyrene (PS), poly(butyl methacrylate) (PBMA) and polytetrahydrofuran (PTHF). The displacement of PS by PBMA appears to be rather slow in the solvent decalin. However, by addition of displacers of low molar mass the exchange rate can be considerably enhanced.

1.6 References

(1) Cohen Stuart, M.A.; Cosgrove, T.; Vincent, B. *Adv. Colloid Interface Sci.* **1986**, *24*, 143.

(2) Kawaguchi, M.; Takahashi, A. *Adv. Colloid Interface Sci.* **1992**, *37*, 219.

(3) Everett, D.H. In " *Basic principles of colloid science*"; Royal Society of Chemistry: London, **1988**.

(4) Pefferkorn, E.; Haouam, A.; Varoqui, R. *Macromolecules* **1988**, *21*, 2111.

(5) Pefferkorn, E.; Elaissari, A. *J. Colloid Interface Sci.* **1990**, *138*, 187.

(6) Pefferkorn, E.; Jean-Chronberg, A.C.; Varoqui, R. *Macromolecules* **1990**, *23*, 1735.

(7) Pefferkorn, E.; Carroy, A.; Varoqui, R. *J. Polym. Sci., Polym. Phys. Ed.* **1985**, *23*, 1997.

(8) Johnson, H.E.; Granick, S. *Macromolecules* **1990**, *23*, 3367.

(9) Grant, W.H.; Smith, L.E.; Stromberg, R.R. *Faraday Discuss. Chem. Soc.* **1975**, *59*, 209.

(10) Lee, J.-J.; Fuller, G.G. *J. Colloid Interface Sci.* **1985**, *103*, 569.

(11) Scheutjens, J.M.H.M.; Fleer, G.J. In "*The effects of polymers on dispersion properties*"; Tadros, T.F., Ed.; Academic Press: London, **1981**

(12) Frantz, P.; Granick, S. *Phys. Rev. Lett.* **1991**, *66*, 899.

2 MEASUREMENT OF ADSORPTION BY REFLECTOMETRY

2.1 Introduction

The use of ellipsometry for studying adsorbed layers of, e.g., polymers, proteins or surfactants on various substrates has been known for a long time[1]. Quite recently a new, simple reflectometric technique was developed at AKZO laboratories[2,3]. This technique offers the possibility of a continuous measurement of the adsorbed amount.

In a reflectometer a linearly polarised light beam is reflected from the surface, and the reflected beam is split into its parallel and perpendicular components using a polarising beamsplitter. The intensities of the normal and parallel polarisation directions (with respect to the plane of incidence) are measured continuously. Upon adsorption the ratio of these intensities changes, and after calibration the adsorbed amount is obtained from this change.

The high sensitivity for adsorption of the method lies in the fact that the reflecting substrate used carries a thin film of material with a refractive index different from the substrate itself. Reflectometry appears to be insensitive to the concentration profile of the adsorbed layer, which could be considered as a loss in information as compared to ellipsometry. However, advantages of reflectometry are that it is much simpler -and cheaper-, and that a continuous measurement is obtained over short time-scales. The time resolution is determined by the response time of the light detectors (photo diodes) and the signal processing electronics. It is well below 1 s. For this reason reflectometry is very suitable for the measurement of adsorption kinetics on the time scale of seconds to minutes. Particularly, transport processes between bulk and surface occur at these time scales.

In this chapter we want to discuss the applicability of reflectometry for adsorption measurements in various systems. With the help of an optical model the reflectivity of the adsorbing surface is calculated, and the sensitivity of the method and optimal optical conditions will be discussed.

In most cases, the optical contrast between adsorbate and solution is rather low, and the adsorbed amounts are very small (typically ≈ 1 mg/m^2). The resulting change in the reflectivity of the surface is therefore also very low. A well-known method to increase the sensitivity is the use of a substrate with a high refractive index upon which a thin film of the adsorbent is prepared. Optically the thin film causes a favourable phase shift in the reflected beam. A suitable thickness is typically in the range of

20-200 nm. For reflectometry, the use of a thin film appears to be essential in order to obtain enough sensitivity. In this chapter we consider the substrate silicon, which is commercially available in the form of polished wafers.

The first application to be discussed is the adsorption from aqueous solutions on silicon covered with a thin silica film. However, in studying polymer adsorption organic solvents are equally important, since many polymers are not soluble in water. The optical contrast between an organic solvent (or dilute solution) and silica is often very low, or even absent for many solvents. Therefore a closer examination of these systems is useful, which will be our second topic. Thirdly we will discuss the use of thin films other than silica. Using various techniques it is possible to prepare thin films of many materials (such as polystyrene, titanium oxide, indium tin oxide) on silicon[4-7] This makes reflectometry suitable for adsorption studies on a variety of substrates.

2.2 Methods

In this section we first describe the optical model used for the reflectivity calculations and the relation between adsorbed amount and optical constants of the adsorbate. Then the experimental setup is discussed, and an expression for the calibration of the adsorbed amount from the reflected intensities is derived. Finally we discuss some conditions for using reflectometry for quantitative adsorption measurements.

2.2.1 Optical model

Our aim is to calculate the parallel and perpendicular reflectivities of the surface, denoted by R_p and R_s, respectively. (The subscript s is from the German "senkrecht", meaning perpendicular.) Due to the presence of a dielectric film and a more or less diffuse adsorbed layer, the refractive index in the interface may vary with z (the distance in normal direction) in a complicated way. A natural way to deal with this is to consider the interface as a stack of flat, parallel layers. For such a system one can use the method of Hansen, which is based on the exact matrix formalism of Abeles[8,9].

In Hansen's method the system is modelled as a series of flat, parallel layers of uniform refractive index. Any number of layers ≥ 2 can be used. A layer is fully characterised by its thickness and refractive index. The situation for a silicon wafer with a thin silica film is schematically drawn in fig. 2.1. In order to satisfy the assumptions of the method the film

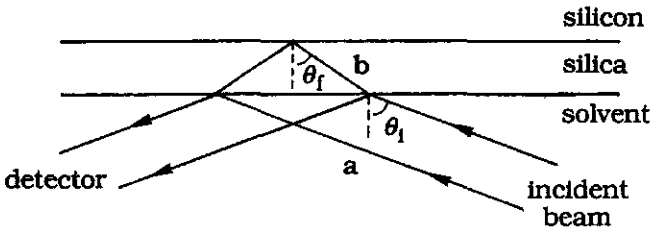

Figure 2.1. Principle of reflectometry. The reflectivity of the surface is determined by the Fresnel coefficients of the phase boundaries as well as by interference in the reflected beam between rays of the incident beam that reflect on the solvent/silica and silica/silicon interface (marked 'a' and 'b', respectively). The effect of an adsorbed layer is qualitatively comparable to a (small) growth of the oxide layer.

thickness must be much smaller than the diameter of the incident beam. In practice, the oxide film thickness is typically ≈100 nm.

The reflectivities R_p and R_s of the oxidised wafer are determined by the Fresnel reflection coefficients at the two-phase boundaries (solvent/silica and silica/silicon), and by interference in the reflected beam. The interference depends on the phase difference in the reflected beam between rays of the incident beam that are reflected at the solvent/silica and silica/silicon boundary (in fig. 2.1 those rays are marked 'a' and 'b', respectively). The phase difference ϕ is a function of the thickness d_f and refractive index n_f of the film, and is given by

$$\phi = \frac{4\pi d_f n_f \cos\theta_f}{\lambda_0} \tag{2.1}$$

In this equation λ_0 is the wavelength in vacuum of the light used and θ_f is the angle of the beam in the silica layer, defined with respect to normal incidence. Using Snell's law θ_f can be calculated from the angle of incidence θ_i. The effect of an adsorbed layer is qualitatively comparable to a small increment in the thickness d_f of the oxide layer, and thus to a small shift of ϕ. For an exact computation of R_p and R_s the reflectivities at all phase boundaries as well as the phase shifts in all intermediate layers have to be accounted for. This is done by Abeles' method. Multiple reflections in intermediate layers are also incorporated. The computational method is based on a matrix multiplication: each layer of the system is represented by a matrix. The procedure is extensively described in[8]. The calculations show that the sensitivity of reflectometry strongly depends on ϕ, and thus on the film thickness d_f and the angle of incidence θ_i.

For the calculations we have to adopt some model for the concentration

profile $c(z)$ of the adsorbate, and this profile $c(z)$ should be converted to a refractive index profile $n(z)$. In a real adsorbed layer the concentration profile will usually be some decreasing function of the distance z. As a first approximation we can replace this function by a single step profile. The refractive index n_a of such a homogeneous layer of thickness d_a is related to the adsorbed amount Γ by

$$n_a = n_s + \left(\frac{dn}{dc}\right)\frac{\Gamma}{d_a} \tag{2.2}$$

where n_s is the refractive index of the solvent, and dn/dc is the refractive index increment of the adsorbing material in solution. The quantity Γ / d_a is the concentration in the adsorbed layer. For multilayer profiles eq. 2.2 has to be applied to each layer, and the total adsorbed amount is obtained by summation over the layers.

2.2.2 Experimental setup

The experimental setup is schematically shown in fig. 2.2. A linearly polarised He/Ne laser beam (1) enters the cell through a 45° glass prism (2). The laser beam reflects on the adsorbing surface, for which we use a strip cut from an oxidised silicon wafer (3). The laser beam leaves the cell through the glass prism (2). For the detection we apply a method originally

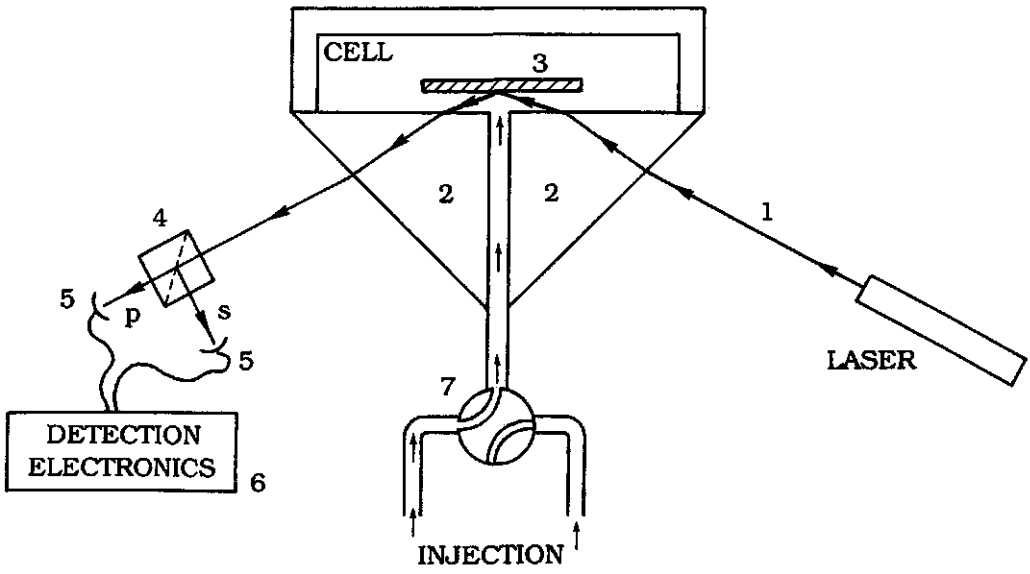

Figure 2.2. Schematic diagram of the experimental setup. For explanation of numbers, see text.

developed at AKZO Research Laboratories Arnhem[2]. The reflected beam is split into its parallel (p) and perpendicular (s) components (with respect to the plane of incidence) by means of a polarising beamsplitter cube (4). Both components are detected by photo-diodes (5) and the resulting signals are fed into an analogue divider (6) to give the output signal S, defined in eq. 2.3 below. At the beginning of an experiment the cell is filled with solvent. The signal due to a surface without adsorbate is called S_0. Solution is introduced into the cell by means of an injection system (7) which is connected to the cell by tubing and a horizontal cylindrical hole drilled in the glass prism (2). The flow system will be extensively discussed in the next chapter. The increment $\Delta S = S - S_0$ is recorded.

2.2.3 Calibration

The reflected intensities I_p and I_s for parallel and perpendicularly polarised light, respectively, are combined to the output signal S of the reflectometer which is defined as[1]

$$S = \frac{I_p}{I_s} \tag{2.3}$$

The reflected intensities I_p and I_s can be expressed in the incident intensities I_p^0 and I_s^0, the reflectivities R_p and R_s of the substrate, and loss factors f_p and f_s, respectively

$$I_p = f_p R_p I_p^0 \tag{2.4.a}$$

$$I_s = f_s R_s I_s^0 \tag{2.4.b}$$

The factors f_p and f_s account for losses at the reflecting surfaces of the prisms and the beamsplitter, and for differences in detection efficiency between the two photo diodes. Combination of eqs. 2.3 and 2.4 gives

$$S = f \frac{R_p}{R_s} \tag{2.5}$$

---

[1]Originally S was defined by AKZO as $(I_s - I_p)/(I_s + I_p)$. This definition was also used in chapter 3. In order to simplify detection electronics we redefined S. Upon adsorption I_s and I_p usually change in opposite directions (see section 2.3), so that according to AKZO's definition essentially a change in $I_s - I_p$ is measured, the sum $I_s + I_p$ in the denominator being approximately constant. Normally we have $I_s \approx I_p$ (see chapter 3), under which condition there is a simple relation between both definitions of S: S(AKZO) ≈ {1 − S(eq. 2.3)}/2.

where $f = f_p I_p^0 / f_s I_s^0$. The factor f depends on I_p^0 and I_s^0, and thus on the (adjustable) polarisation angle of the laser. For a given value of this angle, f is a constant. Note that the signal S is insensitive to fluctuations in the total light intensity as long as the polarisation angle is constant.

For each experiment the constant f can be determined from the initial values of S and R_p/R_s

$$f = \frac{S_0}{\left(R_p / R_s\right)_0} \tag{2.6}$$

where the subscript 0 indicates the initial situation on a bare surface. The value of $(R_p/R_s)_0$ follows from the optical model.

Due to adsorption the reflectivity of the surface will alter, and for the corresponding change ΔS of the output signal we can write, using eq. 2.5:

$$\Delta S = f\left\{\left(\frac{R_p}{R_s}\right)_\Gamma - \left(\frac{R_p}{R_s}\right)_0\right\} \tag{2.7}$$

where the subscript Γ indicates the presence of an adsorbed layer. With eqs. 2.6 and 2.7 it is possible to relate ΔS to a change in R_p/R_s. From a calculation with the optical model the corresponding adsorbed amount Γ can be determined using eq. 2.2 or a more complicated version for a multilayer profile. In most cases R_p/R_s turns out to be linear in Γ. Then the term in between braces in eq. 2.7 equals $\Gamma\, \mathrm{d}(R_p/R_s)/\mathrm{d}\Gamma$. For this case we can write for the adsorbed amount Γ by combination of eqs. 2.6 and 2.7:

$$\Gamma = \frac{\Delta S}{S_0}\frac{1}{A_s} \tag{2.8}$$

where the sensitivity factor for adsorption A_s is defined as

$$A_s = \frac{1}{\left(R_p / R_s\right)_0}\frac{\mathrm{d}R_p / R_s}{\mathrm{d}\Gamma} \tag{2.9}$$

The optical model gives R_p/R_s as a function of Γ, from which A_s follows immediately. Note that A_s according to eq. 2.8 equals the relative change in S per unit adsorbed amount, which is why we call it sensitivity factor.

For the calculation of R_p/R_s the film thickness d_f of the adsorbent is needed. If the refractive index n_f is known, then d_f can be determined with the reflectometer. To this end first the factor f is determined from a wafer with known values of n_f and d_f, for which $(R_p/R_s)_0$ can be

calculated. Then S of the wafer with unknown d_f is measured and from the value of R_p/R_s thus found the thickness d_f is calculated. If both n_f and d_f are unknown, they have to be determined by another method, e.g., ellipsometry.

2.2.4 Conditions for using reflectometry

In order to assess the results of the reflectivity calculations it is useful to define some conditions necessary for accurate adsorption measurements with reflectometry.

(i) The useful range of R_p/R_s is about $10^{-2} - 10^{2}$. These limits originate from the limited polarisation separation of the beamsplitter, and the polarisation of the incident laser beam.

(ii) The sensitivity should not be too low, e.g., $A_s > 0.005\ m^2/mg$. Noise and drift in our experiments are mainly caused by temperature fluctuations. Effects of evaporation at the free solution/air interface as well as long term temperature fluctuations of the whole setup seem to play a role. The lower limit for A_s will therefore strongly depend on the quality of the temperature control and the required accuracy. The value of 0.005 m^2/mg is rather arbitrary, and is mainly based on our experience.

(iii) For a quantitative determination of Γ it is desirable that the relation between R_p/R_s and Γ is linear, so that A_s is a constant which is independent of Γ.

(iv) For a quantitative determination of Γ the sensitivity A_s should not depend on the concentration profile of the adsorbed layer.

2.3 Results of reflectivity calculations

In this section we discuss the use of reflectometry under various circumstances. All calculations were carried out for λ_0=632.8 nm, which is the usual wavelength of low pressure He/Ne lasers.

2.3.1 Adsorption from water onto silica

Figure 2.3 is a compilation of reflectivity calculations for adsorption from aqueous solutions onto a Si-wafer covered with a thin film of SiO_2. First we discuss figs. 2.3.a/b; figs. 2.3.c/d will be considered after discussion of figs. 2.4 and 2.5.

In fig. 2.3.a the reflectivities R_p and R_s are given as a function of the angle of incidence θ_i for the water/silicon interface in the absence (dotted curves) or presence (full curves) of a thin silica film. The dashed curves ($d_f = 0$) correspond to the Fresnel-reflectivities. For this case we see that

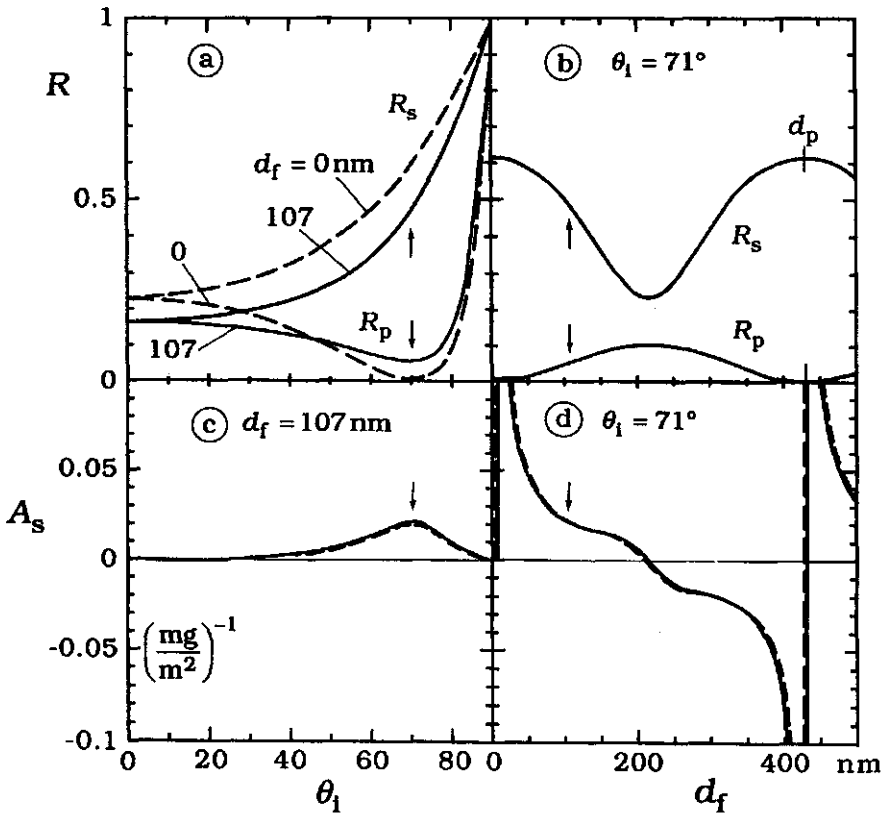

Figure 2.3. Reflectivity for adsorbed layers from aqueous solution on oxidised silicon. In **a** and **b** the reflectivities R_p and R_s of silicon covered with a thin silica film without adsorbate are given as a function of θ_i and d_f, respectively. In **a** the dashed curves represent R_p and R_s for the silicon/water interface (d_f=0) and the full curves are for d_f=107 nm, corresponding to ϕ=90° in eq. 2.1. Figure **b** is calculated at the Brewster angle for silicon/water. The thickness d_p of a period for which ϕ=360° is indicated by a vertical tick along the curves. Arrows indicate the optimal experimental conditions. In figs. **c** and **d** the sensitivity factor A_s for adsorption is given as a function of θ_i and d_f, respectively. The full and dashed curves are for block-profiles with Γ=1 and 5 mg/m^2, respectively. The similarity of both curves indicates that A_s is nearly independent of the adsorbed amount Γ.

Parameters: λ_0=632.8 nm, n_{Si}=3.80, n_f=1.460, n_s=1.333, n_a=1.3598, d_a=5 or 25 nm. The values for d_a correspond to Γ=1 and 5 mg/m^2 if dn/dc=0.134 cm^3/g, which is the value for PEO in water.

R_p = 0 at ≈ 71°, which is called the Brewster angle for the water/silicon interface. The Brewster angle θ_{Br} is given by $\theta_{Br} = \text{arctg}(n_{Si}/n_s)$.

In presence of a silica film R_s is lower for every θ_i, and for R_p a cross-over occurs at ≈47°, which is the Brewster angle for the water/silica

interface. For θ_i<47° the reflectivities R_p and R_s change in the same direction, if the silicon is oxidised; consequently the change in R_p/R_s is only small. The effect of an adsorbed layer is qualitatively comparable to that of a thickness increment of the oxide film, and thus for θ_i<47° only a small effect from the adsorbate on R_p/R_s is expected. However, for θ_i>47° the situation is more favourable, because R_p and R_s change in different directions, the relative change in R_p/R_s being most pronounced at the Brewster angle for the water/silicon interface.

In fig. 2.3.b the effect of the silica film thickness d_f on R_p and R_s at θ_{Br} (water/silicon) is shown. The reflectivities R_p and R_s vary periodically with the film thickness. The thickness d_p of the period is 429 nm, which value is given by the condition that the phase-shift ϕ equals 2π, or, with eq. 2.1, $d_p = \lambda_0 / 2n_f \cos\theta_f$. Furthermore we note that for $d_f \approx 107$ nm ($\approx d_p/4$) and 320 nm ($\approx 3d_p/4$) the slope of the curves is at an extreme value, which indicates that at these film thicknesses R_p and R_s are most sensitive to an adsorbed layer.

We choose θ_i=71° ($=\theta_{Br}$) and d_f=107 nm ($=d_p/4$) for a calculation of R_p/R_s as a function of the adsorbed amount Γ. For the adsorbed layer a single step concentration profile was taken, and Γ was varied by changing d_a according to eq. 2.2 at a fixed value of n_a. For dn/dc we took the value of poly(ethylene oxide), which is 0.134 cm^3/g[10]. This is a typical value for many organic solutes in aqueous solution. In fig. 2.4 the full curve represents the outcome of the calculations, whereas the dashed line is a linear extrapolation of the initial part.

The variation of R_p/R_s with Γ is linear up to 5 mg/m^2 and the deviation of linearity at 10 mg/m^2 is only a few percent. For adsorbed layers of polymers, proteins or surfactants Γ=5 mg/m^2 is already very high and therefore we conclude that for adsorption from aqueous solutions on a silica film we can use a linear conversion between R_p/R_s and Γ. From the slope of the curve and the intercept with the ordinate we determine from eq. 2.9 that the sensitivity A_s equals 0.022 m^2/mg. This means that the reflectivity ratio R_p/R_s changes about 2.2 % per mg/m^2 adsorbed. Note that the value of $R_p/R_s \approx 0.1$ is well within the limits set out before.

In order to check if there is any effect of the concentration in the adsorbed layer on the sensitivity A_s we varied this concentration at a fixed value of Γ of 1 mg/m^2 by changing d_a and n_a according to eq. 2.2, keeping the product $(n_a - n_s)d_a$ constant. In fig. 2.5 the results are presented as $A_s(d_a)$. Some representative values of n_a are indicated. The value of A_s is practically the same for all reasonable densities of the

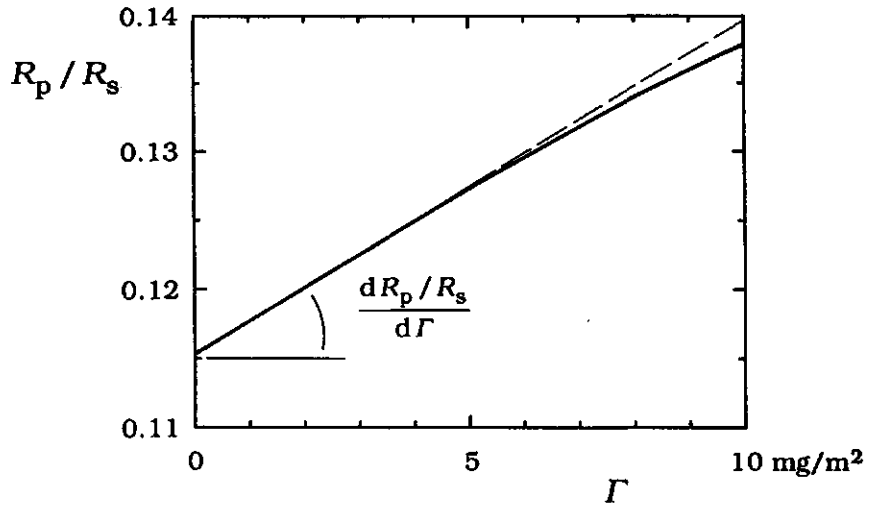

Figure 2.4. Calculated effect of the adsorbed amount Γ on the reflectivity ratio R_p/R_s for adsorption from aqueous solution on oxidised silicon. The full curve gives calculated values, the dashed line is a linear extrapolation. Note the very good linearity up the high adsorbed amounts. From the graph we calculated the sensitivity factor A_s according to eq. 2.9. The result is A_s=0.022 m^2/mg. Parameters: d_f=107 nm, and θ_i=71°, corresponding to the optimal values indicated in fig. 2.3 by arrows. Other parameters same as in fig. 2.3. For variation of Γ the value of n_a is fixed, and d_a is varied according to eq. 2.2.

adsorbed layer. It is concluded that the signal S measures Γ irrespective of the concentration in the adsorbed layer. Reflectometry is nearly insensitive to the thickness of an adsorbate layer (at constant Γ) but gives an accurate result for the adsorbed amount.

We now come to the discussion of figs. 2.3.c/d in which A_s is plotted as function of θ_i and d_f, respectively. For determination of A_s according to eq. 2.9 the slope $d(R_p/R_s)/d\Gamma$ was set equal to $\Delta(R_p/R_s)/\Delta\Gamma$, and A_s was calculated for two values of $\Delta\Gamma$: 1-0 and 5-0 mg/m^2. If both values of A_s are the same, the linearity between R_p/R_s and Γ is perfect. For convenience in the further discussion we introduce a linearity index $L_{5/1}$, which is defined as $L_{5/1}=A_s$(5-0 mg/m^2)/ A_s(1-0 mg/m^2). Figure 2.3.c shows that the sensitivity has a maximum around the Brewster angle for water/silicon. This implies that 71° is the optimum value of θ_i, but from the broadness of the peak it is concluded that the precise setting is not very important. For all θ_i the linearity index $L_{5/1}$ is slightly lower than 1. For example, in the range $58<\theta_i<77°$ the linearity index $L_{5/1}$ is above 0.95, which is quite satisfactory for most experiments.

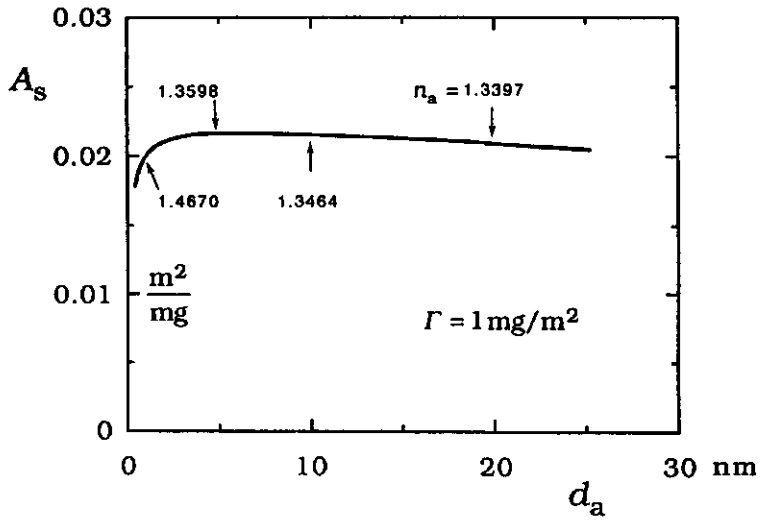

Figure 2.5. Effect of the adsorbed layer thickness d_a on the sensitivity A_S, for adsorption from aqueous solution on oxidised silicon. Same parameters as in fig. 2.4, except for n_a which was varied according to $(n_a - n_s)d_a$ =constant, where the constant corresponds to Γ=1 mg/m^2.

Finally fig. 2.3.d shows that a silica film thickness in the range of about 60-150 or 270-360 nm is most suitable for experiments. In these regions the absolute value of A_s is in between 0.016 and 0.039 m^2/mg and that of $L_{5/1}$ in the range 0.93-1.05, which is again quite satisfactory. In between these two regions A_s becomes rather low and S is then far from linear. For $d_f / d_p \approx 0$ or 1 the curves $A_s(d_f)$ diverge because $A_s \propto 1/R_p$ (see eq. 2.9) and $R_p \approx 0$ for these film thicknesses. However, $R_p \approx 0$ is not suitable for reflectometry, since too high demands are put on the polarisation of the laser and separation by the beamsplitter under this condition. Furthermore, in order to obtain A_s with reasonable precision a very accurate calibration of the film thickness would be needed.

2.3.2 Adsorption from organic solvents on silica

In using organic solvents for adsorption studies on silica films the refractive index of the solvent n_s may be lower, higher, or, indeed, equal to that of the silica film, which is n_f=1.46. Therefore, these systems deserve special attention. We start with an example where the refractive index of solvent and silica film are nearly matched. Thereafter, the influence of n_s will be discussed systematically.

Let us consider the adsorption of polystyrene from decalin. We studied this system extensively and the results are described in chapters 5-7. The

refractive index of decalin is 1.473, which is only slightly higher than that of the silica film (n_f=1.46). The refractive index increment of polystyrene in decalin is 0.120 cm^3/g[10]. This is comparable to the value of 0.134 for poly(ethylene oxide) in water, which was used for the calculations shown above. The results of the reflectivity calculations for the adsorption from decalin are presented in the same form as those for adsorption from aqueous solutions. Figures 2.6-8 are the analogues for decalin of figs. 2.3-5 for water.

Comparison of figs. 2.3.a (water) and 2.6.a (decalin) shows that the shape of the curves for $R_p(\theta_i)$ and $R_s(\theta_i)$ in the presence of a thin silica film is the same in decalin and water. The Brewster angle for decalin/silicon θ_{Br}=68.8°. This is only 1.9° lower than that for water/silicon. However, in the presence of a thin silica film, there is an important difference between both solvents: at the Brewster angle $R_p \approx 0$ in decalin, whereas in water $R_p \approx 0.05$. Obviously, this is caused by the low contrast between the silica film and decalin. Because in decalin R_p is very low, the Brewster angle is in this solvent not suitable for reflectometry.

A suitable angle should be at least a few degrees off the Brewster angle. In fig. 2.6.c $A_s(\theta_i)$ is plotted, again (as in fig. 2.3.c) calculated from Γ= 1 (full curve) and 5 mg/m^2 (dashed). It is seen that close to the Brewster angle A_s oscillates between highly negative and highly positive values. From the large difference between both curves we infer that the linearity is poor in this region. This behaviour is caused by the Brewster condition $R_p \approx 0$, as noted before. However, at the flanks of the oscillation both curves cross each other which means that, by definition, $L_{5/1}$=1 and here the linearity is excellent. The angles at which $L_{5/1}$=1.00 are found to be 60° and 74°, and the corresponding values of A_s are 0.019 and -0.036 m^2/mg, respectively. These values for A_s are comparable to the optimal value found for adsorption from aqueous solution.

For the optimal angle θ_i=60° we calculated the dependence of R_p and R_s (fig. 2.6.c) and A_s (fig. 2.6.d) on the silica film thickness. Again, like in water, R_p, R_s and A_s vary periodically with d_f. The period d_p equals 446 nm in decalin, which is slightly higher than in water (d_p= 429 nm). The slopes of the curves $R_p(d_f)$ and $R_s(d_f)$ are again steepest at $d_f / d_p \approx 1/4$ and 3/4, like in water, but now these thicknesses correspond to a maximum in the absolute value of A_s. The large difference between the curves for $A_s(d_f)$ in water and decalin is due to the fact that fig. 2.3.d (water) is at the Brewster angle and fig. 2.6.d (decalin) is not.

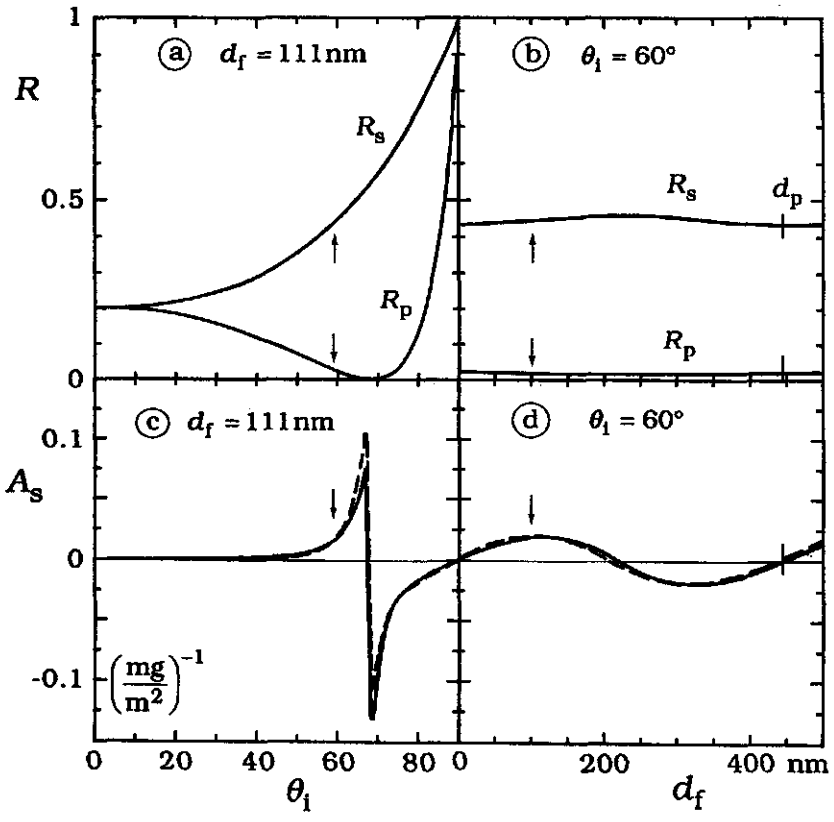

Figure 2.6. Reflectivity for adsorbed layers from decalin on oxidised silicon. The solvent (n_s=1.473) and silica film (n_f=1.460) are nearly refractive index matched. Figures **a** and **b** give the reflectivities R_p and R_s in the absence of an adsorbed layer as a function of θ_i and d_f, respectively. In figs. **c** and **d** the sensitivity A_s for adsorption is given as a function of θ_i and d_f, respectively. The meaning of the full and dashed curve is the same as in fig. 2.3.c/d. Arrows indicate the optimal experimental conditions. Parameters: n_s=1.473, n_a=1.497, d_a=5 or 25 nm. The values for d_a correspond to Γ=1 and 5 mg/m^2 if dn/dc=0.12 cm^3/g, which is the value for PS in decalin. Other parameters the same as in fig. 2.3.

The maximum found for $A_s(d_f)$ is rather broad and the linearity index $L_{5/1}$≈1.00 in this region. Thus, $L_{5/1}$=1.00 at d_f=116 and 307 nm, and within a range of about 40 nm around these points, the deviations from $L_{5/1}$=1.00 are not more than ±0.05. As a check of the linearity the results of a calculation of R_p/R_s as a function of Γ at d_f=111 nm (= $d_p/4$) and θ_i=60° are shown in fig. 2.7 (full curve). The dashed curve is again a linear extrapolation of the initial part. The linearity is indeed excellent. Note that the value of $R_p/R_s \approx 0.05$, which is within the acceptable limits set out

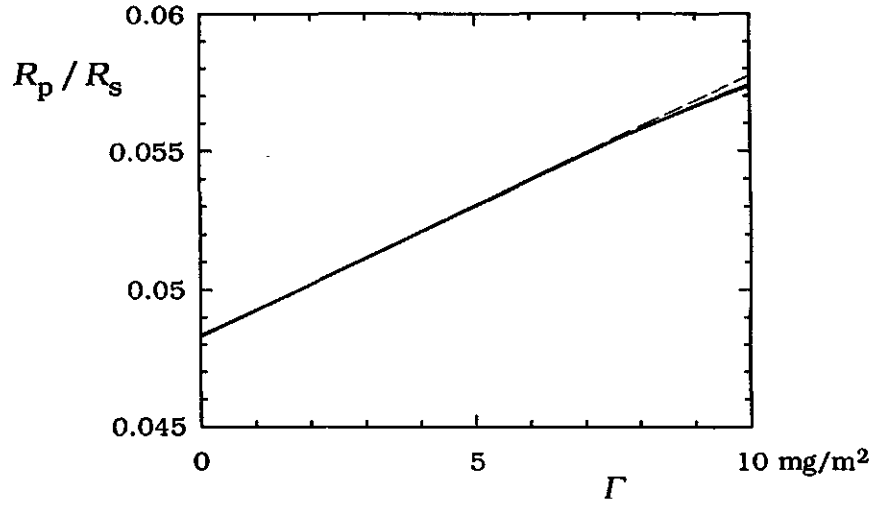

Figure 2.7. Effect of the adsorbed amount Γ on the reflectivity ratio R_p/R_s for adsorption from decalin on oxidised silicon, calculated analogously to fig. 2.4. Parameters: d_f=111 nm, and θ_i=60°; others as for fig. 2.6.

before for this quantity. Finally, fig. 2.8 shows that also in decalin the value of A_s is not sensitive to variations in the thickness of the adsorbed layer as long as the adsorbed amount Γ is kept constant.

We conclude that for reflectometry in decalin about the same sensitivity can be obtained as in water, namely $A_s \approx 0.02$ m^2/mg (at θ_i=60°). The optimal silica film thickness in decalin ranges from about 95-135, or 285-325 nm, which is about the same as in water. However, in decalin $\theta_i = \theta_{Br}$ (≈69°) is highly undesirable, whereas in water it was the optimal angle. The reason is the poor contrast between decalin and the silica film. In decalin θ_i=60° or 74° is a suitable angle, giving sufficiently high values of A_s and excellent linearity between R_p/R_s and Γ.

We now turn to a discussion of adsorption on thin silica films from solvents with other refractive indices. We will consider the range $1.3<n_s<1.6$, which covers almost any organic solvent. Upon changing the solvent we can adjust θ_i or d_f in the experiments in order to obtain enough sensitivity (A_s high) and a good linearity ($L_{5/1}$≈1.00). Our goal is to find for each solvent a useful combination of θ_i and d_f.

With respect to d_f we found that both in water (n_s=1.333) and decalin (n_s=1.473) a broad range centred around ≈115 nm gave satisfactory results. We therefore decided to keep this parameter fixed at d_f=111 nm, which was the value we used for the calculations in decalin. We then calculated for a series of n_s the angular dependence of the reflectivity and

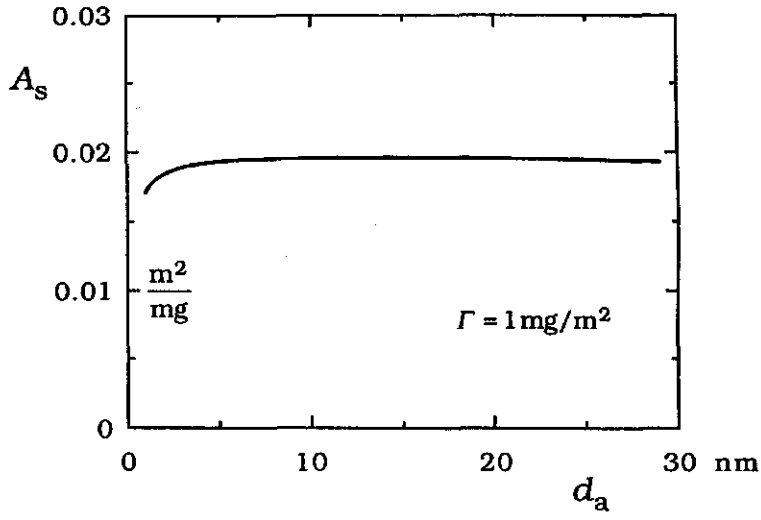

Figure 2.8. Effect of the adsorbed layer thickness d_a on the sensitivity A_s for adsorption from decalin on silica, calculated analogously to fig. 2.5. Same parameters as for fig. 2.7

sensitivity, and from this we determined for each n_s the angle θ_i^{opt}, where the linearity is optimal. Depending on n_s the optimal angle θ_i^{opt} corresponds to a value of $L_{5/1}$ that is exactly 1 or a value very close to it. The result for $A_s(n_s)$ and $\theta_i^{opt}(n_s)$ of this optimalization is represented by dashed curves in figs. 2.9.a and b, respectively. The first thing to note is that over the entire range of n_s the sensitivity A_s is of the order 0.01-0.03 m^2/mg, which implies that with reflectometry on silica films enough sensitivity can be obtained in any solvent.

For $n_s \geq 1.47$ the criterion of optimal linearity provides us with a clear choice for θ_i^{opt}, because in this range of n_s, like for decalin in fig. 2.6.c, the curves $A_s(\theta_i)$ calculated for Γ=1 and 5 mg/m^2 cross, which means that a single point with $L_{5/1}$=1.00 exactly exists. The corresponding angle is θ_i^{opt}. From fig. 2.9.b it is seen that θ_i^{opt} decreases from ≈60 to 52° going from n_s=1.47 to 1.6. This decrease is related to the fact that for $n_s > n_f$ the critical angle for total reflection on a solvent/silica interface is less than 90°. For n_s=1.6 this critical angle is already as low as 65°.

For n_s<1.47 the criterion of optimal linearity leads to a curve for $A_s(n_s)$ with a pronounced maximum at n_s=1.42, just below the refractive index of the silica film. This rather sharp peak implies that both the refractive index of the solvent and that of the silica layer have to be known precisely in order to have an accurate estimate of A_s. Experimentally it would be more convenient if $A_s(n_s)$ changed more gradually. Fortunately for n_s<1.47 we

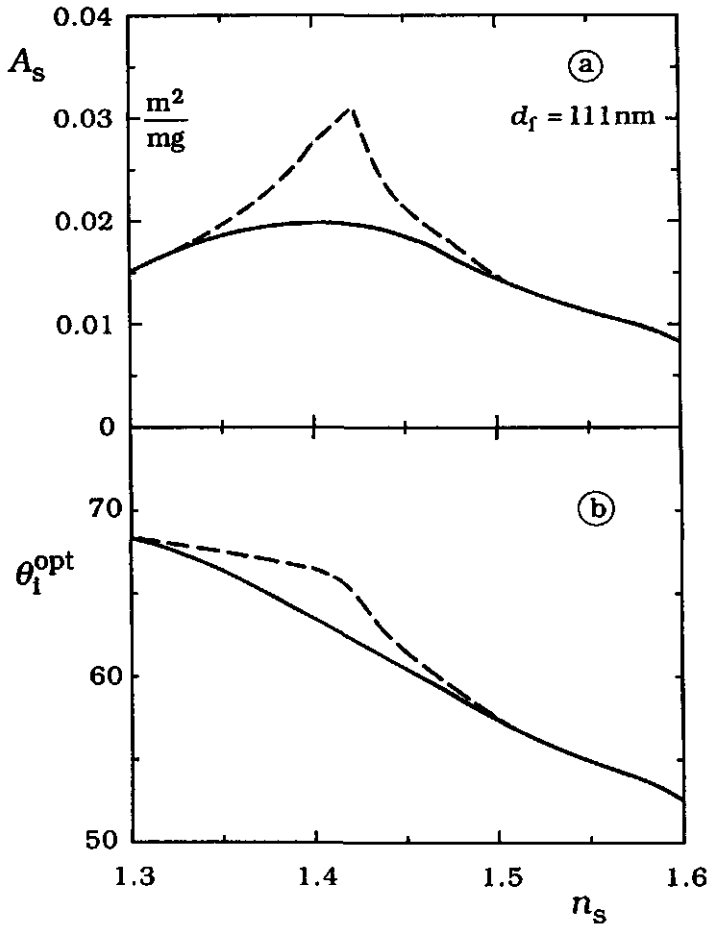

Figure 2.9. Optimal conditions for adsorption on silica as a function of the refractive index n_S of the solvent. The optimal angle of incidence θ_i^{opt} and the corresponding sensitivity A_S are plotted as a function of the solvent refractive index n_S in figs. **a** and **b**, respectively. For explanation, see text. Parameters: d_f=111 nm, others the same as for fig. 2.3.

do not have to obey the criterion of optimal linearity too strictly, because in this range of n_S a situation arises like that in fig. 2.3.c for water: $L_{5/1}$ is slightly lower than 1.00 for every θ_i and the dependence of $L_{5/1}$ on θ_i is only small. This means that in fact in a broad range of θ_i the linearity is sufficient.

We then decided to choose rather arbitrarily for $\theta_i^{opt}(n_S)$ a more or less linearly decreasing curve (full in fig. 2.9.b) and to calculate the corresponding value of A_S (full in fig. 2.9.a). The result is a more gradual change of A_S with n_S, as was desired. It turns out that for this curve the linearity is still very good: $L_{5/1}$ ranges from 0.97 at n_S=1.3 to 1.01 at

n_s=1.6, and in between it is nowhere out of these limits. The full curve in fig. 2.9.b must be looked upon as a practical suggestion for the choice of θ_i as a function of the refractive index of the solvent.

For $n_s \approx n_f$ there is almost no reflection at the solvent/silica interface and one might wonder whether for this case the concentration and optical properties of the adsorbed layer become important in determining the reflectivity of the surface. In order to change the refractive index of the adsorbed layer at constant concentration and constant adsorbed amount we performed calculations in which the sign of dn/dc was reversed. (Negative values for dn/dc indeed occur for some polymer/solvent combinations). The sign reversal of dn/dc means a drastic change in the position of n_a relative to that of n_s and n_f. The result for $A_s(\theta_i)$ is, however, practically the same, except for a change of sign of A_s. When at constant Γ the concentration in the adsorbed layer is varied (like in fig. 2.3 or 2.8), nowhere a strong dependence of A_s on the concentration is found. We conclude that for the adsorbed layer neither the concentration profile nor the sign of dn/dc are important in determining A_s and θ_i^{opt}.

The physical background why the sensitivity is still retained when n_s is close to n_f may be the following. In the absence of an adsorbed layer there is only one reflective surface, namely the silica/silicon interface. With an adsorbed layer present, the optical contrast between this layer and the solvent gives a second plane of reflection, at a distance d_f from the first. The sensitivity is mainly determined by interference between the two reflected beams, and thus depends strongly on their phase difference, which is determined by eq. 2.1. The main effect of the silica film is to provide an optimal optical spacing between the adsorbed layer and the underlying silicon.

We conclude that in principle reflectometry is suitable for adsorption measurements on silica using any solvent. For a thickness of the silica layer of about 110 nm the obtained sensitivity A_s varies between 0.01 and 0.02 m^2/mg, when the angle of incidence is decreased linearly from 69° at n_s=1.3 to 52° at n_s=1.6. However the angle of incidence should be chosen with care.

2.3.3 Adsorption on other thin films

As was already pointed out in the previous (sub)section the function of a thin silica film is to create a favourable optical phase shift in the reflected beam. This function can also be fulfilled by thin films of other materials, and therefore reflectometry can also be used for adsorption studies on

other materials, provided thin films of these materials can be prepared. Fortunately a number of techniques are available, and in our laboratory we already used reflectometry with films of polystyrene, indium/tin oxide and titanium oxide on silicon wafers[11]. In this section we want to establish the sensitivity and optimal optical conditions as function of the refractive index of the film.

For most films the refractive index will be higher than that of silica, e.g., many metal oxides have n_f around 2. Therefore, in most cases $n_s << n_f$ and we will have a situation that resembles the adsorption from aqueous solutions on silica which was discussed before. For the calculations we therefore decided to keep the refractive index of the solvent fixed at n_s=1.333, which is the value for water. For θ_i we chose θ_{Br}(silicon/water)=71°, which is the optimal angle for adsorption from aqueous solution on silica, as discussed before.

In fig. 2.10, we check the influence of the film thickness d_f for two types of films: n_f=1.46 (full curve), and n_f=1.90 (dashed curve). The sensitivity A_s is plotted as a function of d_f / d_p, where d_p is the thickness of a period as defined before. The first thing to note is that both films show the same type of behaviour on this normalised thickness scale, although d_p is different by a factor of almost 2. For silica it was already discussed before that $d_f / d_p \approx 1/4$ or 3/4 is most favourable for reflectometry. We can now generalise this conclusion to films of other refractive index. Note that with increasing n_f the value of d_p decreases. Accordingly, the useful range of d_f narrows. This implies that higher demands are made upon the accuracy of preparing films of a specified thickness when n_f increases. A practical suggestion to overcome this problem may be to prepare a two film layer: first a silica film of about 100 nm and then a extremely thin film of a few nm of the other material. As long as the thickness of the second layer is small as compared to that of the silica, the optical properties of the second layer are only of little importance.

For n_f=1.9 around d_f / d_p=0.5 we observe in fig. 2.10 a kind of oscillation of A_s. The reason is a sort of Brewster condition: R_s is close to zero (and not R_p as for water). At θ_i=71° and d_f / d_p=1/2 the perpendicular reflectivity R_s shows as a function of n_f a minimum with $R_s \approx 0$ at n_f=1.8. In terms of fig. 2.3.b this means that in the minimum $R_s \approx 0$ for n_f=1.8. In the minimum at n_f=1.8 the oscillation in fig. 2.10 is even much stronger than at n_f=1.9. The angle at which $R_s \approx 0$ for d_f / d_p=1/2 decreases with increasing value of n_f.

In order to obtain a curve for $A_s(n_f)$ under optimal conditions, we

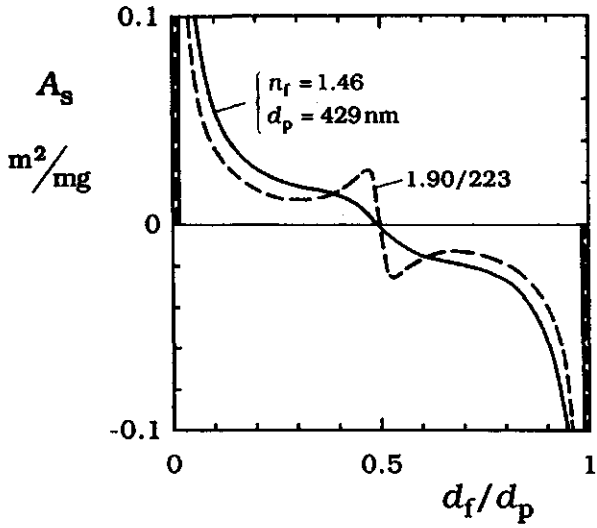

Figure 2.10. Film thickness dependence of the sensitivity A_s for adsorption from aqueous solution on a high and low refractive index thin film. The sensitivity A_s is plotted as a function of the normalised thickness d_f / d_p, where d_p is the film thickness for which $\phi=2\pi$. Values of n_f and d_p as indicated. Around $d_f / d_p \approx 1/4$ or 3/4 favourite conditions for reflectometry occur (see text). Parameters: $\theta_i=71°$, $\Gamma=1$ mg/m^2, others as for fig. 2.3.

calculated $A_s(n_f)$ for a variable thickness d_f, which was determined by the condition that $d_f = d_p / 4$. The result is shown in fig. 2.11 for 3 values of θ_i, as indicated. Like in fig. 2.3.c/d the full and dashed curves are calculated for $\Gamma = 1$ and 5 mg/m^2.

In fig. 2.11 we can roughly distinguish three regions: $n_f<1.5$, $1.5<n_f<2.5$, and $n_f>2.5$. For $n_f<1.5$ the optical contrast between solvent and film is rather low, and effects occur quite comparable to those already discussed for adsorption from organic solvents on silica. Therefore, we will not go into more detail here. The middle region of $1.5<n_f<2.5$ is the most important, since it covers a large range of materials. The calculations show that for $\theta_i=70°$ in this region $A_s>0.015$ m^2/mg, which is quite satisfactory for performing reflectometry. Also, the small difference between the dashed and full curve for $\theta_i=70°$ shows that A_s is (almost) independent of Γ, which facilitates quantitative interpretation of experimental data.

For $n_f>2.5$ the situation is more complicated since the reflectivity R_p of the surface decreases strongly. The reason for this is the higher Brewster angle for the solvent/adsorbent interface as n_f increases, and the concomitant decrease of the reflectivity of the film. For example, for $n_f=3.0$ the value of θ_{Br}(water/film) equals 66.0° and R_p(surface) is 0.01 at this

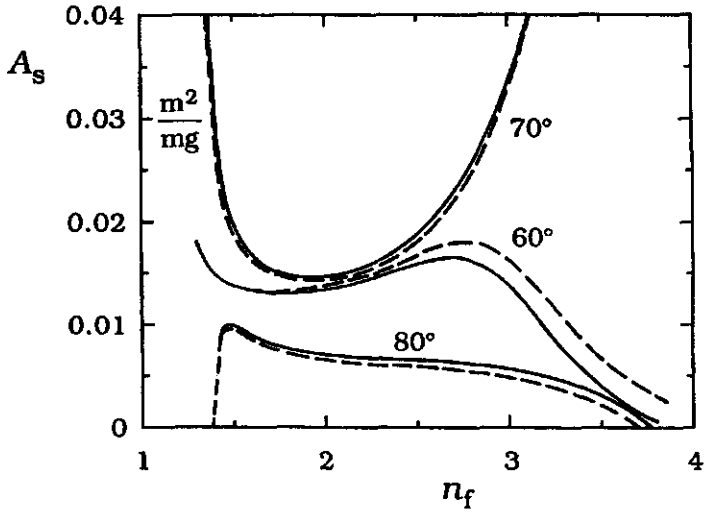

Figure 2.11. Effect of the film refractive index n_f on the sensitivity A_s for adsorption from aqueous solution for three different values of θ_i, as indicated. The full and dashed curves are for block-profiles with Γ=1 and 5 mg/m^2, respectively. They are calculated for a (variable) film thickness, given by $d_f = d_p / 4$. Other parameters as for fig. 2.3.

angle. Coupled with the increase of θ_{Br}(solvent/film) the useful range of θ_i narrows. Qualitatively, the reason for this is that $\theta_i < \theta_{Br}$(solvent/film) is unfavourable for reflectometry since R_p and R_s change in the same direction upon adsorption, as was already pointed out in the discussion of fig. 2.3.a. For θ_i=70° we think that reflectometry is possible for n_f<3; above this value R_p becomes too low. By taking θ_i somewhat higher or lower the range for reflectometry can probably be extended up to $n_f \approx 3.5$.

We conclude that thin films of practically all dielectric materials prepared on silicon wafers can be used for adsorption studies with reflectometry. For films with 1.5<n_f<2.5 in aqueous solution $\theta_i = \theta_{Br}$ is ideal, and the value of A_s does then only weakly depend on n_f.

2.4 Conclusions

In this chapter we performed model calculations in order to investigate the possibilities of reflectometry for adsorption measurements on silicon wafers coated with a thin film of adsorbent.

In our reflectometer the ratio between the reflected intensities of parallel and perpendicular light is defined as the output signal. In many cases a change in this ratio is proportional to the adsorbed amount Γ, irrespective of the concentration profile of the adsorbed layer. The proportionality constant is called the sensitivity factor A_s; its value follows from the

model.

Calculations were made for adsorption from aqueous solution or organic solvents on thin silica films, and for adsorption from aqueous solutions on other types of films. For all systems studied we found that by careful choosing the angle of incidence and the film thickness a sensitivity is obtained of the order of 1-2% change in reflectivity per 1 mg/m^2 adsorbed, which is enough for accurate determination of the adsorbed amount.

For adsorption on silica a film thickness of about 110 ± 20 nm seems to be a good choice in all solvents. The optimal angle of incidence decreases roughly linearly from about 70° for water (n_s=1.333) to about 52° for a solvent with n_s=1.6.

For adsorption from aqueous solution on other thin films an angle of incidence of 70° can be used for a film with $1.5<n_f<2.5$. The value of A_s is only weakly dependent on n_f in this range of n_f. For $n_f>2.5$ the situation is more complicated due to the low reflectivity of the surface, but by choosing carefully the angle of incidence reflectometry should be possible up to $n_f \approx 3.5$.

2.5 References

(1) Azzam, R.M.A.; Bashara, N.M. In " *Ellipsometry and Polarized Light*"; North-Holland: **1977**.

(2) AKZO *Eur. Patent Application No. 88200230.6.*

(3) Heuvelsland, W.J.M.; Oldenzeel, M. *Chemisch Weekblad* **1989**, 307.

(4) Bange, K.; Otterman, C.R.; Anderson, O.; Jeschkowski, U.; Laube, M.; Feile, R. *Thin Solid Films* **1991**, *197*, 279.

(5) Phillips, R.W.; Dodds, J.W. *Appl. Opt.* **1981**, *20*, 40.

(6) Vorotilov, K.A.; Orlova, E.V.; Petrovsky, V.I. *Thin Solid Films* **1992**, *207*, 180.

(7) Yoldas, B.E.; O'Keeffe, T.W. *Appl. Opt.* **1979**, *18*, 3133.

(8) Hansen, W.N. *J. Optical Soc. Am.* **1968**, *58*, 380.

(9) Born, M.; Wolf, E. In " *Principles of Optics*"; Pergamon Press: Oxford, **1975**, 5th ed.

(10) "*Polymer Handbook*"; Brandrup, J.; Immergut, E.H., Eds.; John Wiley and Sons: New York, **1989**, 3rd ed.; p. VII-409.

(11) Elgersma, A.V.; Zsom, R.J.L.; Lyklema, J.; Norde, W. *Colloids Surf.* **1992**, *65*, 17.

3 KINETICS OF POLYMER ADSORPTION IN STAGNATION POINT FLOW

This chapter is reprinted from Colloids and Surfaces, 51 (1990) 141-158.

The reflectometer described in this chapter is an earlier version with an output signal S defined by eq. 3.6, in contrast with the present definition of S by eq. 2.3. As a consequence, the sections 3.2.3 ("Reflectometry") and 3.2.4 ("Calibration and sensitivity") only pertain to the reflectometer described in this chapter. (Corresponding information for the present reflectometer is all found in section 2.2.). The output signal was redefined in order to obtain simpler detection electronics. The change in the definition of S has no consequences for the interpretation of the experimental results; they may be directly compared to those in the other chapters.

Colloids and Surfaces, 51 (1990) 141–158
Elsevier Science Publishers B.V., Amsterdam

Kinetics of polymer adsorption in stagnation point flow

J.C. Dijt[1], M.A. Cohen Stuart, J.E. Hofman and G.J. Fleer

Laboratory for Physical and Colloid Chemistry, Agricultural University, P.O. Box 8038, 6703 HB Wageningen (The Netherlands)

(Received 3 April 1990; accepted 25 June 1990)

Abstract

The kinetics of adsorption of poly(ethylene oxide) from water onto silica in stagnation point flow are studied using a reflectometric technique.

It is shown that with reflectometry an absolute and continuous determination of the adsorbed mass per unit area can be obtained. For the stagnation point flow, the maximum rate of mass transfer to the surface is theoretically calculated. This rate is compared to the observed adsorption rate and it is concluded that mass transfer is the rate-determining step up to 75% or more saturation, depending on the molecular weight. Plateau adsorbed amounts obtained are in good agreement with those found by others. The molecular weight dependence of the diffusion constant agrees with scaling theory and the plateau adsorbed mass is in accordance with the theory for polymer adsorption from good solvents.

3.1 INTRODUCTION

The rate of adsorption of small molecules is determined mainly by two processes: (i) transport towards the surface by diffusion and/or convection; and (ii) attachment to the interface. Changes in the shape of the molecule may play a role, but they are expected to be very rapid and, therefore, not very important for the kinetics of adsorption. Flexible polymers, on the other hand, have many internal degrees of freedom and, therefore, reconformation processes at the surface are much more likely and deserve attention. Recent experiments [1–3] seem to indicate that at least part of the reconformation occurs on a timescale of seconds or more. These processes might well affect the adsorption kinetics, especially if both are on the same timescale.

One may distinguish three kinetic contributions: transport to the surface, attachment and reconformation. In order to assess the role of each of the three contributions it is necessary to measure the kinetics of adsorption under well-defined hydrodynamic conditions. For such measurements, the mass transfer (convection and diffusion) can be calculated and therefore it becomes possible

[1]To whom correspondence should be addressed.

0166-6622/90/$03.50

to study unambiguously the interfacial processes, i.e., attachment and reconformation.

Most kinetic studies so far have been carried out with some version or other of the depletion method, i.e., by monitoring changes in the concentration of free polymer in a dispersion of small adsorbent particles [4–6]. In our opinion, this method is less suitable for the purpose described above, since the hydrodynamic conditions in a stirred suspension are highly non-uniform and very difficult to specify. Unless due attention is paid to these aspects, it is impossible to decide whether mass transfer from the bulk or interfacial processes are rate determining.

Well-defined hydrodynamics are best obtained in simple geometries, such as with a macroscopically flat surface as the adsorbent. Then a direct method to determine adsorbed amounts is needed. Although various optical techniques have been used for this, in most cases no use was made of well-defined hydrodynamics to control the transport conditions [7–10]. We decided to use reflectometry in order to obtain a continuous measurement of the adsorbed amount and, following the work done on deposition of colloidal particles [11], a stagnation point flow to handle the mass transport towards the surface. The principle is sketched in Fig. 1b. A jet of solution impinges perpendicularly on a surface. A stagnation point forms at the spot where the axis of the impinging jet intersects with the surface. The polymer is deposited rather homogeneously at and around the stagnation point and is detected by means of a polarized laser beam reflected at the stagnation point.

The rate of mass transfer in this kind of stagnation point flow can be calculated in great detail, so that the rate of polymer arriving at the collector (per unit surface area) is known. By varying the experimental conditions (flow velocity, concentration, molecular weight) this rate can be varied over a wide range. Whether or not a molecule will attach may depend on many variables, such as surface coverage, state of preadsorbed molecules, adsorption energy, coulombic interaction, rate of shear at the interface, etc.

The highest deposition rate is of course obtained when the surface is still bare. Each molecule that touches the surface will then attach with a certain probability β that depends perhaps on interactions between molecule and surface,and shear rate. For short range polymer–surface interactions, and low shear rates, one expects $\beta = 1$. This will probably be the case for many neutral-polymer/substrate systems. As a consequence, the initial rate of adsorption in such cases should closely correspond to the maximum rate of mass transfer from the bulk.

As the adsorbed amount increases, it becomes progressively more difficult for molecules to find space for attachment, so that the adsorption rate will first decrease, and eventually become zero at saturation. One might expect that the attachment probability depends not only on the number of preadsorbed molecules, but also on their conformation, so that β is not only a function of the

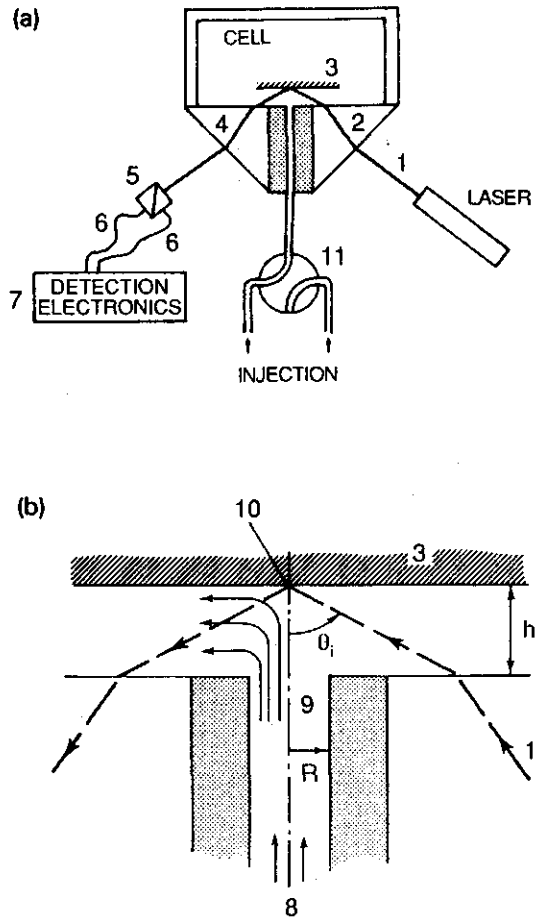

Fig. 1. (a) Schematic diagram of the experimental setup. (b) Detail of the stagnation point region. For explanation of the numbers, see text. For all experiments: $h = 1.1$ mm, $R = 0.65$ mm and $\theta_i = 70°$.

adsorbed amount, but also of time. Our measurements should be able to check that hypothesis.

3.2 EXPERIMENTAL METHODS

We first describe the experimental setup, followed by a brief outline of the underlying theory: mass transfer in stagnation point flow, and determination of the adsorbed amount by reflectometry. Our final goal is to compare the calculated mass transfer rate towards the surface with the observed adsorption rate.

3.2.1 *Experimental setup*

The experimental setup is schematically shown in Fig. 1a and b. A polarized He/Ne laser beam (1) enters the cell through a 45° glass prism (2). The laser beam reflects on the adsorbing surface, for which we use a strip cut from an oxidized silicon wafer (3). The angle of incidence θ_i is equal to the Brewster angle for the silicon–water interface. The laser beam leaves the cell through a second 45° glass prism (4). For the detection we applied a method originally developed at AKZO Research Laboratories, Arnhem [12]. The beam is split into its parallel and perpendicular components (with respect to the plane of incidence) by means of a polarizing beamsplitter cube (5). Both components are detected by photodiodes (6) and the resulting signals are electronically combined (7) to give the output signal S, defined in Eqn (6) below.

A stagnation point flow (Fig. 1b) is obtained by pumping solvent or polymer solution (8) into the cell through a cylindrical channel (9) of radius R, drilled in a piece of solid PMMA which is mounted between the two prisms. The distance between the end of the cylindrical channel and the adsorbing surface is h. Flow lines are indicated schematically in the left hand side of Fig. 1b. The channel is perpendicular to the silicon wafer, and the intersection of its symmetry axis with the surface is called the stagnation point (10). This point is positioned such that it coincides with the reflection spot of the laser beam. With the help of a two-way valve (11) it is possible to switch from solvent to polymer solution or vice versa. Two automatic burettes (Methrom) were used as pumps.

3.2.2 *Stagnation point flow*

The hydrodynamics and deposition of colloidal particles in stagnation point flow are extensively discussed by Dabros and Van de Ven [13]. Here, we will only be concerned with their final equations describing the diffusive/convective mass transport and with simplifications that can be made when polymer molecules are used instead of colloidal particles.

Because of the relatively small size and good hydrodynamic permeability of polymer coils, hydrodynamic interactions between surface and polymer can be neglected. This implies that the polymer moves with the undisturbed fluid velocity.

The significance of convection effects relative to diffusion in the mass transport to the surface is characterized by the Péclet number Pe, which for spherical particles of radius a and diffusion coefficient D is defined as:

$$Pe=\frac{2a^3\nu\bar{\alpha}Re}{R^3D} \tag{1}$$

In this equation, ν is the kinematic viscosity, $\bar{\alpha}$ a dimensionless streaming

intensity parameter which will be discussed below, R the radius of the inlet tube, and Re the Reynolds number, given by

$$Re=\frac{UR}{\nu} \tag{2}$$

where U is the mean fluid velocity at the end of the inlet tube. For most polymers Pe is very small, typically of the order of 10^{-8}.

Dabros and Van de Ven expressed the flux J of particles (coils) towards the surface (per unit area) as:

$$J=\frac{Dc}{a}Sh \tag{3}$$

where c is the polymer concentration and the Sherwood number Sh a complicated function of the Péclet number. In the limit of very small Pe, this function takes the simple form

$$Sh=0.616Pe^{1/3} \tag{4}$$

Combining Equations (1), (3) and (4) an expression for J can be easily derived

$$J=0.776\nu^{1/3}R^{-1}D^{2/3}(\bar{\alpha}Re)^{1/3}c \tag{5}$$

This equation is valid if the perfect sink boundary condition applies, i.e., $c=0$ at the surface. Also, any specific interactions between particles and surface are assumed to be negligible.

The parameter $\bar{\alpha}$ reflects the intensity of the flow near the surface, which depends on the Reynolds number, the radial distance to the stagnation point and on the geometry of the cell, characterized by the ratio h/R, where h is the distance between collector surface and inlet tube and R the radius of the tube (Fig. 1b). Dabros and Van de Ven [13] have calculated $\bar{\alpha}$ numerically for various cases and Fig. 2 taken from their paper gives $\bar{\alpha}$ in the stagnation point as a function of Re for two values of h/R. In our cell, $h/R=1.7$. It is seen that $\bar{\alpha}$ is roughly proportional to Re.

Due to the finite thickness of the laser beam the adsorption is measured not only in the stagnation point itself, but also in a (small) area around it. Strictly speaking, in the calculation of J we should therefore correct for the radial dependence of $\bar{\alpha}$ and the intensity profile of the laser beam. For example at a radial distance $\frac{1}{2}R$ from the stagnation point the light intensity is half of its maximum value and the flux J at this distance is found to be 7% lower than in the stagnation point itself. In our further calculations of J we will neglect the radial dependence of $\bar{\alpha}$ and we will use its value in the stagnation point. We thereby overestimate J somewhat.

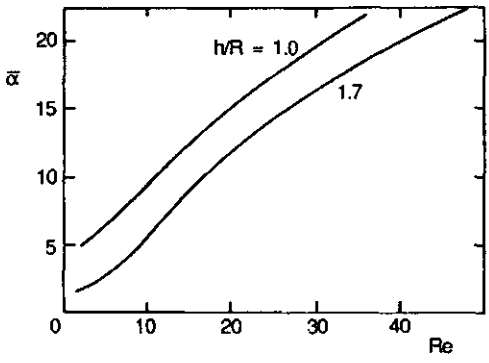

Fig. 2. Dependence of the dimensionless flow intensity parameter $\bar{\alpha}$ on the Reynolds number Re, for two values of h/R. The figure is taken from Ref. [13].

3.2.3 *Reflectometry*

The technique of reflectometry makes use of the fact that the adsorption of polymer causes a change in the reflectivity of the substrate. In our setup the reflected intensities I_s and I_p for the perpendicular and parallel polarization components, respectively, are continuously measured and electronically combined to give the output signal S defined as:

$$S=\frac{I_s-I_p}{I_s+I_p} \tag{6}$$

Note that S is normalized by the total light intensity and is therefore not affected by fluctuations in the laser light intensity. Using light reflection theory we show below that S is proportional to the adsorbed amount Γ (mass/unit area), where the proportionality constant depends on the oxide layer thickness d_{ox}. A method to determine d_{ox} and conditions for optimal sensitivity will be discussed.

The reflected intensities I_s and I_d can be expressed in the incoming light intensities I_s° and I_p°, the reflectivities R_s and R_p of the substrate, and loss factors f_s and f_p, respectively:

$$I_s=f_sR_sI_s^\circ \tag{7a}$$

$$I_p=f_pR_pI_p^\circ \tag{7b}$$

The factors f_s and f_p account for losses at the reflecting surfaces of prisms and beamsplitter. Combining Eqns (6) and (7) we find:

$$S=\frac{R_s-fR_p}{R_s+fR_p} \tag{8}$$

where $f\equiv f_pI_p^\circ/f_sI_s^\circ$. The factor f depends on I_s° and I_p°, i.e., on the (adjustable)

polarization angle of the laser. For a given value of this angle, f is a constant which can be determined by a suitable calibration method, described below.

3.2.4 *Calibration and sensitivity*

The sensitivity of the reflectometer, $dS/d\Gamma$, depends on $dR_s/d\Gamma$, $dR_p/d\Gamma$ and on the constant f. In order to obtain $dR_s/d\Gamma$ and $dR_p/d\Gamma$ we have numerically calculated the reflectivity of an Si/SiO_2 surface with adsorbed polymer using Hansen's method based on the exact matrix formalism of Abeles [14]. To this end the system is optically modelled as a set of flat, parallel layers of uniform refractive index. A schematic drawing and values for the optical constants are shown in Fig. 3.

Due to interference in the oxide layer, R_s and R_p change with oxide thickness d_{ox}. In order to determine d_{ox} for each wafer we used a calibration wafer for which d_{ox} had been ellipsometrically measured. The reflectivities R_s and R_p of the calibration wafer (without adsorbed polymer) were calculated from the known value of d_{ox}. Together with a measurement of S of this wafer this gives the constant f [Eqn (8)]. Then, for a wafer of unknown d_{ox} the value of S is measured and the ratio R_s/R_p for this wafer is calculated. Finally, this R_s/R_p value is converted back into the corresponding d_{ox} value by means of the numerical calculation.

For the calculation of $dS/d\Gamma$ some model for the adsorbed polymer has to be adopted. In a real polymer layer the polymer concentration will usually be some continuously decreasing function of the distance from the surface. As a first approximation we replace this function by a single step function. Below we show by means of calculations that the actual concentration profile has no significant influence on $dS/d\Gamma$. If the single, homogeneous layer has thickness d_p and refractive index n_p, the adsorbed amount Γ is given by:

$$\Gamma = \frac{(n_p - n_s)d_p}{dn/dc} \tag{9}$$

where n_s is the refractive index of the solution and dn/dc the refractive index

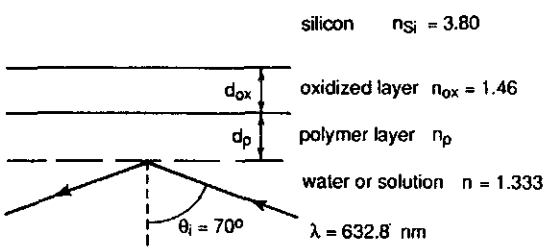

Fig. 3. Schematic illustration of the layer model used for light reflection. The values used for the optical constants of silicon, oxidized layer, polymer layer and water are indicated.

increment of the polymer–solvent system. For PEO in water, $dn/dc=0.136$ ($cm^3\ g^{-1}$) [15].

In order to see if there is any effect of the polymer conformation (i.e., of the segment density) on S, we calculated S for an adsorbed layer with a fixed Γ of 0.5 mg m^{-2}, but with n_p and d_p varying according to Eqn (9). The results for $S(d_p)$ are presented in Fig. 4. Some representative values of n_p are indicated along the curve. The value of S is practically the same for all reasonable densities of the polymer layer. It is concluded that the signal S measures Γ, irrespective of the polymer conformation in the adsorbed layer.

The relation between S and Γ was checked by varying d_p while keeping n_p constant. Results are given in Fig. 5. It is clearly seen that S is nearly proportional to Γ up to adsorbed amounts of 4.0 mg m^{-2}.

The sensitivity $dS/d\Gamma$ also depends on f. In order to find the optimal value

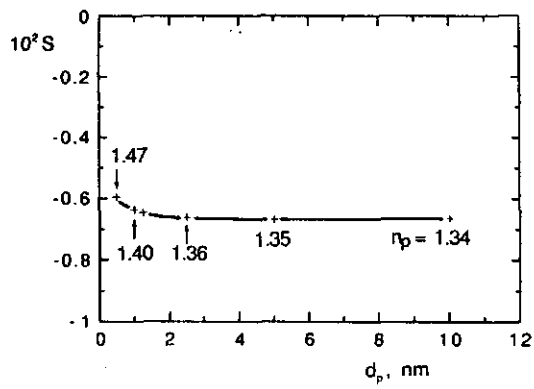

Fig. 4. Calculated effect of the polymer layer thickness d_p on S, at a fixed adsorbed amount Γ of 0.5 mg m^{-2}. For the oxide layer thickness, $d_{ox}=90$ nm was taken.

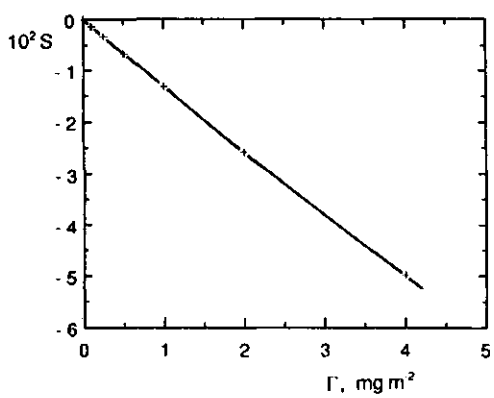

Fig. 5. Calculated effect of the adsorbed amount Γ on the output signal S. Parameters: $d_{ox}=90$ nm, $n_p=1.3608$.

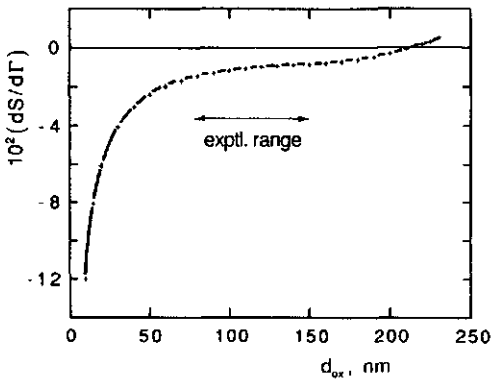

Fig. 6. Effect of oxide layer thickness on the sensitivity for polymer adsorption. Calculations were made for $\Gamma=0.5$ mg m^{-2}, $d_p=2.5$ nm and $n_p=1.3608$.

of f we first differentiate Eqn (8) with respect to Γ, where we should keep in mind that $df/d\Gamma=0$:

$$\left(\frac{dS}{d\Gamma}\right)=2f\left\{\frac{R_s}{R_p}+f\right\}^{-2}\left\{\frac{1}{R_p}\left(\frac{dR_s}{d\Gamma}\right)-\frac{R_s}{R_p}\left(\frac{dR_p}{d\Gamma}\right)\right\} \tag{10}$$

By taking the derivative of $dS/d\Gamma$ with respect to f, one easily shows that the sensitivity $dS/d\Gamma$ has a maximum for $f=R_s/R_p$. According to Eqn (8), $S=0$ at this value of f. Therefore, we set $S=0$ at the beginning of each experiment by adjusting the polarization angle of the incident beam.

The dependence of $dS/d\Gamma$ on the oxide layer thickness d_{ox} is shown in Fig. 6. We used wafers with d_{ox} varying between 80–150 nm. Although for very thin layers ($d_{ox}<20$ nm) the sensitivity is much higher, it was found during experiments that for such thin layers the signal to noise ratio became less. For very thin layers R_p/R_s is almost zero and hence the incident laser beam is nearly completely polarized in the parallel direction. The strong rise in the noise level is possibly caused by small fluctuations in the polarization angle of the laser, which under these conditions strongly affect f and thus S. Also, the light intensity on the detectors is then very low so that electronic noise may become important.

3.2.5 *Alignment*

For an accurate comparison of the adsorption rate and the mass transfer rate J the laser beam should be reflected precisely in the stagnation point of the flow, and the distance h (Fig. 1b) should be known. Vertical adjustment of the laser beam could easily be done by visual inspection of the reflection of the laser beam against the inlet tube. For horizontal alignment this was not possible. According to theory, J is maximal in the stagnation point. We therefore

adjusted the position of the cell parallel to the wafer until the observed adsorption rate was at a maximum. The distance h was measured by selecting from a set of spacers of known thickness, the one that just fitted between the collector surface and the cell wall. We estimate this gives an error in h of $\pm 5\%$.

3.3 MATERIALS

3.3.1 *Oxidized silicon wafers*

Highly pure silicon wafers of the Czochralsky-type were purchased from Wacker Chemitronic GmbH (F.R.G.). For all experiments wafers from the same batch were used. We oxidized the wafers in an oven in ambient air at 1000 °C for 1 h. Between wafers we found oxide layer thicknesses ranging between 80–150 nm. The very broad range is possibly due to differences in the atmospheric moisture content at which the various wafers were oxidized. After oxidation, the wafers were cut into strips 1.5 cm wide. Gloves were used to avoid contamination of the surfaces.

The strips were cleaned by red glowing in a natural gas flame for about 5 s. After cleaning they were immediately used for an experiment. With this cleaning technique each strip could be recycled at least 10 times, with very good reproducibility of the adsorption experiments and without any detectable growth of the oxide layer.

Wet cleaning methods, like treatment with chromic or nitric acid at room temperature or with mixtures of hot H_2O_2/NH_3 followed by H_2O_2/HCl [16] were far less successful. Results were less reproducible when strips were used repeatedly. SEM photographs of substrates that had been in contact with chromic acid for several days showed a severe roughening of the surface.

Monodisperse poly(ethylene oxide), PEO (for $M < 20\,000$ the manufacturer denotes these polymers as 'polyethylene glycol', PEG), was purchased from Polymer Laboratories and was used without further purification. Their

TABLE 1

Polymer samples

M_w (g mol^{-1})	M_w/M_n	δ_h, (nm)[a]
7 100	1.03	2.1
23 000	1.08	3.7
56 300	1.05	5.7
105 000	1.06	7.8
246 000	1.09	11.8
400 000	1.08	15.0
847 000	1.16	21.6

[a]The values of δ_h were taken from Ref. [22].

molecular weights and degree of polydispersity are given in Table 1. The polymer was dissolved in deionized water at room temperature and solutions were stored for at most 3 days, at 4 °C before use. Solutions were deaerated under vacuum for 30 s and during experiments they were kept in a water bath at a constant temperature of approximately 23.0 °C.

3.4 RESULTS AND DISCUSSION

.4.1 *Typical result for adsorption of PEO*

An example of a typical experiment is given in Fig. 7. Before $t=0$ only solvent is pumped into the cell. It usually takes several minutes after the start of the solvent flow before S is constant. This is due to the high sensitivity of the measurement for temperature gradients, which affect the refractive index of the solvent. As soon as the baseline was sufficiently stable the flow was switched at $t=0$ from pure solvent to polymer solution, thus starting adsorption. Initially, Γ increases linearly with time. In this part of the curve the adsorption rate $d\Gamma/dt$ is not reduced by previously deposited polymer and we denote $d\Gamma/dt$ in this region as the initial adsorption rate $(d\Gamma/dt)_{t=0}$. Below, we will compare $(d\Gamma/dt)_{t=0}$ with the maximum mass transfer rate J as given by Eqn (5). Close to saturation there is a decrease in the adsorption rate. We shall analyse this regime at the end of this section. When the adsorption had stopped increasing we switched back to pure solvent. No desorption takes place. This is probably due to the strong attachment of a long polymer chain to the surface with a large number of segments. For molecular weights below 10^5 g mol^{-1} some desorption is observed, the extent of which increases with decreasing M and reaches 15% for $M=7100$ g mol^{-1}. This trend reflects the decrease in adsorption energy per chain when M decreases.

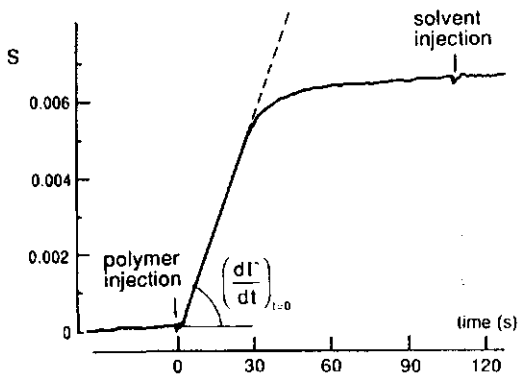

Fig. 7. Example of a typical experiment for PEO adsorption. $M=400\,000$ g mol^{-1}, $c=10$ mg dm^{-3}, $Re=12.2$ and $dS/d\Gamma=-8.9\cdot10^{-3}$ m^2 mg^{-1}.

3.4.2 *Initial adsorption rate*

PEO adsorbs on silica with high affinity [17]. During the attachment of a neutral, flexible PEO molecule we do not expect any energy barriers and, therefore, it is reasonable to test the assumption that J equals $(d\Gamma/dt)_{t=0}$. In order to do this we measured $(d\Gamma/dt)_{t=0}$ for a broad range of mass transfer conditions, varying the polymer concentration c, the Reynolds number Re and the molecular weight M.

Figure 8 is a double-logarithmic plot of $(d\Gamma/dt)_{t=0}$ as a function of c, for three values of Re. As predicted by theory $(d\Gamma/dt)_{t=0}$ increases with an increase in c or Re. For all curves the slope is nearly unity. Hence, $(d\Gamma/dt)_{t=0}$ is indeed proportional to c, in good agreement with Eqn (5).

In Fig. 9 the dependence of $(d\Gamma/dt)_{t=0}$ (points) and J (solid curves) on Re,

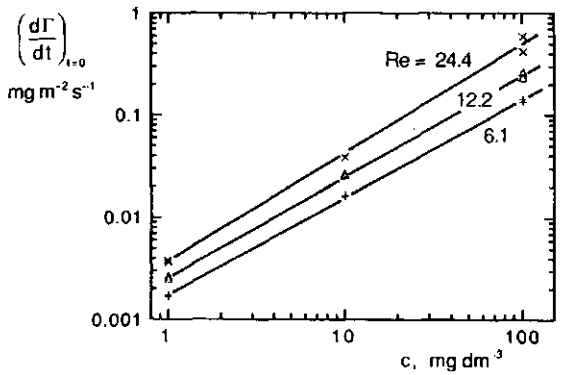

Fig. 8. Effect of PEO concentration on initial adsorption rate for three values of the Reynolds number Re. $M = 246\,000$ g mol^{-1}.

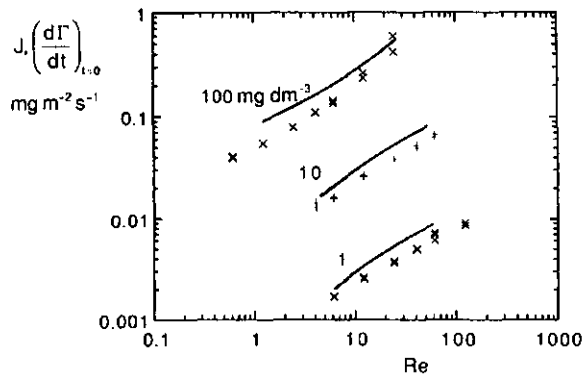

Fig. 9. Effect of the Reynolds number on the initial adsorption rate at three concentrations. The symbols represent the experimentally observed $(d\Gamma/dt)_{t=0}$, the solid curves give J as calculated according to Eqn (5). $M = 246\,000$ g mol^{-1}.

for three concentration levels, is shown on a double-logarithmic scale. The theoretical curves for J are calculated using values of $\bar{\alpha}$ from Fig. 2. We used the value for the diffusion constant obtained by Sauer and Yu [18] by dynamic light scattering. In Fig. 2 we see that for our flow cell $\bar{\alpha}$ is roughly proportional to Re and, hence, according to Eqn (5) we expect that the curves for J in Fig. 9 have a slope of about 2/3. This is indeed the case. In Fig. 9 the value of J from Eqn (5) is somewhat higher than $(d\Gamma/dt)_{t=0}$ for the entire range of Re studied, but theoretical and experimental curves run nearly parallel and we conclude that the agreement is quite good.

Note that over the experimental range $(d\Gamma/dt)_{t=0}$ changes by more than a factor of 200. In the fastest experiment $(d\Gamma/dt)_{t=0}$ is approximately 0.4 mg $m^{-2}\,s^{-1}$, meaning that full saturation is reached in less than 2 s.

The absolute difference between J and $(d\Gamma/dt)_{t=0}$ may be a real effect in the sense that the polymer capture probability of the surface β is smaller than 1, or it may be explained by errors in experiment and/or calculations. From a theoretical point of view we see no reason to suppose that $\beta<1$. PEO is a neutral polymer and so charge repulsion is absent. Hydrodynamic drag is unlikely because the polymer molecules are too small and permeable for that. Slipping along the surface is also not to be expected, because Re is low throughout and no divergence between theory and experiment is seen in the dependence on Re.

Experimental errors, on the other hand, can be numerous. It was already noted in the discussion of $\bar{\alpha}$ that we slightly but systematically overestimate J, due to the size of the reflection spot of the laser beam. Also, when the actual alignment of the reflection spot is (somewhat) off-centre, J is again overestimated. An error in the distance h affects $\bar{\alpha}$, and thus J, especially at low Re (see Fig. 2). Other possible sources of errors are the optical constants needed for the calculation of the sensitivity, and the diffusion constant taken from Ref. [18], used for the calculation of J. All these effects could easily explain

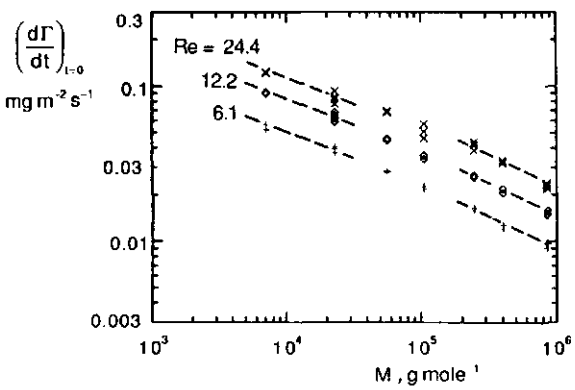

Fig. 10. Effect of molecular weight on the initial adsorption rate for three values of the Reynolds number. Polymer concentration 10 mg dm^{-3}. The dashed lines are drawn with a slope according to the scaling theory (see text).

the difference between J and $(d\Gamma/dt)_{t=0}$, and there is no reason to expect that $\beta \neq 1$. Therefore we conclude that the initial adsorption rate is completely determined by the maximal mass transfer rate from the bulk solution.

Figure 10 is a double-logarithmic plot of the effect of the molecular weight M on $(d\Gamma/dt)_{t=0}$, for three values of Re. The decrease in $(d\Gamma/dt)_{t=0}$ with increasing M is caused by the lowering of the diffusion constant with increasing chain length. Polymer solution theory states that the diffusion constant of a polymer scales as $D \sim M^{-\gamma}$. For low M, where Gaussian statistics apply, γ equals 0.5. For high M, γ equals 0.588, the value for coils swollen by excluded volume. The transition between these regimes is rather broad for D, about 2 decades in M [19]. In Fig. 10, a gradual increase in γ from $M = 10^4$ to 10^6 g mol^{-1} is indeed seen. Dashed lines are drawn according to the theoretical limits of γ. It is seen that the experiments are entirely consistent with scaling theory. This result corroborates our conclusion that $(d\Gamma/dt)_{t=0}$ is entirely controlled by the bulk mass transfer rate.

3.4.3 *Maximum adsorbed amount*

Figure 11 shows the effect of M on the adsorbed amount of Γ_{max} in the plateau region for a bulk polymer concentration of 10 mg dm^{-3}. For the highest molecular weights ($M = 400\,000$ and $847\,000$ g mol^{-1}) the maximum adsorption was not entirely reached during the experiments. Here we used for Γ_{max} the value at the end of the experiment. We found no influence of the flow rate on Γ_{max} and therefore values of Γ_{max} for $Re = 6$, 12 and 24 are plotted together in one figure. For $M = 246\,000$ g mol^{-1} we measured Γ_{max} for concentrations ranging between 1 and 100 mg dm^{-3}. No effect of c on Γ_{max} was observed. It is concluded that the values of Γ_{max} for $c = 10$ mg dm^{-3}, given in Fig. 11, are well within the plateau region of the adsorption isotherm. The theory of polymer

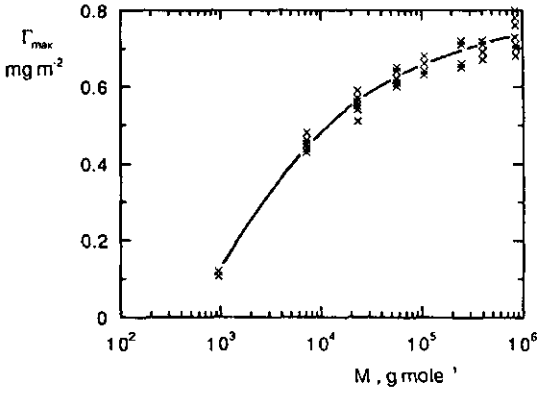

Fig. 11. Effect of molecular weight on the maximum adsorption. For all experiments $c = 10$ mg dm^{-3}. The strips used were cut from the same wafer. $Re = 6.1$, 12.2 or 24.4.

adsorption from good solvents predicts that Γ_{max} increases rather strongly with growth of the chain length for low M, whereas for high M the dependence becomes less [20, 21]. Water is a good solvent for PEO and the shape of the curve in Fig. 11 is in good agreement with theory, at least qualitatively.

From batch adsorption experiments with colloidal silica particles Killmann et al. [17] found maximum adsorbed amounts of 0.653 mg m^{-2} for $M=86\,000$ g mol^{-1} to 0.68 mg m^{-2} for $M=996\,000$ g mol^{-1}. Van der Beek and Cohen Stuart [22] reported for the same type of experiment a value of $\Gamma_{max}=0.61$ mg m^{-2} for $M=570\,000$ g mol^{-1}. With a strip cut from a different wafer we found Γ_{max} 20% lower than given in Fig. 11. All these results are in reasonable agreement, taking into account that the state of the silica surface may vary somewhat and have an effect on adsorption. Our method gives roughly the same adsorbed amounts as those reported in the literature, which corroborates our calibration procedure.

3.4.4 *Adsorption rate near saturation*

From the analysis of $(d\Gamma/dt)_{t=0}$ we have concluded that $\beta=1$ on a bare surface. Of course, at saturation, $\beta=0$. In between one expects a more or less gradual decrease in β. To examine the effect of M on β we plotted Γ as a function of $t(d\Gamma/dt)_{t=0}$ (Fig. 12). In such a plot, all initial slopes are reduced to unity. We see that for low M there is a remarkably sharp transition between $\beta=1$ and 0. For longer coils the linear region extends to higher adsorbed amounts and the transition to $\beta=0$ is more gradual. In all cases, bulk mass transfer is rate limiting up to at least 75% coverage.

Possibly comparable results are those published by Pefferkorn et al. [5]; they are rather similar. These authors studied the adsorption rate of poly(acrylamide) on modified glass beads in a stirred vessel. The inlet rate of

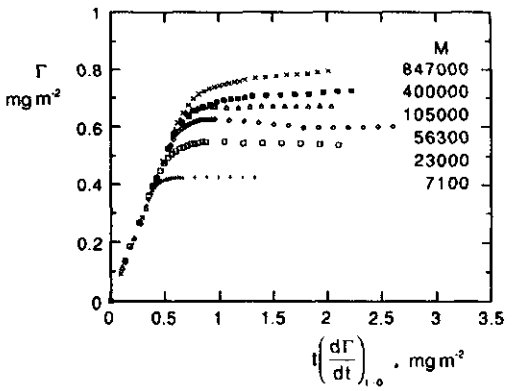

Fig. 12. Comparison of the adsorption rate near saturation for different molecular weights. Polymer concentration 10 mg dm^{-3}, $Re=12.2$.

polymer in the vessel was constant. A linear increase of Γ with time was found up to 50–80% of saturation, depending on pH and temperature. It is likely that in this region the mass transfer (in this case the inlet of polymer in the vessel) was also rate limiting.

At present we only have a tentative explanation for the observed behaviour in Fig. 12. A gradual decrease in β can be an effect of either polydispersity in the sample or of the previously adsorbed polymer. With highly polydisperse samples we found that the adsorption rate decreases continuously from the beginning of the experiment onwards, i.e., the adsorption curves had a strongly rounded shape. It is conceivable that the gradual decrease in β in Fig. 12 is a result of some polydispersity, although we used samples with a narrow distribution of molecular weights. However, a clear increase with M in the size of the transition region in β is observed, whereas the degree of polydispersity remains more or less the same (Table 1). We conclude that polydispersity cannot entirely explain Fig. 12.

The effect of the preadsorbed molecules can perhaps be understood as follows. Imagine that it takes a free polymer molecule some time, τ, before it has found enough free sites on the surface to be adsorbed by several segments. The time τ will depend on the number of free sites present, which is a function of Γ, and on the possibility of the molecule to form loops between distant free sites, which depends on the molecular weight M. As long as τ is sufficiently small, the maximum rate of mass transfer given by Eqn (5) will be rate limiting. Apparently, for our experiments this condition is fulfilled up to 75% or more of saturation. The fact that even up to high coverage the surface is easily accessible for new molecules becomes understandable when we study the effect of coverage on the thickness of the adsorbed layer. The hydrodynamic layer thickness δ_H of saturated layers of PEO on silica as measured by Van der Beek and Cohen Stuart [22] is given in Table 1. The hydrodynamic layer thickness is mainly determined by the very diluted region of tails and loops. It is seen that for low M, and thus low Γ, δ_H is very small. Here, δ_H is determined by loops and tails of a few segments long. Under these conditions free molecules can come very close to the surface without being disturbed by the adsorbed layer. For higher M, δ_H rises rapidly. The surface then becomes less accessible for free molecules and β decreases. If this reasoning holds, we expect for poor solvents in which much thicker adsorption layers are formed a broader transition region for β.

The longer linear region of the adsorption curve for high M can be explained by the more efficient use of distant sites by longer chains. We may speculate that less flexible chains have more difficulty in forming loops, causing a smaller linear region in the adsorption curve. This has to be checked in subsequent work.

3.5 CONCLUSIONS

With reflectometry the adsorption of polymer on a flat silica surface can be continuously measured and an absolute determination of the adsorbed mass per unit area is obtained. A stagnation point flow is a good method for a quantitative control of the mass transfer rate of polymer from the bulk solution to the surface. In the adsorption kinetics it is therefore possible to distinguish between mass transfer from the solution and surface related processes.

For monodisperse PEO the mass transfer is rate limiting up to 75% or more of saturation, depending on molecular weight. For long chains the transition from a completely mass transfer controlled adsorption rate to a saturated layer starts at a higher adsorbed amount and is more gradual than for short chains.

The adsorbed amount in a saturated layer is in good agreement with that reported in the literature [17,22]. The dependence of the maximum adsorption on the molecular weight follows the theory of polymer adsorption from good solvents [20,21].

From the molecular weight dependence of the mass transfer rate of PEO the diffusion constant was found to follow the scaling theory [19], i.e., a gradual transition in the diffusion constant from the region of Gaussian statistics to that of excluded volume is observed.

3.6 ACKNOWLEDGEMENTS

We gratefully acknowledge Dr R. Zsom, AKZO laboratories, Arnhem, for making available essential information about AKZO's patented reflectometer [12].

We also thank Dr J. Marra, Philips laboratories, Eindhoven, for the ellipsometric determination of oxide layer thicknesses.

3.7 REFERENCES

1 M.A. Cohen Stuart and H. Tamai, Macromolecules, 21 (1988) 1863.
2 M.A. Cohen Stuart and H. Tamai, Langmuir, 4 (1988) 1184.
3 E.G.M. Pelssers, M.A. Cohen Stuart and G.J. Fleer, J. Chem. Soc. Faraday Trans., 86 (1990) 1355.
4 E. Pefferkorn, A. Carroy and R. Varoqui, Macromolecules, 18 (1985) 2252.
5 E. Pefferkorn, A. Carroy and R. Varoqui, J. Polym. Sci. Polym. Phys. Ed., 23 (1985) 1997.
6 C. Orgeret-Ravanat, P. Gramain, P. Déjardin and A. Schmitt, Colloids Surfaces, 33 (1988) 109.
7 B.K. Lok, Y.-L. Cheng and C.R. Robertson, J. Colloid Interface Sci., 91 (1983) 104.
8 B.K. Lok, Y.-L. Cheng and C.R. Robertson, J. Colloid Interface Sci., 91 (1983) 87.
9 J.F. Tassin, R.L. Siemens, W.T. Tang, G. Hadziioannou, J.D. Swalen and B.A. Smith, J. Phys. Chem., 93 (1989) 2106.
10 Y. Zhang, Y. Levy and J.C. Loulergue, Surf. Sci., 184 (1987) 214.

11 Z. Adamczyk, T. Dabros, J. Czarnecki and T.G.M. Van de Ven, Adv. Colloid Interface Sci., 19 (1983) 183.
12 Eur. Patent Application No 88200230.6.
13 T. Dabros and T.G.M. Van de Ven, Colloid Polym. Sci., 261 (1983) 694.
14 W.N. Hansen, J. Optical Soc. Am., 58 (1968) 380.
15 P. Molyneux, Water-Soluble Synthetic Polymers: Properties and Behavior, Vol. 1, CRC Press, Boca Raton, FL, 1983, p. 39.
16 W. Kern and D.A. Puotinen, RCA Rev., June (1970) 187.
17 E. Killmann, H. Maier, P. Kaniut and N. Gütling, Colloids Surfaces, 15 (1985) 261.
18 B.B. Sauer and H. Yu, Macromolecules, 22 (1989) 786.
19 G. Weill and J. des Cloizeaux, J. Phys. Paris, 40 (1979) 99.
20 J.M.H.M. Scheutjens and G.J. Fleer, J. Phys. Chem., 83 (1979) 1619.
21 M.A. Cohen Stuart, T. Cosgrove and B. Vincent, Adv. Colloid Interface Sci., 24 (1986) 143.
22 G.P. Van der Beek and M.A. Cohen Stuart, J. Phys. Paris, 49 (1988) 1449.

4. KINETICS OF POLYMER ADSORPTION AND DESORPTION IN CAPILLARY FLOW

4.1 Introduction

The rate of adsorption of polymers is mainly determined by two processes: (i) transport of the polymer by convection and/or diffusion from the solution to the surface, and (ii) attachment to the interface. The second step may consist of the reconformation of the chain towards an adsorbed state, and of the formation of entanglements between different molecules. When the adsorption takes place from a well-defined flow, the rate of transport can be calculated and thereby separated from the attachment step. In a previous paper[1] we showed in this way that for the adsorption of poly(ethylene oxide) (PEO) from water onto silica the transport is rate limiting until close to saturation. A similar behaviour was found in time-dependent ATR-IR measurements by Van der Beek et al.[2] with polytetrahydrofuran, by Johnson and Granick[3] with poly(methyl methacrylate), and by Frantz et al.[4] with polystyrene. For all these polymers it was found that 70-100% of the plateau value of the isotherm adsorbs already in the first few minutes after introduction of the polymer solution in the cell. It is likely that this rapid initial adsorption was mass transfer limited, although not always a quantitative analysis was made. The mass transfer limitation seems to be a general feature for uncharged homopolymers.

However, it is quite possible that in adsorbed layers processes occur that are not revealed by merely following the adsorbed amount. We therefore decided to study a different property of interfacial layers, namely the hydrodynamic thickness δ_h. Generally, we expect that the hydrodynamic thickness is a rather sensitive quantity to the conformation of adsorbed molecules. For instance, in equilibrated adsorbed layers of long chains the non-adsorbed ends of the molecules ('tails') protrude far into the solution, determining almost completely the hydrodynamic thickness[5]. However, these tails contribute only slightly to the adsorbed amount. We therefore expect that the hydrodynamic thickness can be used as a probe of the tails, whereas the adsorbed amount cannot be used as such. A claim that δ_h can indeed be used to monitor reconformations was made earlier by Cohen Stuart and Tamai[6,7]. They concluded from streaming potential measurements on the adsorption of poly(ethylene oxide) and poly(vinyl pyrrolidone) on glass that a thickness relaxation of the adsorbed layer

could be observed following a short, pulsewise injection of polymer in the capillary.

Another reason for monitoring the adsorption process by means of the hydrodynamic layer thickness is the high sensitivity of δ_h to the adsorbed amount of high molecular weight polymers at saturation. It may be interesting to study changes in such layers, for instance those due to desorption. The amounts of long chains desorbed into solvent are expected to be very low, due to the high adsorption energy per chain. Therefore desorption of long chains is very difficult to study via the adsorbed amount, but we expect much larger changes in the hydrodynamic thickness. Experimental information on desorption is only available for low molecular weights of PEO (<100 kg/mole)[1]. By reflectometry we observed that in about 10 minutes only a small amount (up to 10%) desorbs when a flow of pure solvent is applied. When a polymer solution is injected again, re-adsorption till the original saturated level occurs. No quantitative analysis was possible, but the reversibility of the adsorption suggests that no barrier to desorption is present. This leads us to the interesting question whether the desorption rate, just as the adsorption rate, is mainly determined by mass transfer between the bulk solution and the interfacial region.

A suitable method to obtain the hydrodynamic thickness under well-defined hydrodynamic conditions is the measurement of streaming potentials in glass capillaries. Cohen Stuart and Tamai[6,7] showed that by this method the adsorption of uncharged polymers can be studied as a function of time. By using a suitable injection system one can switch quickly between a flow of polymer solution or of pure solvent.

For a correct analysis of our data it is necessary to know how the adsorbed amount changes under the hydrodynamic conditions of the experiments. Therefore, we will first carefully consider the mass transfer in a capillary, both for adsorption and desorption conditions.

4.2 Local equilibrium concept

Both for adsorption and desorption the steady-state rate of mass transfer in a capillary is given by the equation of Lévêque[8]. The flux J of polymer is a function of the mean fluid velocity v_m, of the diffusion constant D of the polymer, and of the concentration difference $c_b - c_s$, where c_b and c_s are the polymer concentrations in the bulk solution and in the subsurface region, respectively:

$$J = k(c_b - c_s) \tag{4.1.a}$$

where the transport coefficient k is given by

$$k = 0.855\left(\frac{D^2 v_m}{Rz}\right)^{1/3} \tag{4.1.b}$$

In this equation , R is the radius of the capillary, and z the lateral distance downstream from the capillary entrance. Both c_b and c_s are assumed to be independent of z. For adsorption we have $c_b > c_s$ and $J>0$, whereas in desorption experiments (where $c_b = 0$) we must have $J<0$.

At a fixed flow rate the flux of polymer is only determined by the concentration difference $c_b - c_s$ between bulk solution and surface. The bulk solution concentration c_b is either maintained at a constant level (adsorption), or is zero (desorption in pure solvent). The problem is to find a reasonable expression for c_s.

From reflectometry on the adsorption of PEO we know that the adsorption rate is mass transfer limited till close to saturation[1]. This mass transfer limitation implies that the attachment to the interface is faster than the arrival of new molecules. This, in turn, leads us to the assumption that the adsorbed layer and its immediate surroundings are continuously in a local equilibrium. Then the adsorption isotherm $\Gamma(c_s)$ applies near the surface, where c_s is the local equilibrium concentration of non-adsorbed molecules. These free molecules can take part in diffusion and convection, and therefore this local equilibrium concentration should also be used in eq. 4.1.

In the case of local equilibrium the difference between the kinetics of adsorption and that of desorption can be qualitatively explained using an adsorption isotherm (fig. 4.1). According to eq. 4.1 the mass transfer rate is proportional to $c_b - c_s$. For an adsorption experiment c_b is the concentration of the flowing polymer solution, which may be chosen arbitrarily, e.g., at the value indicated by the vertical dashed line in figure 1. The concentration c_s is, at each Γ, given by the adsorption isotherm. Now the mass transfer rate for adsorption is proportional to the (horizontal) distance from c_b to a point on the isotherm. According to the isotherm, the (sub)surface concentration is very small indeed until close to saturation, making the concentration difference between bulk and surface and, hence, the mass transport constant. Then, also the adsorption rate is constant till close to saturation.

For desorption the same reasoning leads to totally different kinetics.

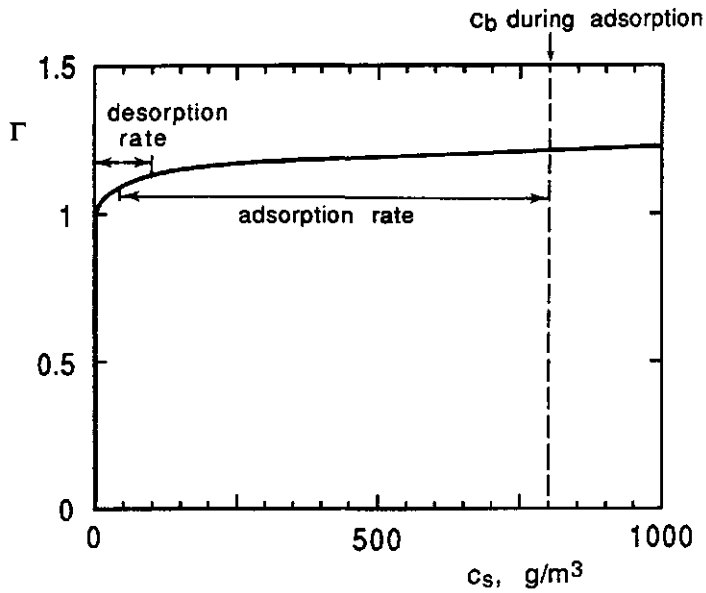

Figure 4.1 Illustration of adsorption and desorption rates using the local equilibrium concept. The full curve is an equilibrium adsorption isotherm $\Gamma(c_s)$. The ad- and desorption rates are proportional to $c_b - c_s$, where c_b is the bulk solution concentration. For adsorption c_b has a constant (non-zero) value, and the rate is proportional to the lower horizontal bar. For desorption c_b = 0 and the rate is represented by the upper bar. In this example, the adsorption isotherm was calculated with the theory of Scheutjens and Fleer. The adsorbed amount Γ is given in equivalent monolayers. The bulk volume fraction as given by the theoretical model was converted to ppm (g/m^3) using a specific volume of 10^{-3} m^3/kg. Number of statistical segments r=100, solvency parameter χ=0.5, segmental adsorption energy χ_s=1.0, cubic lattice with λ_0=2/3.

Now c_b is zero and the concentration difference $c_b - c_s$ is completely determined by the surface concentration. The desorption rate is given by the distance from an isotherm point to the ordinate axis (see fig. 4.1). According to the isotherm c_s, and thus the rate of mass transport decreases sharply upon a minute desorption. Thus the desorption rate decreases continuously during desorption. For a high affinity adsorption isotherm of a polymer the concentration c_s drops over decades for only a small decrease in the adsorbed amount. If Γ has decreased so far that the 'vertical section' of the isotherm is entered, the desorption rate is hardly measurable because c_s is then extremely small. As will be derived below, for a typical polymer adsorption isotherm the adsorbed amount decreases linearly with log$t$.

These typical differences between adsorption and desorption kinetics depend highly on the shape of the adsorption isotherm. If the isotherm

would be linear over the concentration range $0 < c_s < c_b$, adsorption and desorption rates would follow the same pattern. However, it is well known that polymer adsorption isotherms show a pronounced high-affinity character, making desorption much slower than adsorption. The isotherm given in fig. 4.1 was calculated with the theory of Scheutjens and Fleer[9,10] but any other high-affinity isotherm would lead to the same general conclusions. In the following sections we will consider the kinetics of adsorption and desorption quantitatively in order to be able to make a quantitative comparison between experiment and theory. For the case of desorption we shall make an explicit assumption about the isotherm shape.

4.2.1 Adsorption

In the analysis of the adsorption experiments we want to answer the question whether the observed change in the streaming potential can be interpreted in a way similar to the results found by reflectometry in stagnation point flow[1]. There we found that the adsorption rate was mass transfer limited, except for the final approach to saturation, which was much slower.

The analysis of the streaming potential experiments involves three steps. First, the adsorbed amount $\Gamma(t,z)$ as a function of time t and position z in the capillary is calculated, using the mass transfer equation in combination with reflectometric data on the adsorption of PEO. Then the adsorbed amount $\Gamma(t,z)$ is converted into the hydrodynamic layer thickness $\delta_h(t,z)$ by means of an experimental relation between the two quantities. Finally, from the local hydrodynamic layer thickness $\delta_h(t,z)$ the expected streaming potential $V_s(t)$ is calculated.

Before we calculate $\Gamma(t,z)$ with the transport equation, we first examine the adsorption kinetics of PEO from a stagnation point flow as found by reflectometry[1]. In this type of experiment the flow of polymer solution hits the surface perpendicularly. A typical example is shown in fig. 4.2. From these experiments we concluded that the initial adsorption rate equals the maximum mass transfer rate, i.e. c_s equals zero initially. Only close to saturation $d\Gamma/dt$ starts to decrease. In order to incorporate the approach to saturation in the transport equation we define an adsorption probability β as:

$$\beta = \frac{d\Gamma/dt}{(d\Gamma/dt)_0} \tag{4.2}$$

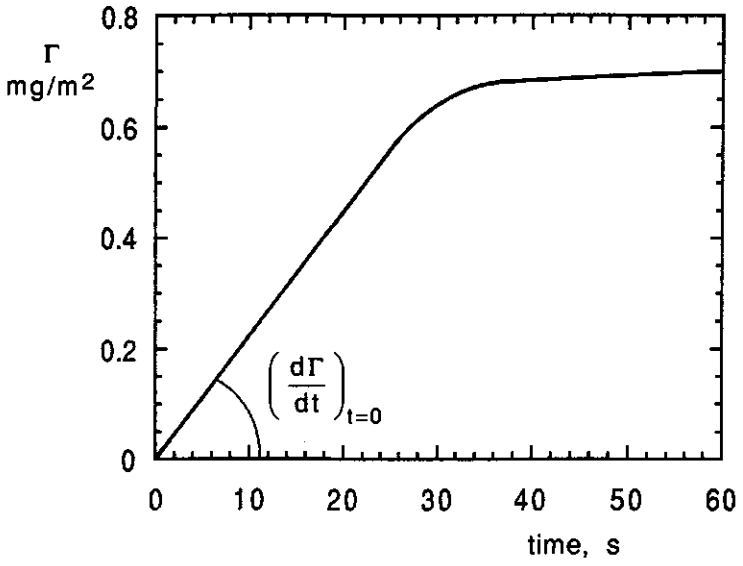

Figure 4.2 Adsorption kinetics of PEO from water, using stagnation point flow towards an oxidised silicon wafer. M = 105 kg/mole, c_b = 10 (g/m^3), Reynolds number Re = 6.1.

Clearly, in the initial, linear regime $\beta = 1$, and at saturation $\beta = 0$. In the transition region we found that, at least qualitatively, β only depends on Γ, and not on mass transport conditions. From the reflectometry experiment we can now determine $\beta(\Gamma)$ and we can use this in combination with eq. 4.1 to calculate $d\Gamma/dt$ in the capillary:

$$\frac{d\Gamma(t,z)}{dt} = J_0(z)\beta(\Gamma) \tag{4.3}$$

where $J_0(z)$ is the flux J of polymer at $c_s = 0$ and position z in the capillary. From this $\Gamma(t,z)$ is obtained by integration:

$$\Gamma(t,z) = \int_{t=0}^{t} J_0(z)\,\beta(\Gamma)\,dt \tag{4.4}$$

where the injection of polymer solution in the capillary starts at t=0 (i.e., $\Gamma(0,z) = 0$).

The next step, the conversion of $\Gamma(t,z)$ into $\delta_h(t,z)$ will be done using static, equilibrium data of Γ and δ_h at saturation. The experimental results needed to establish the relation between Γ and δ_h will be given in section 4.4, and therefore at the moment we simply assume that

$$\delta_h(t,z) = f(\Gamma(t,z)) \tag{4.5}$$

where f is a monotonously increasing function of Γ, which can be

determined experimentally.

We now want to find from $\delta_h(t,z)$ the streaming potential $V_s(t)$ between the two ends of the capillary. For a surface homogeneously covered with polymer Cohen Stuart et al.[11,12] showed that the streaming potential V_s is related to the hydrodynamic layer thickness δ_h by

$$V_s = V_s^0 e^{-\kappa\delta_h} \tag{4.6}$$

where V_s^0 is the streaming potential of the bare capillary and κ^{-1} is the Debye screening length. This equation is valid as long as (i) $\delta_h < \kappa^{-1}$, (ii) the polymer is uncharged, and (iii) the adsorbed layer is homogeneous. However, during the adsorption the coverage in the capillary is not homogeneous, but it depends on z as is seen from eq. 4.1. Therefore eq. 4.6 cannot be used directly to calculate $V_s(t)$. In order to overcome this restriction, we will assume that eq. 4.6 can be applied to small sections of the capillary for which the adsorbed layer can be considered to be homogeneous. The streaming potential of the whole capillary is obtained as the sum of the contributions of the individual sections. Equation 4.6 applied to a small section of the capillary turns into

$$dV_s = e^{-\kappa\delta_h} dV_s^0 \tag{4.7}$$

dV_s and dV_s^0 are the contributions to the streaming potential due to a length dz of the section with and without polymer adsorbed, respectively. In a bare capillary this contribution is the same everywhere, and therefore dV_s^0 is proportional to V_s^0 and the length dz of the section

$$dV_s^0 = V_s^0 \frac{dz}{L} \tag{4.8}$$

where L is the length of the capillary. Finally, the streaming potential $V_s(t)$ of a capillary inhomogeneously covered with polymer is obtained by combining eqs 4.7 and 4.8, and by integrating over the length of the capillary

$$V_s(t) = \frac{V_s^0}{L} \int_0^L e^{-\kappa\delta_h(t,z)} dz \tag{4.9}$$

With eqs. 4.1-5, in combination with 4.9 we can now calculate $V_s(t)$ as it should be expected on the basis of the adsorption kinetics as found by reflectometry. These latter kinetics were mass transfer limited, except for the final approach to saturation. The calculated time dependence $V_s(t)$ can be compared directly to experimental results.

4.2.2 Desorption

In order to describe the desorption of polymer in a flow of pure solvent we will derive in this section a desorption equation which is based on the mass transfer equation in combination with the local equilibrium concept.

When solvent is injected into a capillary with an adsorbed polymer layer the mass transfer will take place from the surface region (concentration c_s) to the bulk solution, where $c_b = 0$. We assume that continuously a local equilibrium exists between the adsorbed layer and the solution directly adjacent to it, as is discussed above. In this case, according to eq. 4.1, the desorption rate can be written as:

$$\frac{d\Gamma}{dt} = -k c_s(\Gamma) \tag{4.10}$$

where $c_s(\Gamma)$ is the inverse of the adsorption isotherm $\Gamma(c_s)$. In order to get an impression of the shape of the adsorption isotherm we performed model calculations with the theory of Scheutjens and Fleer. In fig. 4.3 adsorption isotherms of homopolymers of 100 and 1000 statistical segments for good ($\chi = 0$) and θ-solvents ($\chi = 1/2$) are shown. The concentrations of interest are those below $c < 100$ g/m^3. It is seen that for all cases the slope $p = d\Gamma / d\log c$ is nearly constant over several decades of c, its value being

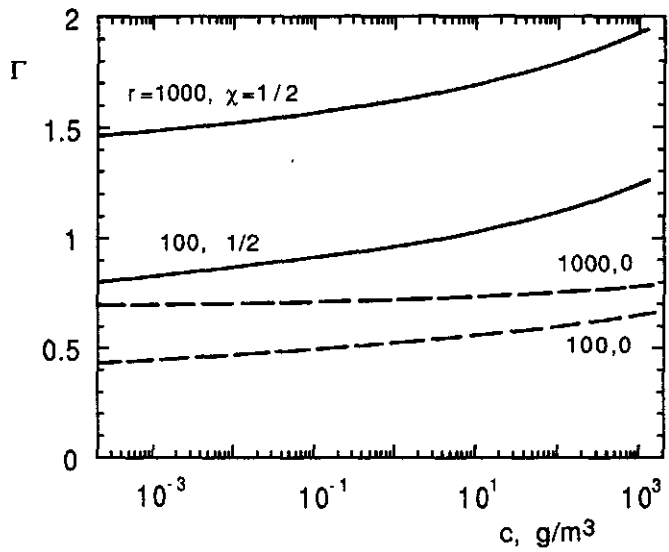

Figure 4.3 Theoretical adsorption isotherms $\Gamma(\log c)$ for homopolymers, showing that the slope $d\Gamma/d\log c$ is constant over several decades of c. The isotherms are calculated with the Scheutjens-Fleer theory, using the same parameters as in fig. 4.1, except for the chain length r and the solvency parameter χ (indicated).

of the order of a few percent per decade. As long as the slope p is constant, we can describe the adsorption isotherm equation as $\Gamma - \Gamma_0 = p\log(c_s / c_s^0)$, where Γ_0 and c_s^0 refer to some reference point of the isotherm (for example, the point $\Gamma(c_b)$ in fig. 4.1). Equivalently,

$$c_s = c_s^0\, 10^{(\Gamma-\Gamma_0)/p} \tag{4.11}$$

Taking for c_s^0 and Γ_0 the values at the start of the solvent injection (at $t=0$) we obtain a simple differential equation for $\Gamma(t)$ by substitution of eq. 4.11 into eq. 4.10. Integrating this from $t=0, \Gamma=\Gamma_0$ to t, Γ we find:

$$\Gamma = \Gamma_0 - p\log(1 + t/\tau) \tag{4.12}$$

where $\tau = 0.43p/kc_s^0$. This equation describes the kinetics of the mass transfer controlled desorption of polymer, and is graphically shown in fig. 4.4, for two values of p/Γ_0. In our experiments τ is typically well below 1 s, and the time-scale well above (≈15 min.), so that Γ is expected to decrease essentially as $p\log(t/\tau)$. A few remarks are in place at this point.

To our knowledge eq. 4.12 is the first theoretical expression for the desorption rate that has ever been derived. It is expected to apply whenever a constant flow of solvent is maintained, i.e., the desorbed material is transported away. Nevertheless, the desorption is for all practical cases far from complete, even after long times, due to the

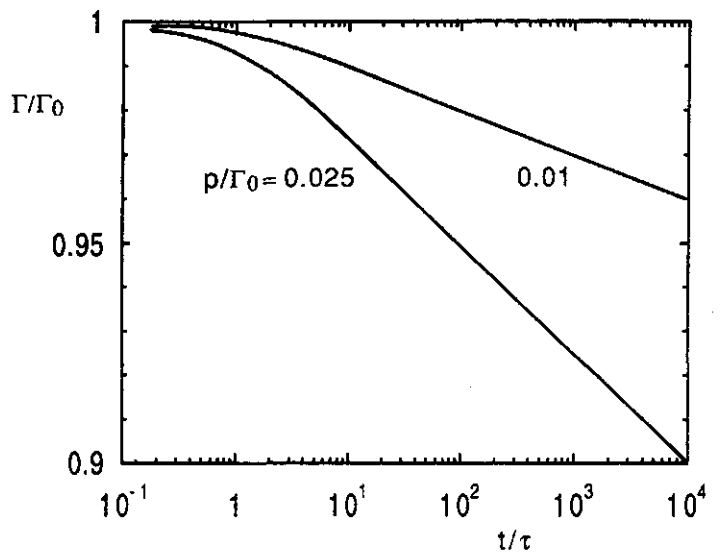

Figure 4.4 Mass-transfer-controlled desorption kinetics according to eq. 4.12 for a polymer with a high affinity adsorption isotherm, for $p/\Gamma_0 = 0.025$ and 0.01. For times $t > 5\tau$ the slope $d\Gamma/d\log t$ equals $-p$.

logarithmic dependence on time. The reason is, obviously, the (extremely) low value of c_s obtained after some desorption has taken place.

For $t>5\tau$ we see that the slope $d\Gamma/d\log t$ equals $-p$, whereas the slope of the adsorption isotherm $d\Gamma/d\log c$ is $+p$. Thus the coupling of the mass transfer with the local equilibrium concept leads to a remarkable congruence between the shape of the desorption curve $\Gamma(\log t)$ and the adsorption isotherm $\Gamma(\log c)$. The equality $d\Gamma/d\log t = -d\Gamma/d\log c$ can be used as an experimental check on the local equilibrium assumption, and, hence, on eq. 4.12. However, a direct check on eq. 4.12 is difficult to carry out since p, and thus also the desorbed amounts for polymers are usually very small. The key idea in our experiments is to follow the hydrodynamic thickness δ_h (rather than Γ) over time, and to compare these data to static values of δ_h at various concentrations. Since $d\Gamma = (d\Gamma/d\delta_h)d\delta_h$, where $d\Gamma/d\delta_h$ is constant as long as points of the same Γ are compared, we can equally well test whether $d\delta_h/d\log t = -d\delta_h/d\log c$.

Finally, we expect that the desorption equation even holds for polymers where the local equilibration takes some time. An effect of equilibration on the desorption can only be observed when its rate is lower than the mass transfer rate. Since the mass transfer rate falls by orders of magnitude upon a small desorption, the same applies to the equilibration rate that can be observed. In fact, it is likely that the mass transfer rate is nearly always lower than the equilibration rate, and thus rate determining.

4.3 Experimental setup and materials

The experimental setup used is schematically drawn in fig. 4.5. A glass capillary (length 20 cm, inner diameter 0.30 mm) is mounted between an inlet valve and a flask at the outlet side. The electronic inlet valve is connected to two bottles containing solvent and polymer solution, respectively. The bottles were under 0.300 atm N_2 with respect to the outlet pressure and through the valve either of the two solutions was injected into the capillary. An electronic pressure control was used, and the pressure drop over connecting tubes and valve was found to be negligible. Hydrostatic pressure differences were at most 1% of the applied N_2 overpressure. Under the conditions of the experiment the Reynolds number was 127 and the entrance length according to the Boussinesq expression[13] approximately 1.3 mm. The flow can thus be considered to be laminar over nearly the whole length of the capillary. The total flux was 1.79 mL/min and the wall shear rate 11300 s^{-1}

The streaming potential was measured with a special high impedance

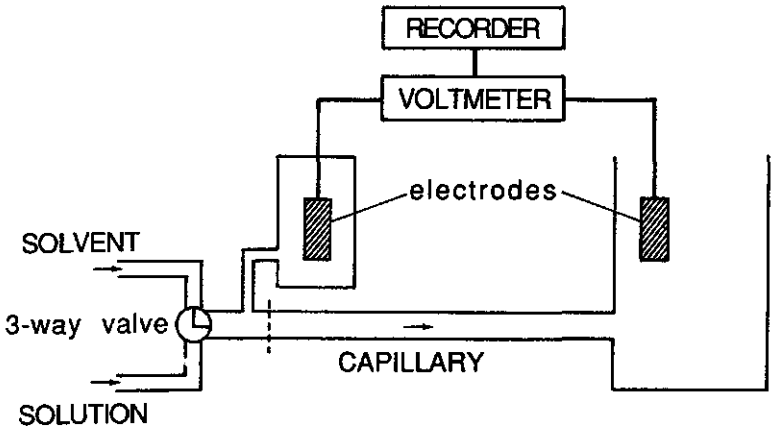

Figure 4.5 Schematic diagram of the experimental setup for measuring the streaming potential in adsorption or desorption kinetics.

voltmeter connected to two reversible Ag/AgCl-electrodes, one of which is in the flask at the outlet side, and the other in a separate vessel connected via a small opening to the space between valve and capillary. The drift in the potential at zero pressure drop was in all cases less than 1% of V_s^0. The dead volume between valve and capillary was estimated from recording the adjustment time of the streaming potential after a switch to a solution of different salt concentration. After 10 s (≈0.3 mL) the adjustment was complete.

As the solvent 1.00 mM NaCl was used throughout. The Debye screening length κ^{-1} for this ionic strength is 10 nm. Monodisperse poly(ethylene oxide) purchased from Polymer Laboratories (see table 4.1) was dissolved without further purification and the solution was stirred for one night at room temperature before use. The glass capillaries were cleaned by immersion for 24 hours in concentrated sulfo-chromic acid, followed by 24 hours in 2 N HNO_3, after which they were stored in the solvent. The streaming potential of the clean capillaries varied between 140 and 155 mV (corresponding to an electrokinetic ζ-potential of 80-90 mV).

Table 4.1 Polymer samples

M_w(kg/mole)	M_w / M_n	M_w(kg/mole)	M_w / M_n
7.1	1.03	105	1.06
23	1.08	400	1.08
56	1.05	847	1.16

The hydrodynamic layer thickness was calculated from the streaming potential using eq. 4.6. The reported thickness is therefore an average over the length of the capillary.

4.4 Results and discussion

In fig. 4.6 we show the result of a typical experiment. First ($t<0$) only solvent is injected and, hence, $\delta_h = 0$. At $t=0$ the valve is switched to polymer solution and we see an increase of δ_h due to the adsorption of polymer. After some time (≈70 s in this example) δ_h has attained a constant level, indicating that the polymer layer is saturated. We indicate the saturated level by δ_h^m. When the valve is switched back to solvent the ensuing decrease in δ_h reflects the desorption of polymer. When polymer is injected again the same level of δ_h^m is reached, but more quickly than the first time. This cycle of desorption and re-adsorption can be repeated many times with reproducible results. The picture sketched for this experiment was found for all molecular weights and all concentrations studied. Only the time scales and layer thicknesses are different. We shall first describe the adsorption kinetics in more detail, followed by an analysis of the (equilibrium) thickness isotherms and, finally, the desorption kinetics.

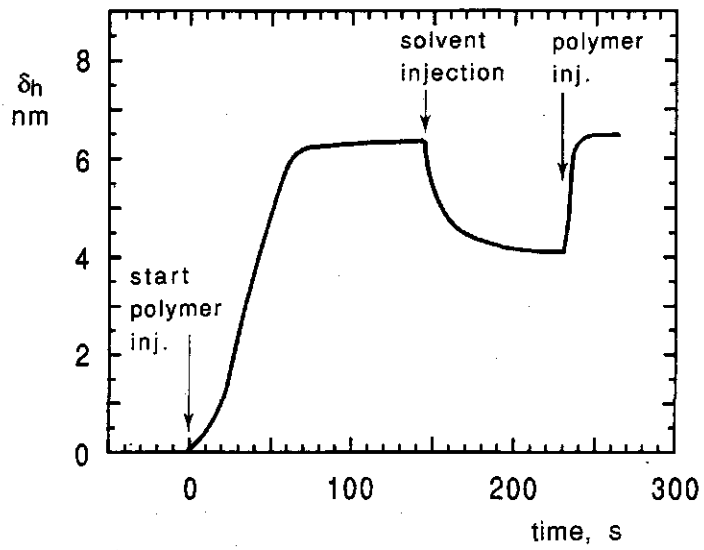

Figure 4.6 Typical example of $\delta_h(t)$ for PEO adsorption in a streaming potential experiment. At $t=0$ the injection of the polymer solution starts, at $t=150$ s this flow was changed into solvent, followed by a switch to the same polymer solution at $t=225$ s. $M=105$ kg/mole, $c=10$ (g/m^3), $Re=127$.

4.4.1 Adsorption kinetics

Before we can apply the adsorption model, we have to establish the relation between δ_h and Γ. Cohen Stuart et al.[14] found from theoretical calculations that for low volume fractions of polymer the relation between δ_h and Γ does not depend on molecular weight. Moreover, their experimental data of PEO adsorbed on polystyrene latex were in good agreement with this result. We therefore decided to measure δ_h and Γ at saturation as a function of molecular weight, using different methods, and to combine these results to a universal curve $\delta_h(\Gamma)$. Adsorbed amounts of PEO on silica in water are available from reflectometry[1] and δ_h^m was measured by the streaming potential technique as described above. All measurements were carried out at the same polymer concentration of 10 g/m^3 and the results are shown in fig. 4.7 as $\delta_h(\Gamma)$. For the two highest molecular weights, δ_h is somewhat greater than κ^{-1}, and therefore the reported values may underestimate the actual δ_h. For comparison, values of δ_h (at a higher concentration) measured by means of dynamic light scattering by Van der Beek and Cohen Stuart[15] are also combined with the reflectometry results and included in fig. 4.7. There is good agreement between values of δ_h found by the latter authors and those obtained from

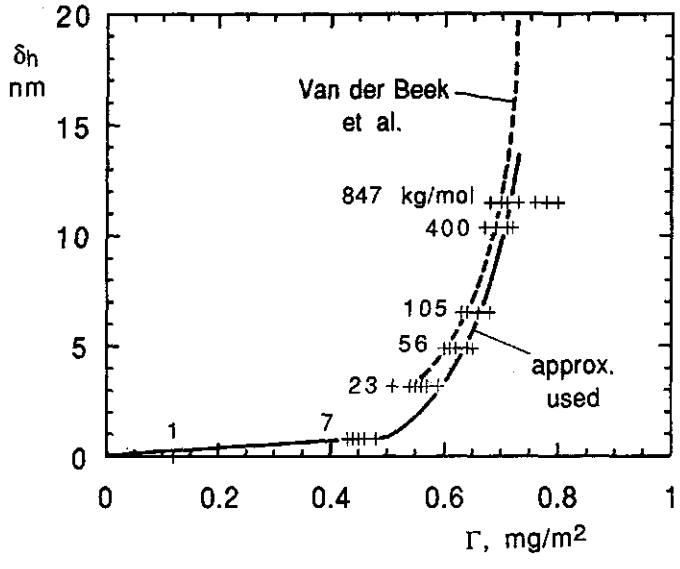

Figure 4.7 Relation between the hydrodynamic layer thickness δ_h and the adsorbed amount Γ for PEO. The + symbols represent the combination of δ_h (from the streaming potential in saturated layers) and Γ (from reflectometry) for different molecular weights (indicated). The dashed curve gives results of Van der Beek and Cohen Stuart[15]. The full curve is the approximation used for further calculations (see text).

the streaming potential, which confirms the idea that both methods measure the same quantity. Also, the shape of the curve $\delta_h(\Gamma)$ is in good agreement with the theoretical predictions of Cohen Stuart et al[14]. We therefore conclude that we can use our present data as an empirical relation $\delta_h(\Gamma)$. In order to have explicit expressions we represented the data by combination of a linear ($\Gamma \leq 0.5$ mg/m^2) and a fourth order polynomial function ($\Gamma > 0.5$ mg/m^2).

Model calculations for the adsorption of PEO of $M = 105$ kg/mole were carried out as described in the theoretical section, using Poiseuilles law to calculate v_m, and a diffusion coefficient of 2.34×10^{-11} m^2/s, which was taken from Sauer and Yu[16]. The result is shown in fig. 4.8. The maximum adsorbed amount is used as a variable parameter to obtain a good fit at saturation. This optimum value was found to be 0.636 mg/m^2. From fig. 4.7 we see that this is well within the experimental range of adsorbed amounts found for this molecular weight. We conclude that there is excellent agreement between model and experiment. We emphasise that the time-scale of the experiment predicted by the model is correct. This

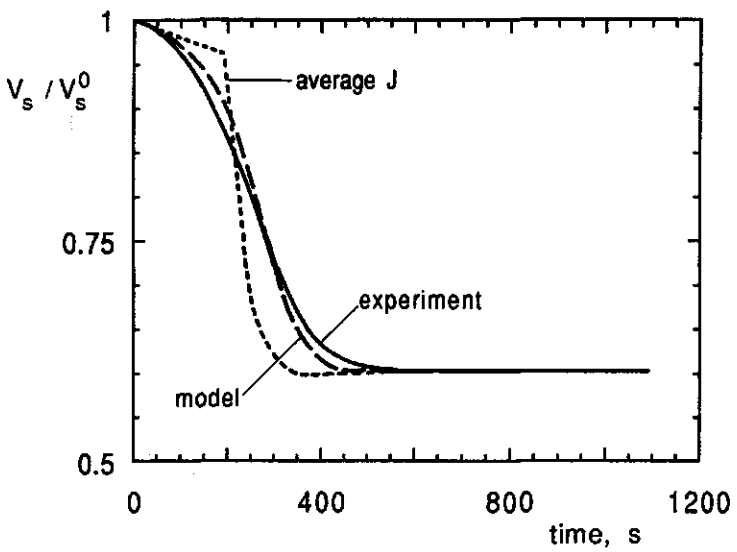

Figure 4.8 Comparison of model calculations and streaming potential experiments for the adsorption of PEO. The full curve represents the experimental V_s / V_s^0 during injection of PEO.(at constant c_b=1 (g/m^3)) The dashed curve was calculated using the Lévêque equation and reflectometric data on the adsorption of PEO, and accounts for the inhomogeneous PEO-deposition. Calculations with an assumed homogeneous mass transfer rate, which equals the average over the length of the capillary, are shown in dotted curve. $M = 105$ kg/mole, and $Re = 127$.

corroborates our conclusion that the adsorption rate of PEO is mass transfer controlled. The precise shape of the dashed curve in fig. 4.8 is explained as follows. The slow increase of δ_h in the first fifty seconds is mainly due to the flat conformation of the polymer at low coverage. The slowing down close to saturation of the decrease of V_s/V_s^0 is largely caused by the rapid decrease of β. We also checked the effect of the variation of the deposition rate along the z-direction. The curve labelled 'average J' is the result of a calculation with a uniform, average mass transfer rate in the z-direction. We see that this leads to a quite different prediction for $V_s(t)$.The sharp kink at $t=200$ s is an artefact resulting from the transition from a linear to a polynomial approximation for $\delta_h(\Gamma)$. We conclude that the deposition rate is non-uniform along the lateral direction. Agreement between theory and experiment is only obtained if this non-uniform deposition is explicitly taken into account.

4.4.2 Thickness isotherms

The measurement of a thickness isotherms $\delta_h^m(\log c)$ and of the desorption kinetics $\delta_h(\log t)$ were done in one experiment for each molecular weight, and proceeded as follows. First, we prepared a saturated polymer layer in equilibrium with a polymer solution of $c=100$ g/m^3, which is the highest concentration studied. Then for a prolonged time pure solvent was injected into the capillary, and the resulting desorption curve recorded. Directly following this, without cleaning the capillary or completely desorbing the polymer, we determined the thickness isotherms $\delta_h^m(\log c)$. In order to do this polymer solutions of decreasing concentration were injected in the capillary, and for each concentration the final thickness δ_h^m was measured. In fig. 4.9.a the resulting thickness isotherms are shown for molecular weights from 7 to 847 kg/mole. For the two highest molecular weights the condition $\kappa\delta_h < 1$ is no longer fulfilled at concentrations above 10 g/m^3, and therefore the reported values of δ_h underestimate the actual ones.

We shall first show that these isotherms really represent equilibrium by giving an illustration of the reversibility of the polymer layer with respect to concentration changes. Figure 4.10 shows a recording of the concentration in the capillary, of the streaming potential and of the pressure when the polymer concentration is switched from $c=2.5$ to 1 g/m^3, with an intermediate period of pure solvent flow. Initially the higher concentration is injected and V_s is stable at 82 mV. When the valve is opened to pure solvent, the polymer concentration in the capillary drops to zero, and the

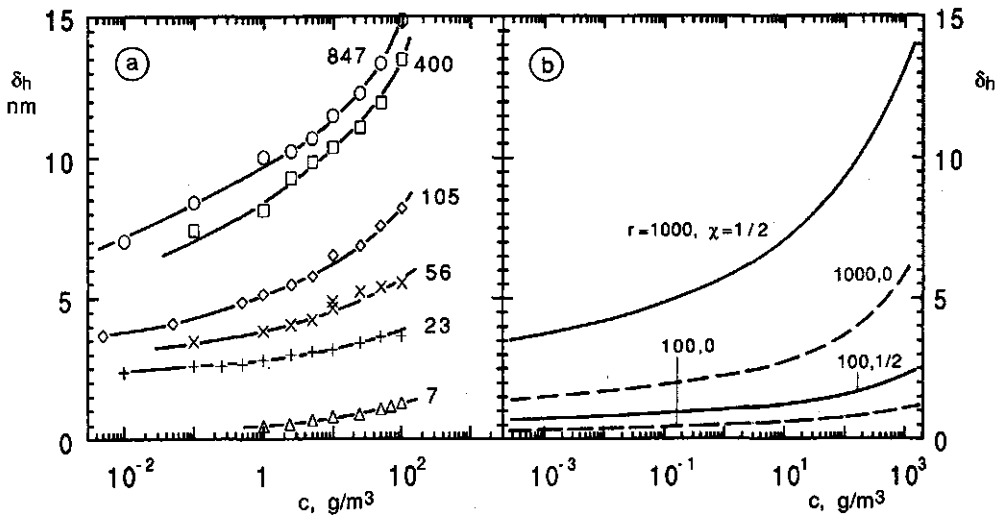

Figure 4.9 Experimental equilibrium thickness isotherms $\delta_h^m(\log c_b)$ for PEO of six different molecular weights (a). Theoretical hydrodynamic layer thickness for the adsorption isotherms of fig. 4.3 (b). Chain length r and solvency parameter χ are indicated. The hydrodynamic constant C_h was assumed to be 1.0, δ_h is given as the number of lattice layers.

streaming potential increases due to desorption. Then the pressure is released for some time in order to replace the polymer solution in the bottle. When the pressure is reapplied and the valve is switched back to the polymer solution of lower concentration, the first 45 s the polymer solution of the higher concentration, which was still in the connecting tubes, passes the capillary. The streaming potential closely follows the changes in the polymer concentration, and stabilises at a level which corresponds to the adsorbed amount for the lower concentration.

It is remarkable to see how fast and completely reversible the streaming potential adjusts itself to the concentration in solution. From this we conclude that the reported values of δ_h^m represent equilibrium. For low concentrations (<0.1 g/m^3) the adjustment time becomes of the order of minutes and (far) more because the rate of mass transfer, which is proportional to the concentration gradient between surface and solution, is very low in that case. In fact, the long time stability of the apparatus determined the lowest concentration (0.005 g/m^3) at which we were able to measure. Finally, it is worth noting that by performing all the measurements in one experiment we can accurately detect thickness differences corresponding to changes in the streaming potential of only about 1%. The results are not complicated by the variations which

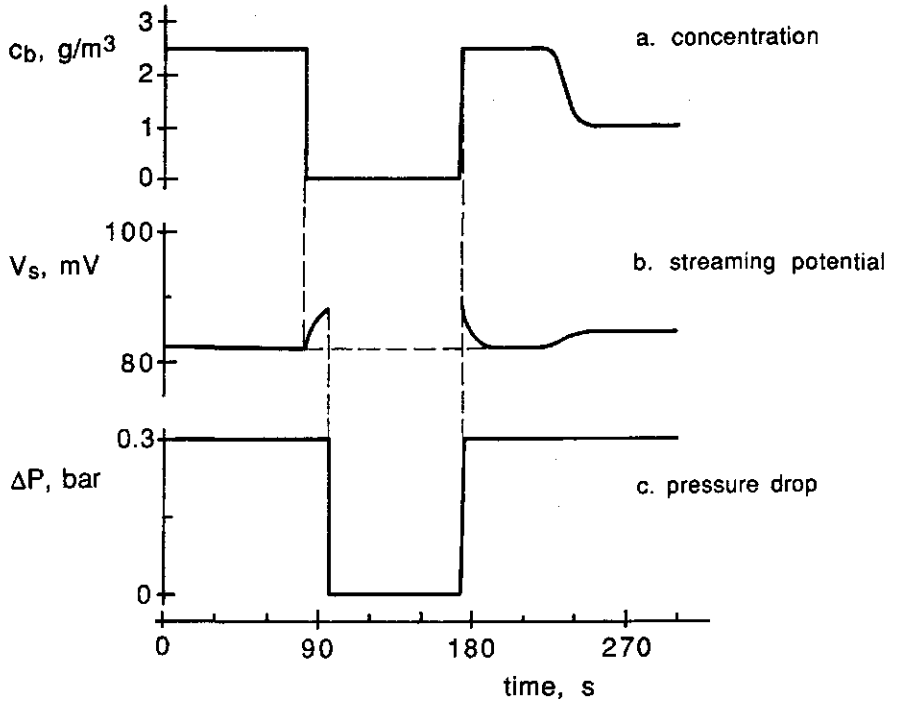

Figure 4.10 Response of the adsorbed layer to changes in the polymer concentration. Initially a polymer solution (c=2.5 (g/m^3)) is flushed through. At t=80 s the valve is switched to pure solvent injection. Between t=96 and 170 s the pressure is released in order to be able to change the polymer solution in the bottle, and directly after this the valve is opened to polymer solution of lower concentration (1 (g/m^3)). The top diagram (a) gives the bulk polymer concentration in the capillary, the middle curve (b) represents the streaming potential, and the lower figure (c) shows the pressure drop over the capillary. M= 105 kg/mole, V_s^0 = 140 mV. For further explanation, see text.

inevitably occur when the capillary is cleaned in between.

For a comparison of the experimental thickness isotherms with their theoretical counterparts, we calculated theoretical δ_h values according to the method described by Cohen Stuart et al[14]. The result for the adsorption isotherms of fig. 4.3 is shown in fig. 4.9.b. Qualitatively, there is good agreement: δ_h, $d\delta_h/d\log c$, and the curvature of the isotherms increase with chain length in both experiment and theory. Note that the chain length dependence of the slope of the thickness isotherms (fig. 4.9) is reversed as compared to the adsorption isotherms (fig. 4.3). This indicates that for long chains δ_h is a much more sensitive quantity to measure than Γ.

In fig. 4.11 the experimental chain length dependence of $d\delta_h/d\log c$ (plusses) is compared to theory (full curves). For the calculations we

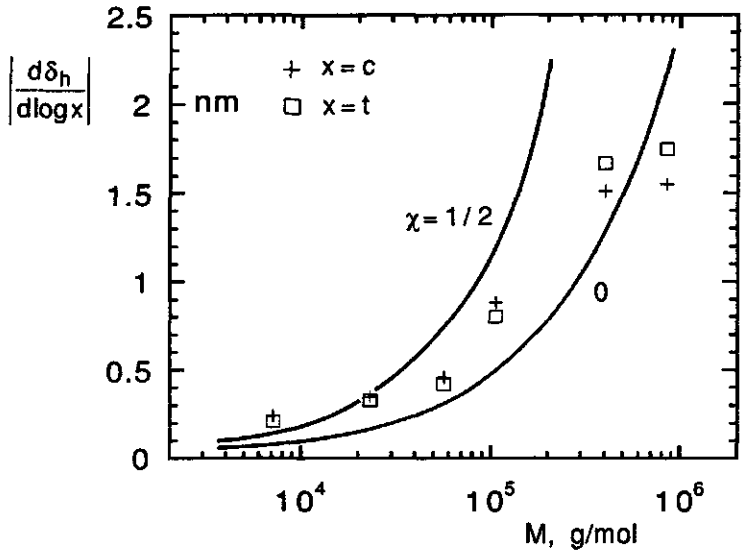

Figure 4.11 Chain length dependence of $d\delta_h/d\log c$ (plusses), $-d\delta_h/d\log t$ (open squares), and $d\delta_h/d\log c$ (full curves) The experimental values of the slopes $d\delta_h/d\log c$ and $-d\delta_h/d\log t$ were calculated from the linear parts of fig. 4.9.a ($c<1$ (g/m^3)) and 4.12.b ($t>50$ s), respectively; the theoretical values of $d\delta_h/d\log c$ were calculated at $c=1$ (g/m^3), using the Scheutjens-Fleer model and assuming 2 EO monomers/statistical chain element. The lattice layer thickness was taken to be 1 nm.

assumed, following Cohen Stuart et al[14], 2 EO monomers /statistical segment and an elementary layer thickness of 1 nm. We see that there is good agreement between theory and experiment. For the two highest molecular weights the condition $\kappa\delta_h < 1$ is no longer fulfilled and therefore the experimental data of $d\delta_h/d\log c$ and $d\delta_h/d\log t$ underestimate the actual values. The results for $d\delta_h/d\log t$ (open squares in fig. 4.11) will be discussed in the next (sub)section.

From a comparison of the theoretical adsorption isotherms of fig. 4.3 with the corresponding thickness isotherms in fig. 4.9.b we see that the concentration range over which the slope $d\Gamma/d\log c$ is constant is wider than for $d\delta_h/d\log c$. Using the equilibrium relation between δ_h and Γ(fig. 4.7) we can convert the isotherms $\delta_h(\log c)$ to $\Gamma(\log c)$. This conversion leads to curves with a constant slope up to higher concentrations, which is in agreement with the theoretical finding. From such a $\Gamma(\log c)$ isotherm we found that for $M=105$ kg/mole the relative slope $d\Gamma/(\Gamma d\log c)$ is 0.024. The theoretical value for $d\Gamma/(\Gamma d\log c)$ for a chain of 1000 segments (≈2 EO monomers/statistical chain element) ranges from 0.015 for $\chi=0.5$ to 0.04 for $\chi=0$. The experimental value is in between these limits, which is

reassuring. For this molecular weight the relative changes in δ_h are about 5 times higher than those in Γ and therefore much easier to detect. For longer chains this factor is still greater. The conversion was also carried out for the other molecular weights. Again the concentration range over which the slope of the isotherm was constant increased, but the slope $d\Gamma/d\log c$ showed no consistent variation with molecular weight. Since $d\Gamma = (d\Gamma/d\delta_h)d\delta_h$, the slope $d\Gamma/d\log c$ is proportional to the slope $d\Gamma/d\delta_h$ of the equilibrium curve $\delta_h(\Gamma)$. Especially for very low and high molecular weights it was not possible to determine $d\Gamma/d\delta_h$ accurately from our results, because the variations in δ_h and Γ, respectively, are very small in those regions (see fig. 4.7). Thus, the conversion of δ_h to Γ prohibits a quantitative comparison of the experimental and theoretical chain length dependence of $d\Gamma/d\log c$. Nevertheless, the qualitative agreement between theory and experiment is excellent.

4.4.3 Desorption kinetics

In fig. 4.12.a the results of the desorption experiments are shown, and, for comparison, the thickness isotherms of fig. 4.9.a are replotted in fig. 12.b. The results apply to desorption starting from a polymer layer in equilibrium with a polymer solution of $c = 100$ g/m^3. At $t = 0$ the injection of pure solvent starts and the layer thickness decreases due to desorption. For the first 10 seconds the desorption curves are dashed because the kinetics in this time interval are affected by the dead volume between valve and capillary so that a steady state is not yet fully established. We see that for $t > 10$ s (full lines) shape and slope of the desorption curves closely correspond to the $\delta_h(\log c)$ isotherms. In fact, figs. 4.9.a and b are virtually mirror images of each other. By connecting points of equal thickness in two corresponding curves it is possible to find at each moment during the desorption the surface concentration c_s according to the thickness isotherm. For instance, for the highest molecular weight c_s is found to be 32, 1.3 and 0.05 g/m^3 at $t = 10$, 100 and 1000 s, respectively. This decrease of c_s with time reflects directly the slower desorption.

Our model for the desorption kinetics predicts that $d\Gamma/d\log t = -d\Gamma/d\log c$. This is only valid under the condition that p ($= d\Gamma/d\log c$) is constant and for times $t > 5\tau$. For $M = 105$ kg/mole we calculated τ as 0.03 s and thus for all t of interest the second condition is fulfilled. With respect to the constancy of the slope p we see in fig. 4.12.b that the curves $\delta_h(\log c)$ are linear up to about 10 g/m^3. As pointed out before, the linear part is even longer after conversion to $\Gamma(\log c)$, and thus also the former

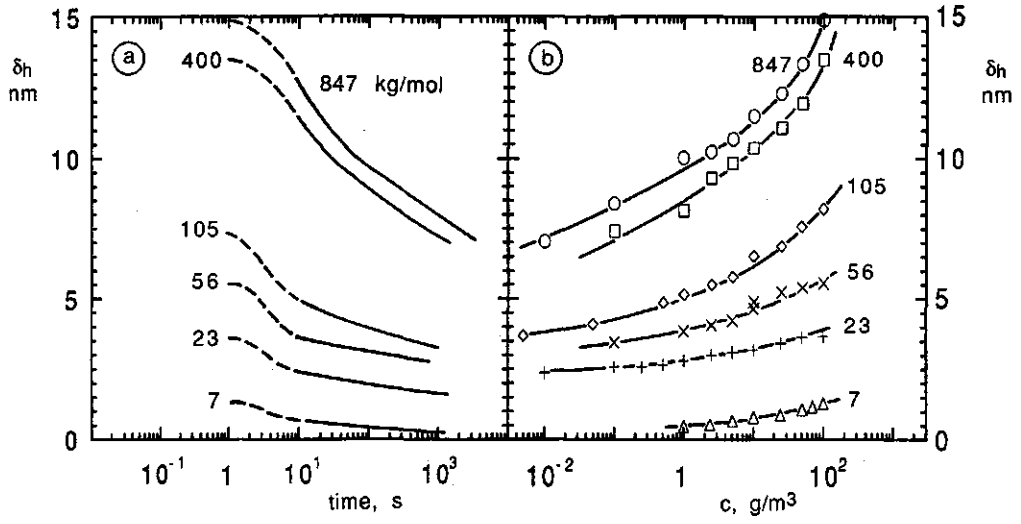

Figure 4.12 Desorption kinetics during injection of solvent (a) and equilibrium thickness isotherms $\delta_h^m(\log c_b)$ of PEO (b). The latter are replotted from fig. 4.9.a. The desorption experiments start at $t=0$ with the injection of pure solvent on a polymer layer initially saturated at $c=100$ (g/m^3). The initial sections ($t<10$ s) are dashed, because the kinetics are still affected by the dead volume between valve and capillary.

condition is met. Consequently, the logarithmic dependence of Γ on c is corroborated. Instead of comparing slopes in terms of Γ we can equally well test whether $d\delta_h/d\log t = -d\delta_h/d\log c$, as pointed out before. In fig. 4.11 we plotted $-d\delta_h/d\log t$ (open squares) and $d\delta_h/d\log c$ (plusses) as a function of chain length. For all molecular weights $-d\delta_h/d\log t$ and $d\delta_h/d\log c$ are nearly equal. This is a strong indication for the correctness of the desorption model.

We also checked whether the absolute value of $d\Gamma/dt$ equals J as predicted by the Lévêque equation. For $M=105$ kg/mole we determined $d\delta_h/dt$ and from this $d\Gamma/dt$ at $t=18$ s. We found 0.6 μg/m^{2}s. Using the value of δ_h at $t=18$ s in the $\delta_h^m(\log c)$ isotherm the equilibrium concentration near the surface is found to be $c_s = 0.35$ g/m^3. The Lévêque equation gives with this c_s $J=0.89$ μg/m^{2}s. We consider this to be in good agreement with the value found for $d\Gamma/dt$, considering the experimental uncertainty that arises from the conversion of $d\delta_h/dt$ to $d\Gamma/dt$ and from reading c_s from a logarithmic concentration scale. We conclude that our model for desorption kinetics is essentially adequate for PEO: the desorption rate is indeed a logarithmic function of time, the slopes $d\Gamma/d\log t$ are quite reasonable (and correspond to the adsorption isotherms), and the desorption process is transport limited. The desorption

is so slow because the (very) low subsurface concentration of polymer allows only a correspondingly low gradient flux.

In two earlier papers Cohen Stuart and Tamai[6,7] attributed the decrease in the layer thickness to a thickness relaxation of adsorbed molecules rather than to desorption. Their main argument against desorption was that the decrease of δ_h continues when the flow is stopped. Using an improved setup we now find that the opposite is true. In fig. 4.13 we compare the increase of V_s upon injection of solvent for two cases: the dashed curve represents continuous injection of solvent, whereas for the full curve the flow is interrupted for about five minutes by the release of the pressure drop over the capillary. It is clearly seen that the increase of V_s stops as long as the flow is absent. This corroborates our present analysis that the decrease is due to desorption. We conclude that the previously claimed thickness relaxation was actually due to desorption of polymer.

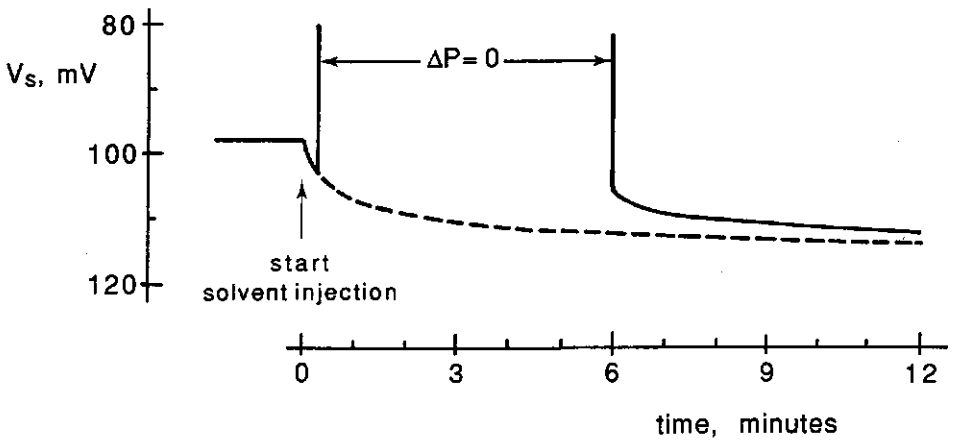

Figure 4.13 Effect of flow on the desorption of polymer. For $t<0$ the polymer layer is saturated at $c=1.0$ (g/m^3), and at $t=0$ the injection of pure solvent starts. The dashed curve represents continuous injection of solvent, whereas the full curve is the result of an experiment, during which the flow of solvent is stopped for some time by release of the pressure drop over the capillary ($\Delta P=0$). Molar mass 105 kg/mole, $V_s^0=159$ mV.

Finally, we want to summarise and discuss the results obtained for the desorption kinetics. We believe that for the first time a quantitative analysis of polymer desorption kinetics has been made and, furthermore, this analysis is also verified by experimental evidence. Using the mass transfer equation and assuming a local equilibrium near the surface, we derived a desorption equation of the form $\Gamma = \Gamma_0 - p\log(t/\tau)$. It is found

that the adsorbed amount decreases linearly with log$t$, and, also, the equilibrium adsorption isotherm Γ(log$c$) and the desorption curve Γ(log$t$) are mirror images: $d\Gamma/d\log t = -d\Gamma/d\log c$. The slope $d\Gamma/(\Gamma d\log c)$ is usually very small for polymers, of the order of a few percent per decade in c. As a result, also the desorbed amount is very small. A sensitive quantity, like the hydrodynamic layer thickness, is needed to observe desorption. From our analysis it has become evident that for a desorption experiment it is essential to remove the desorbed material continuously from the system. By doing this a (small) concentration gradient between surface region and bulk solution is maintained, giving rise to a (correspondingly small) desorption. The adsorbed layer is prevented to establish equilibrium with the bulk solution at an extremely low concentration. Only at the local level (c_s) such an equilibrium should take place. We expect that also for more slowly equilibrating polymers than PEO mass transfer will be rate limiting during desorption, because the mass transfer rate becomes extremely low, and thus rate limiting, after a small amount is desorbed. We therefore presume that eq. 4.12 is a fairly general expression for the desorption of polymers.

4.5 Conclusions

From streaming potential measurements we have obtained the kinetics of adsorption and desorption, and equilibrium thickness isotherms of PEO adsorbed on the wall of a glass capillary. Using the Lévêque equation we found that the rate of adsorption and desorption are determined by the rate of mass transfer towards and away from the surface, respectively. On the time scale of the mass transfer there is near the surface continuously a local equilibrium between free and adsorbed molecules.

The hydrodynamic layer thickness δ_h of PEO adsorbed on silica as calculated from the streaming potential is in good agreement with the results of dynamic light scattering, indicating that both methods measure the same quantity.

Especially for high molecular weights δ_h is sensitive to very small changes in the adsorbed amount Γ, which is mainly due to tails protruding far into the solution. This sensitivity enabled us to perform accurate measurements of the kinetics and thickness isotherms in the region near saturation, under conditions where changes in Γ are hardly measurable. Thickness isotherms were measured down to extremely low concentrations (0.005 g/m^3), and are in good agreement with theoretical predictions.

For the adsorption kinetics we propose a simple model combining the

mass transfer equation with the measured dependence of δ_h on Γ. Excellent, quantitative agreement was found between the predicted and observed δ_h as a function of time. This result is entirely consistent with the kinetics as found by reflectometry.

In the case of desorption into a flow of pure solvent the mass transfer rate is proportional to the surface concentration c_s of non-adsorbed molecules, which according to the local equilibrium concept is determined by the adsorption isotherm of the polymer. Since in the relevant range Γ increases nearly linearly with log$c$, a simple expression for $c_s(\Gamma)$ can be incorporated in the mass transfer equation. This leads to the prediction that Γ falls linearly with log$t$, which constitutes a first result for a desorption equation. Moreover, the slope $-d\Gamma/d\log t$ is predicted to be the same as $d\Gamma/d\log c$. Experimentally we found that the slopes of the equilibrium thickness isotherms and kinetic desorption curves are indeed equal for all molecular weights studied. The absolute value of the observed $d\Gamma/dt$ agrees quite well with the predictions of our model. The relative slope $d\Gamma/(\Gamma d\log c)$ is for polymers usually of the order of a few percent per decade in the concentration c. As a consequence the desorption rate slows down enormously with desorbed amount, and full desorption is therefore impossible in a practical sense. Desorption of polymer by dilution with solvent (where there is no continuous removal of the desorbed material) is impossible. This conclusion is, nevertheless, in complete agreement with thermodynamic equilibrium between the adsorbed layer and the (sub)surface region; it merely reflects that the equilibrium between surface layer and solution is highly biased towards the surface side (high affinity adsorption).

4.6 References

(1) Dijt, J.C.; Cohen Stuart, M.A.; Hofman, J.E.; Fleer, G.J. *Colloids Surf.* **1990**, *51*, 141.

(2) Van der Beek, G.P.; Cohen Stuart, M.A.; Fleer, G.J. *Macromolecules* **1991**, *24*, 3553.

(3) Johnson, H.E.; Granick, S. *Macromolecules* **1990**, *23*, 3367.

(4) Frantz, P.; Leonhardt, D.C.; Granick, S. *Macromolecules* **1991**, *24*, 1868.

(5) Scheutjens, J.M.H.M.; Fleer, G.J.; Cohen Stuart, M.A. *Colloids Surf.* **1986**, *21*, 285.

(6) Cohen Stuart, M.A.; Tamai, H. *Macromolecules* **1988**, *21*, 1863.

(7) Cohen Stuart, M.A.; Tamai, H. *Langmuir* **1988**, *4*, 1184.
(8) Lévêque, A. *Ann. Mines* **1928**, *13*, 284.
(9) Scheutjens, J.M.H.M.; Fleer, G.J. *J. Phys. Chem.* **1979**, *83*, 1619.
(10) Scheutjens, J.M.H.M.; Fleer, G.J. *J. Phys. Chem.* **1980**, *84*, 178.
(11) Cohen Stuart, M.A.; Mulder, J.W. *Colloids Surf.* **1985**, *15*, 49.
(12) Cohen Stuart, M.A.; Waajen, F.H.W.H.; Dukhin, S.S. *Colloid Polym. Sci.* **1984**, *262*, 423.
(13) Bird, R.B.; Stewart, W.E.; Lightfoot, E.N. In " *Transport Phenomena";* John Wiley & Sons: New York, **1960**.
(14) Cohen Stuart, M.A.; Waajen, F.H.W.H.; Cosgrove, T.; Vincent, B.; Crowley, T.L. *Macromolecules* **1984**, *17*, 1825.
(15) Van der Beek, G.P.; Cohen Stuart, M.A. *J. Phys. Fr.* **1988**, *49*, 1449.
(16) Sauer, B.B.; Yu, H. *Macromolecules* **1989**, *22*, 786.

5 ADSORPTION AND DESORPTION KINETICS OF POLYSTYRENE IN DECALIN SOLUTIONS

5.1 Introduction

In chapters 3 and 4 we found that the adsorption and desorption rates of poly(ethylene oxide), PEO, are largely determined by the mass transfer between bulk solution and surface, because of the rapid equilibration of the adsorbed layer. Only for high molar mass polymer ($M \approx 1000\,\mathrm{K}$, where $1\,\mathrm{K} \equiv 1\,\mathrm{kg/mole}$) near saturation a clear decrease of the adsorption rate due to the build-up of the adsorbed layer was observed. In this chapter we want to examine the question whether fast equilibration is a general characteristic of the adsorption of uncharged homopolymers. A reason for the rapid adaptation of adsorbed PEO could be the large flexibility of the polymer chain, which enables fast reconformation during the adsorption process. In view of this argument we chose for the present study polystyrene (PS) , which is much less flexible than PEO due to its bulky styrene side-groups. Polystyrene is available in fractions with a narrow molecular weight distribution, like PEO, and therefore we expect little or no effect of polydispersity on the adsorption kinetics.

In the past 25 years various authors have reported kinetic curves for the adsorption of PS, but in none of these studies[1-12] the adsorption kinetics was investigated systematically under well-controlled conditions. For all these experiments the mass transfer conditions were poorly defined, so that it is often difficult to distinguish between transport and surface processes. However, we will briefly review the main results.

Grant et al.[13] studied the adsorption of PS ($M \approx 10^3\,\mathrm{K}$) from dilute cyclohexane solutions at 36°C, and found a remarkable influence of the substrate: on mercury the adsorption was completed within 1 hr, whereas it took about 72 hr on a chrome surface. Kawaguchi and co-workers[5,8] have studied the adsorption on chrome from solutions of high molar mass PS ($10^2 < M < 10^4\,\mathrm{K}$). As solvents they used cyclohexane[8] and carbon tetrachloride[5], both at 35°C, at which temperature the former is a θ- and the latter a good solvent. The shape of the adsorption curves and the time needed to attain a stable adsorbed amount (2 - 4 hr) were found to be about the same for both solvents and for all molecular weights studied. The final adsorbed amount was much higher in cyclohexane than in carbon tetrachloride, as expected (the amounts were found to be 5 and 1 $\mathrm{mg/m^2}$, respectively, in these solvents).

For the adsorption of PS from cyclohexane solutions onto silica the

results of Vander Linden[9] and Frantz et al.[10] agree rather well. Both groups find that the time to obtain a stable adsorbed amount increases with chain length: from less than 10 minutes for $M \approx 100$K up to several hours for $M \approx 2000$K. All results cited above are obtained for concentrations of 100 g/m^3 or higher. If mass transfer had been rate limiting, then probably the saturated adsorbed amount would have been reached in a few minutes or less. The observed times are much longer. This indicates that the behaviour of PS differs from PEO. Furthermore, some of these results indicate that the adsorption kinetics depend on the chain length and substrate used.

In this chapter we investigate the adsorption kinetics of polystyrene more systematically by using well defined mass transfer conditions, and by varying the concentration, the chain length, the solvent quality and the adsorption energy of the polymer. Obviously, the concentration and chain length of PS can easily be varied. The solvent quality and adsorption energy cannot be directly changed, and therefore we discuss below the possibilities to influence these parameters.

The solvent quality for a polymer can be changed by variation of the temperature or the composition of the solvent. With temperature variation the composition of the solution remains constant, which is an advantage over a change in the solvent composition. However, temperature is also directly related to molecular motions, and these may well affect the adsorption kinetics. For this reason, and because our present reflectometer can only be operated at room temperature, we chose to vary the solvent composition. We decreased the solvent quality by addition of small amounts of a non-solvent. We have to bear in mind that such a non-solvent could also change the effective adsorption energy of the polymer. We therefore decided to use a non-solvent which does not interact with the surface, so that it has little or no influence on the adsorption energy..

Cohen Stuart and Van der Beek[14-17] showed that the effective segmental adsorption energy of a polymer can be varied in a quantitative manner by using mixtures of two solvents, one of which is a displacer of the polymer . We chose a rather strong displacer, so that the amounts needed are relatively small. Therefore, we expect little effect of the displacer on the solvent quality. Moreover, the concomitant changes in the hydrodynamic and optical conditions will be small.

In this chapter we also consider an example of the adsorption kinetics of a low molar mass polystyrene (M= 17 K), that carries at one end a polar, strongly adsorbing iminium ion group. Due to this end group the

adsorption is strongly enhanced. With such an end-capped polymer we can investigate the adsorption kinetics of a short chain at high coverage.

As the experimental technique, reflectometry in a stagnation point flow is used. Since PS is not soluble in water, the use of organic solvents is required when the adsorption of this polymer is studied. The possibilities of reflectometry under these conditions were already extensively discussed in chapter 2. In chapter 3 we showed that with a stagnation point flow well-controlled mass transfer conditions are obtained.

5.2 Experimental

5.2.1 Materials

Polystyrene samples of narrow molar mass distribution were purchased from Polymer Laboratories, and were used without further purification. Their molar masses and degree of polydispersity are listed in table 5.1. According to the manufacturer the three lowest molecular weights have a "vinyl hexane" end-group. From Dr. Furusawa we obtained a Polystyrene with an iminium-ion end-group, and the corresponding homopolymer with a styrene end-group. Both were made by anionic polymerisation, and have a molecular weight of 17 K.

Table 5.1 Polymer samples of polystyrene

code	M, kg/mole	M_w/M_n	code	M, kg/mole	M_w/M_n
1K	1.32	1.09	1030K	1030	1.05
3K	3.25	1.04	3040K	3040	1.04
9K	9.2	1.03	6500K	6500	1.12
66K	66	1.03	20000K	20000	1.3
514K	514	1.05			

The solvent decalin was obtained from Merck ('for synthesis' quality). From an analysis with gas chromatography we determined that it is a 30/70% mixture of the cis- and trans-form, respectively. Before use the decalin was led through a column of zeolite, and stored in bottles containing anhydrous $CaCl_2$. From experiments we concluded that this treatment removes low concentrations of impurities from the decalin which act as displacers of PS. Another treatment in which solid Na was used in stead of $CaCl_2$ was not successful in removing the impurity. This indicates that the contaminant was not water, but probably a polar compound that is not fully degraded by reaction with Na.

In some experiments the solvent decalin was mixed with *n*-hexadecane (Merck, 'for synthesis' quality) or ethyl acetate (Merck, P.A.), which are a non-solvent and a displacer of PS, respectively. Before mixing both additives were purified by the same method as used for decalin.

As the substrate for adsorption, strips cut from an oxidised silicon wafer were used. They were cleaned as described in section 3. By the method described in chapter 3 we determined that the silica film thickness was about 105 nm for all strips used.

In experiments using washing machine cleaned glassware we found that small amounts of impurities were released from the glass into solution. Therefore, we decided to use a more rigorous cleaning treatment for the glassware. Two methods were applied. In the first the glassware was filled with sulfochromic acid and thereafter stored for 24 h, followed by the same treatment with 2 N nitric acid. The final step was rinsing with deionised water and drying at 100°C. The second method consists of a single cleaning step with a solution of 10 g/l $(NH_4)_2S_2O_8$ in concentrated H_2SO_4, followed by rinsing with water and drying.

5.2.2 Methods

All adsorption and desorption measurements were carried out using a reflectometer with stagnation point flow cell as described in chapters 2 and 3. For the experiments in this and the subsequent chapters we used a reflectometer with an output signal S as defined in eq. 2.3. For determination of the angle of incidence θ_i from the decalin solution on the silicon wafer we first measured the angle between the laser and the plane of the silicon wafer. A value of 27.1° was found. Using Snell's law we calculated θ_i as 59.35°, using a refractive index of 1.515 for the glass prism (Melles Griot, BK7 quality).

The sensitivity parameter A_s was calculated as described in chapter 2. The parameters and results are listed in table 5.2. The calculated value of A_s is 0.0174 m^2/mg. The adsorbed amount Γ is calculated from the output signal S and the sensitivity A_s according to eq. 2.8.

For experiments with organic solvents a flow cell and flow system were constructed in which solutions come into contact with glass and Teflon only. Essentially the new cell is the same as in fig. 3.1, but now the cell is made of Teflon and the two prisms (indicated as 2 and 4 in fig. 3.1.a) are replaced by one, through which a cylindrical channel (as inlet for the polymer solution) is drilled from top to base. Teflon valves and tubing were used. The flow of solvent or solution was maintained through the action of

Table 5.2 Sensitivity calculations for adsorption of polystyrene from decalin solution onto silica

Optical parameters		
Silicon	$n = 3.80$	
Silica layer	$n = 1.46$	$d = 105$ nm
adsorbed PS layer (1 mg/m^2)	$n = 1.497$	$d = 5$ nm
decalin solution	$n = 1.473$	
angle of incidence	59.35°	
wavelength	632.8 nm	
refractive index increment PS/decalin	0.120 cm^3/g [18]	
Results		
R_p / R_s without adsorbed polymer	0.0562582	
sensitivity factor A_s	0.0174 m^2/mg	

gravity.

The stagnation point flow for the experiments in decalin is characterised by a distance h between collector surface and inlet tube of 1.3 mm, and a radius R of the inlet tube of 0.75 mm (see fig. 3.1.b). The characteristic ratio h/R equals 1.7. The flow rate was determined from the weight of solution that passed through the flow system in 3 minutes. Using a density of decalin of 0.88 g/cm^3 we find that the volume flow rate is 1.31 ml/min. The corresponding Reynolds number is 3.28. From fig. 3.2 we then find that for h/R = 1.7 the flow intensity parameter $\bar{\alpha}$ is 2.13.

The mass transfer towards the stagnation point is described by eq. 3.5 for the case that the perfect sink boundary condition applies. Here we give a more general version of eq. 3.5, and in order to show the analogy with the transport equation for capillary flow (eq. 4.1) we slightly rewrite eq. 3.5. The flux J of polymer between bulk solution and stagnation point is a function of the mean fluid velocity v_m, at the end of the inlet tube, of the diffusion constant D of the polymer, and the concentration difference $c_b - c_s$, where c_b and c_s are the polymer concentrations in the bulk solution and (sub)surface region, respectively

$$J = k(c_b - c_s) \tag{5.1.a}$$

where the transport coefficient k is given by

$$k = 0.776\left(\frac{D^2 \bar{\alpha} v_m}{R^2}\right)^{1/3} \tag{5.1.b}$$

In eq. 5.1.b, R is the radius of the inlet tube, and $\bar{\alpha}$ is a dimensionless streaming intensity parameter (see chapter 3). Note the analogy of eq. 5.1 with the corresponding expression for capillary flow (eq. 4.1).

The concentration c_b is equal to that of the polymer solution which is injected (for injection of pure solvent, $c_b = 0$). Usually, the (sub)surface concentration c_s is not known beforehand. It is the concentration of non-adsorbed molecules near the surface, that can freely take part in diffusion and convection. The perfect sink boundary condition amounts to the assumption that c_s equals zero. However, also other boundaries conditions can be applied (e.g., that of local equilibrium as in chapter 4).

In order to examine the effect of the addition of the non-solvent *n*-hexadecane on the solvent quality, the cloud point of the PS solutions was measured. To this end a tube containing about 5 ml solution of concentration 500 g/m^3 was placed in a thermostatic bath. The temperature was decreased stepwise by 1 °C and the cloud point was determined visually.

5.3 Results

5.3.1 Adsorption and desorption in decalin solutions

Introductory experiments showed that the reliability and reproducibility of the results is strongly dependent on the degree of purification of solutions and glassware. For example, if an adsorbed polymer is exposed to a non-purified solution, the adsorbed amount of polymer may decrease considerably due to displacement by the pollutant. The sensitivity for contamination of this method originates from the high volume to surface ratio: continuously a fresh solution (containing impurities) is led towards the surface. We therefore start this section by giving an example showing that by our cleaning methods the contamination of solutions has been reduced to an acceptable level.

As the example the adsorption of a low molecular weight PS (9K) is chosen, since adsorption of short chains appeared to be most sensitive for contamination. In fig. 5.1 the result of two experiments is given. Before $t = 0$ only solvent flows through the cell. At $t = 0$ the valve is switched and the injection of polymer solution starts. After about 7 s, which is the time needed to refresh the volume between valve and cell, the signal starts to rise due to adsorption of the polymer. The initial rate $[dS/(S_0 dt)]_0$ which is proportional to the adsorption rate $(d\Gamma/dt)_0$ is indicated. After some 20 - 30 s the surface is saturated and no further adsorption takes place. The saturated level corresponds to an adsorbed amount of about 1 mg/m^2.

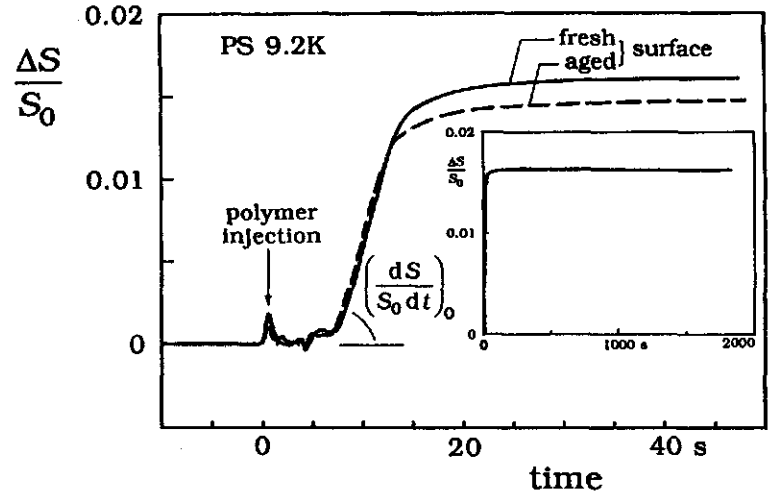

Figure 5.1 Example of the adsorption kinetics of low molar mass PS. The full and dashed curves represent experiments with 3 and 40 min of solvent injection for $t<0$, respectively. The inset shows $\Delta S/S_0$ during prolonged polymer injection. Concentration 50 g/m^3, A_s = 0.0174 m^2/mg.

The difference between both experiments is the time of solvent injection before t=0: 3 and 40 minutes for the full and dashed curve, respectively. The saturated adsorbed amount is about 8 % lower for the experiment with the longer time of solvent injection. If instead of purified solvent (as in fig. 5.1) decalin as received is used, there is almost no adsorption of polymer left after 40 min of solvent injection. This is due to adsorption of contaminants.

The inset of fig. 5.1 shows $\Delta S/S_0$ during prolonged injection of polymer solution for the experiment with the short time of solvent injection before t=0. After rapid initial adsorption the signal remains stable till the end of the experiment, about 30 minutes later. If instead untreated decalin is used, the signal decreases strongly due to displacement by contaminants, becoming nearly zero after ≈2500 s. We conclude that by our cleaning method adsorbing contaminants are effectively removed from the decalin, and that experimental results are hardly effected by contaminants for a period of at least 30 minutes.

5.3.1.1 Initial adsorption rate

For PEO the initial adsorption rate is completely determined by mass transfer from the bulk solution (chapter 3). In order to check whether this is also the case for adsorption of PS from decalin solutions, we varied the

mass transfer conditions by means of the concentration and the chain length of the polymer, and compared the observed initial adsorption rates to the predicted mass transfer rates (eq. 5.1).

The results are presented in fig. 5.2 in a double logarithmic plot of the initial adsorption rate $(d\Gamma/dt)_0$ as a function of molecular weight M, for concentrations of 5 and 50 g/m^3, respectively. From the graph can easily be determined that $(d\Gamma/dt)_0 \propto c$. This is in agreement with eq. 5.1, as long as the (sub)surface concentration c_s is negligibly small as compared to the concentration c_b in the bulk. As discussed in chapter 3, we have no reason to suppose that this is not the case for adsorption on a bare surface. The initial adsorption rate decreases with M due to the slower diffusion of longer chains.

Polymer solution theory states that the diffusion constant of a polymer scales as $D \propto M^{-\gamma}$. Under θ-conditions, where Gaussian statistics apply, $\gamma = 0.5$ for every M. In a good solvent a transition occurs from $\gamma = 0.5$ for low M to 0.588 for high M, due to the swelling of long chains by excluded volume. The transition between these regimes is rather broad and extends over about two decades in M[19]. In fig. 5.2 the slopes of the dashed and dotted lines are drawn according to $\gamma = 0.5$ and 0.588, respectively. For $M > 10\,\mathrm{K}$ there is excellent agreement between the experiment and the scaling theory for θ-solvents. Only for extremely short chains ($M < 10\,\mathrm{K}$),

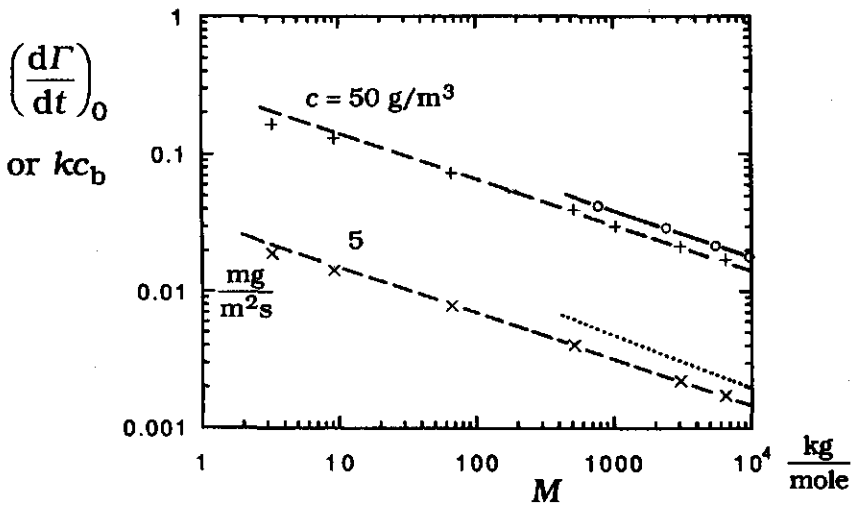

Figure 5.2 Effect of molar mass on initial adsorption rate for two concentrations. Crosses and plusses refer to $c = 5$ and 50 g/m^3, respectively. The dashed and dotted lines are drawn with a slope according to the scaling theory for θ- and athermal solvents, respectively. Circles represent a calculation of the mass transfer rate kc_b, see text.

which actually consist of less than 100 monomeric units, the experiments deviate slightly from scaling theory.

From the agreement between experiment and the theory for polymer diffusion constants in solution we conclude that the measured dependence of $(d\Gamma/dt)_0$ on M reflects the molecular weight dependence of the diffusion constant in solution, and is thus in agreement with mass transfer controlled adsorption. Moreover, from the slope of the curve at high values of M it follows that at ≈ 22 °C decalin is (nearly) a θ-solvent for PS. From measuring D by dynamic light scattering, Tsunashima et al. concluded that the θ-temperature of PS in trans-decalin is 20.4 °C[20,21], which is in good agreement with our result. We have to realise, however, that Tsunashima used pure trans-decalin and that our result applies to a 70/30 mixture of the trans and cis-form. Finally we note that the initial adsorption rate gives a remarkably accurate measurement of the chain length dependence of the diffusion constant. With the same method we observed for aqueous solutions of PEO with increasing M a transition in D, which is characteristic for good solvents (chapter 3).

The above considerations suggest that $(d\Gamma/dt)_0$ of PS from decalin solutions is entirely determined by transport through solution, and thus equals the maximum mass transfer rate kc_b (c_s=0 in eq. 5.1). A further check is to compare the quantitative values of $(d\Gamma/dt)_0$ and kc_b. In order to be able to calculate k we used the values for D as given by Tsunashima et al.. The calculated maximum mass transfer rate is shown as open circles in fig. 5.2. The calculated value of kc_b is about 20 % higher than the experimental value for $(d\Gamma/dt)_0$. As discussed already for the adsorption of PEO in chapter 3, one expects on theoretical grounds that $(d\Gamma/dt)_0 = kc_b$. The discrepancy is easily explained by errors in D and the calibration of the signal. Therefore, it is likely that the initial adsorption rate of PS from decalin solutions is entirely determined by mass transfer from the bulk, as was found before for PEO from water.

5.3.1.2 Adsorption rate at higher coverage

Figure 5.1 shows that the adsorption rate $d\Gamma/dt$ is constant up to about $\Delta S/S_0 = 0.01$, and then decreases gradually to zero in the plateau region. The decrease in $d\Gamma/dt$ is caused by the build-up of the adsorbed layer. Below, we investigate how the adsorption rate at higher coverage depends on the chain length and the concentration of the polymer.

In order to be able to examine the effect of M on the adsorption kinetics we plotted in fig. 5.3 the adsorbed amount Γ as a function of $t(d\Gamma/dt)_0$ on a

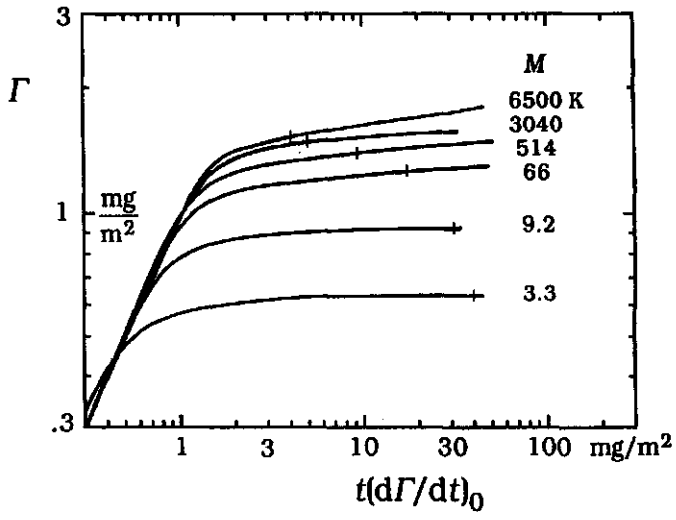

Figure 5.3 Comparison of the adsorption kinetics for different molar masses. The initial slope is normalised to unity. Note the double logarithmic scaling. Vertical tics along the curves indicate $t = 4$ min of polymer injection. Concentration 50 g/m^3.

double logarithmic scale for a series of M. In such a plot all initial slopes are normalised to unity. Since it was concluded before that $(d\Gamma/dt)_0$ is determined by mass transfer for all molar masses, the initial tangent represents mass transfer controlled adsorption. With increasing M the mass transfer limited region extends up to higher Γ. This behaviour was also found for PEO (compare fig. 3.12). However, for all chain lengths of PS we find a *gradual* transition from the transport limited region to the final value, in contrast with the *sharp* transition for the low molar masses of PEO ($M < 100$K, fig. 3.12). For the two lowest molar mass samples of PS (3K and 9K) the final value corresponds to a stable, saturated level. For longer chains the final level is not completely constant, $d\Gamma/dt$ being finite even after long times (note the logarithmic scaling). The adsorption rate in the plateau region was found to increase considerably if less well purified decalin was used. Therefore, in our opinion it is possible that the slow increase of Γ in the plateau region is an undesired side-effect. However, it may also be a 'real' effect related to polymer adsorption kinetics of long, stiff chains.

The effect of the concentration on the adsorption kinetics of a high molar mass sample (3000K) is shown in fig. 5.4 for four concentrations in the range 5 - 50 g/m^3. The adsorbed amount Γ is plotted as a function of the product ct of concentration and time. The initial slope $[d\Gamma/d(ct)]_0$ is the same for each concentration studied, which again shows that initially

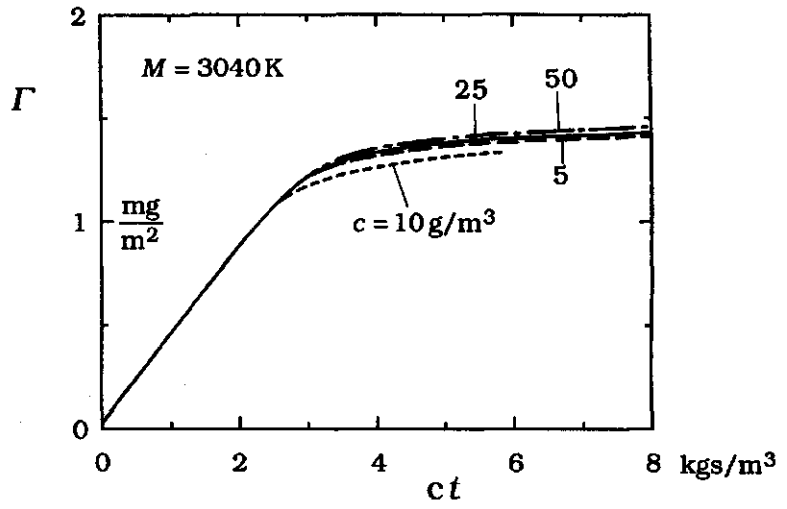

Figure 5.4 Effect of polymer concentration on adsorption rate. Note that Γ is plotted as a function of the product ct of concentration and time. Concentrations as indicated.

$d\Gamma/dt \propto c$, in agreement with the transport equation 5.1. In fig. 5.4 the curves $\Gamma(ct)$ for different c coincide within experimental error, not only in the initial part, but also at higher coverage and in the final level. This implies that $d\Gamma/dt$ is proportional to the solution concentration for each value of Γ. No influence of the age of the adsorbed layer on $d\Gamma/dt$ is observed in these experiments. Similar results are obtained for other molecular weights. Only for very short chains (M = 3K and 9K) this result could not be verified with certainty because the saturated levels for these samples are somewhat concentration dependent.

It turns out that it is possible to analyse the kinetic curves $\Gamma(t)$ in terms of a two-step process: transport of free molecules from the bulk solution, followed by attachment to the interface. From this analysis a rate constant for the attachment can be extracted.

The transfer part is described by eq. 5.1. According to this equation the polymer flux to the surface is proportional to the concentration difference $c_b - c_s$ between bulk solution and surface region. For the attachment step we suppose that the adsorption rate $d\Gamma/dt$ is proportional to the concentration c_s of free molecules near the surface, with an attachment rate constant $K(\Gamma)$ which depends on the adsorbed amount Γ

$$\frac{d\Gamma}{dt} = K(\Gamma)c_s \qquad (5.2)$$

In a steady state situation the flux J (eq. 5.1) equals the adsorption rate $d\Gamma/dt$ (eq. 5.2). However, during adsorption $d\Gamma/dt$ usually decreases in time, so that a real steady state does not exist. Since the changes in $d\Gamma/dt$ are slow as compared to the rate of adjustment of the flux from solution, continuously a quasi-steady state exists, where $J \approx d\Gamma/dt$. After elimination of c_s from eqs. 5.1 and 5.2 the following expression is obtained

$$\frac{c_b}{d\Gamma/dt} = \frac{1}{k} + \frac{1}{K(\Gamma)} \tag{5.3}$$

If $K(\Gamma) >> k$, then $d\Gamma/dt = k c_b$ and the adsorption rate is mass transfer limited ($c_s \cong 0$). If $K(\Gamma) << k$, then $d\Gamma/dt = K(\Gamma)\, c_b$ and the adsorption is entirely determined by the attachment step ($c_s \cong c_b$).

Since the initial adsorption rate of PS is completely determined by mass transfer (see 5.3.1.1), the transport coefficient k equals $(d\Gamma/dt)_0 / c_b$. Hence $1/K(\Gamma)$ is given by

$$\frac{1}{K(\Gamma)} = c_b\left(\frac{1}{d\Gamma/dt} - \frac{1}{(d\Gamma/dt)_0}\right) \tag{5.4}$$

Equation 5.4 can be used to extract from a kinetic curve $\Gamma(t)$ the attachment rate constant $K(\Gamma)$.

As an example we analysed one of the curves in fig. 5.4 ($c = 50$ g/m^3), and plotted in fig. 5.5 $K(\Gamma)$ (full curve) and k (horizontal dashed line) as a function of the adsorbed amount Γ. For Γ up to about 0.5 mg/m^2 the deviation of $d\Gamma/dt$ from $(d\Gamma/dt)_0$ is so small, that $K(\Gamma)$ cannot be determined. In the point where the curves cross ($k = K(\Gamma)$) the adsorption rate is half of its initial value. With increasing adsorbed amount $K(\Gamma)$ decreases sharply (note the logarithmic scaling). This means that due to the build-up of the adsorbed layer the attachment to the surface becomes more and more difficult.

For PS, at any coverage $d\Gamma/dt \propto c_b$ (fig. 5.4), so that the value of the left hand side of eq. 5.3 is independent of $d\Gamma/dt$ or c_b. Consequently, the same applies to $K(\Gamma)$. This means that for polystyrene $K(\Gamma)$ is independent of the mass transfer conditions. It is a rate constant which is entirely determined by the attachment step to the surface. In section 5.4 we will extensively discuss our view of the attachment step. Since we are not able to give a quantitative interpretation to $K(\Gamma)$, we decided to present and compare the experimental results in this chapter in their original form. Note however, that from each curve $\Gamma(t)$ we could extract $K(\Gamma)$, and that we could thus compare and discuss results in terms of $K(\Gamma)$.

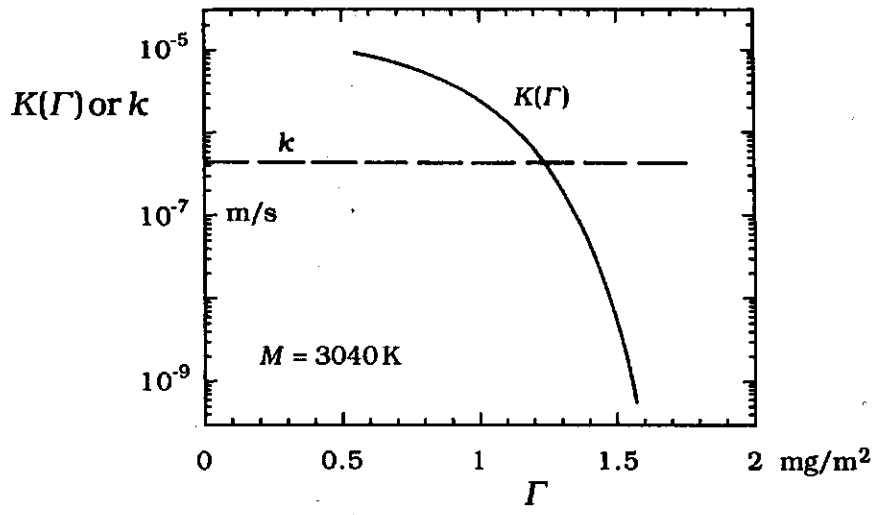

Figure 5.5 Attachment rate constant $K(\Gamma)$ and transport coefficient k as a function of the adsorbed amount Γ. Polymer concentration 50 g/m^3.

5.3.1.3 Final adsorbed amount

In order to examine the effect of the chain length on the final adsorbed amount Γ_f we plotted in fig. 5.6 $\Gamma_f(M)$ for a polymer concentration of 50 (open circles) and 500 g/m^3 (open squares). At the lower concentration Γ_f is the value of Γ at $t(d\Gamma/dt)_0$ = 30 mg/m^2 (fig. 5.3). At the higher concentration Γ_f is the adsorbed amount at $t \approx 25$ min. For comparison, results of Vander Linden and Van Leemput[22] for the adsorption of PS from cyclohexane on silica dispersions at 35 °C and c=2000 g/m^3 are given in open triangles. The meaning of the filled symbols will be discussed in section 5.3.2.

First we discuss the effect of the concentration on the curve of Γ_f as a function of M. For M up to ≈ 20 K the values for Γ_f can be determined unambiguously, since the adsorbed amount attained a constant stable level for those chains lengths (fig. 5.3). Moreover, the adsorption is reversible with respect to concentration changes between 5 and 500 g/m^3, as will be shown in the next (sub)section. Therefore we conclude that the final adsorbed amount Γ_f for $M < 20$K represents equilibrium values. For $M > 20$K the adsorption rate at the end of the experiment was not yet zero, and thus Γ_f does not correspond to equilibrium. The higher value of Γ_f at c=500 as compared to 50 g/m^3 can be explained from the proportionality between $d\Gamma/dt$ and c. In terms of fig. 5.4, the product ct is much higher for c=500 than 50 g/m^3, and thus Γ_f for the higher concentration is nearer to equilibrium than for the lower concentration.

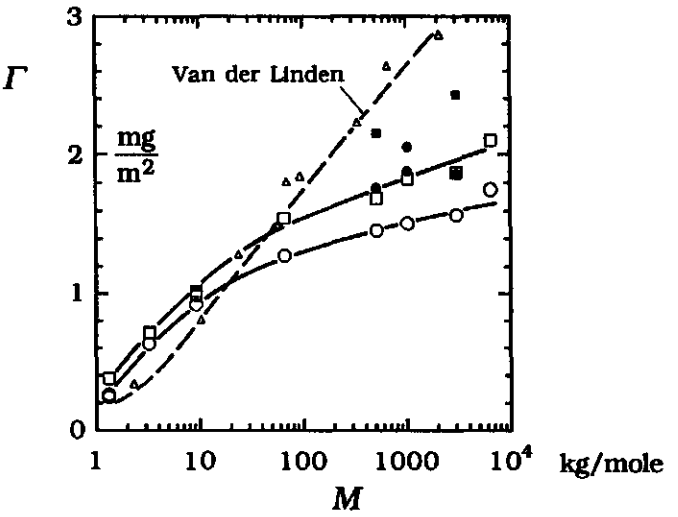

Figure 5.6 Effect of molar mass on final adsorbed amount in decalin solutions (open symbols) and 96.5/3.5 (w/w) mixtures of decalin and *n*-hexadecane (filled symbols). Circles and squares refer to $c = 50$ and 500 g/m^3, respectively. For comparison, results of van der Linden for PS adsorbing from cyclohexane (34 °C) on silica are included (triangles).

The fact that the rate of the attachment step is proportional to the solution concentration implies that equilibrium is attained at certain value of the *product ct*. Thus the time needed to establish equilibrium is inversely proportional to solution concentration. This could well be the reason for the often encountered strong decrease in Γ_f at low concentrations in experimentally determined adsorption isotherms. For example, Van der Linden[9] determined an adsorption isotherm of monodisperse PS (M = 300 K) from cyclohexane at 35 °C on silica dispersions after stirring for 2 h. For $c > 500$ g/m^3 the isotherm showed a plateau value of 2 mg/m^2. For $c <$ 500 g/m^3 the adsorption gradually decreased, and at 20 g/m^3 only 0.95 mg/m^2 was adsorbed. For an equilibrium adsorption isotherm we would not expect such a strong concentration dependence. However, for c = 20 g/m^3 the value of ct was only 4% of that for c = 500 g/m^3, and it was possibly insufficient to reach equilibrium.

Comparison in fig. 5.6 of our results with those of Vander Linden and Van Leemput shows the following trends. For low molar mass Γ_f in decalin is somewhat higher than in cyclohexane. According to the Scheutjens-Fleer theory curves of Γ vs. log$M$ shift to the left with increasing adsorption energy per segment. The difference at low M may thus be an indication that the adsorption energy in decalin is somewhat higher than in

cyclohexane. At high M the value of Γ_f in decalin is lower than in cyclohexane. Presumably, Γ_f in decalin is still below the equilibrium value. In addition, the solvent quality for PS in decalin could be better than in cyclohexane, which would correspond to lower adsorption levels. The second argument is supported by results of Chin and Hoagland[23]. These authors reported that for high M adsorbed amounts in decalin at 22 °C were about half the value of those in cyclohexane at 35 °C. For both solvents the adsorbed amounts were about twice as high as the values given here. This may be a result of the different substrate used: Chin and Hoagland used chrome.

5.3.1.4 Desorption

In this (sub)section we want to investigate whether the desorption rate of PS into a flow of pure solvent is limited by mass transfer away from the surface or by detachment from the adsorbed layer. In chapter 4 an expression for the mass transfer limited desorption of polymer was derived (eq. 4.12). In this equation local equilibrium near the surface between adsorbed layer and adjacent solution is assumed. The adsorbed amount Γ at any time t after the start of solvent injection on a polymer layer initially in equilibrium at an adsorbed amount Γ_0 and concentration c_0 is given by

$$\Gamma = \Gamma_0 - p\log(1 + t/\tau) \tag{5.5}$$

where p is the slope $d\Gamma/d\log c$ of the adsorption isotherm and the time constant τ is given by $0.43p/kc_0$. For $t >> \tau$ a simple correlation between the desorption rate and adsorption isotherm exists: $d\Gamma/d\log t = -d\Gamma/d\log c$. The desorption was studied as a function of the chain length. For $M > 100$ K no detectable desorption of PS into a flow of pure solvent occurs over a period of ≈ 30 min. According to the Scheutjens-Fleer theory the slope p of the adsorption isotherm decreases with increasing M. For long chains p/Γ_0 is of the order of 1 % or less. Due to this low value of p no considerable desorption of long chains is expected, unless t is very long, much longer than the time-scale of a typical desorption experiment in our set-up. Thus, the experimental result of no-desorption is consistent with the model of mass transfer limited desorption, but gives, of course, no proof for this model.

For short chains some desorption is observed in a flow of pure solvent. The results of four desorption experiments with a sample of $M = 9.2$ K are given in fig. 5.7. Initially, for $t < 0$ a polymer solution of a concentration as indicated is injected. The adsorbed amount remains at a constant

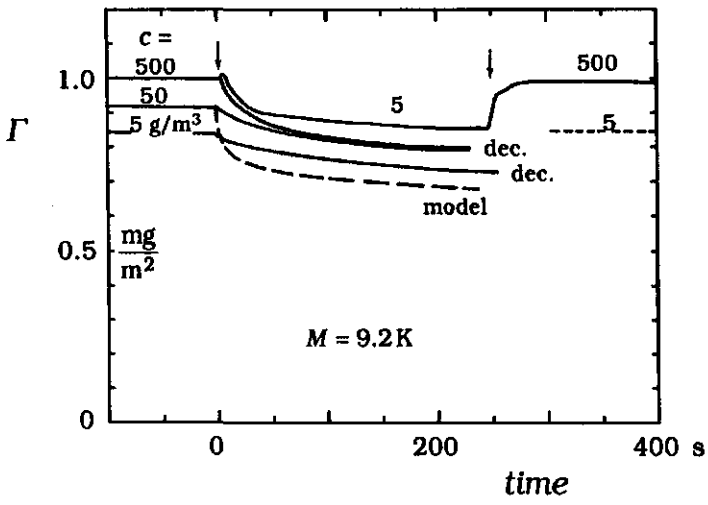

Figure 5.7 Desorption kinetics for $M = 9.2$ K. Initially, for $t < 0$, polymer solution is injected, and the adsorbed layer is saturated at a concentration as indicated. At $t = 0$ the injection of pure decalin (dec) or a solution of lower concentration ($c = 5$ g/m^3) starts. For one of the experiments, at $t \approx 250$ s the original solution is reinjected. For comparison, the saturated level for $c = 5$ g/m^3 is indicated by a dotted line to the right. The dashed curve is the result of a model calculation, as discussed in the text.

saturated level, which increases with concentration. Then, at $t = 0$, the valve is switched to injection of pure solvent or a solution of lower concentration, as indicated. The dashed curve is the result of a model calculation, as discussed below. For all experiments Γ decreases due to desorption. In the case of a concentration jump from $c = 500$ to 5 g/m^3 the desorption rate is initially the same as for a jump from $c = 500$ g/m^3 to pure solvent, probably because the concentration gradient between surface and bulk solution is almost the same. After some time the curves diverge, and the one for injection of polymer solution approaches a new, stable level. The adsorbed amount at that level corresponds to the saturation at this concentration, which is, for comparison, indicated by a dotted line. If at $t = 250$ s the solution of higher concentration is injected again, the original saturated level is quickly re-established. This experiment shows that the adsorption is reversible with respect to changes in solution concentration. For this low M the saturated adsorbed amounts represent equilibrium values, and the initial values for $c = 5$, 50 and 500 g/m^3 give three points of the adsorption isotherm. The almost equal distance between the saturated levels for the 3 concentrations indicates that the slope $p = d\Gamma/d\log c$ of the isotherm is indeed constant over the range studied. A value for p of 0.08 mg/m^2 per decade in c is found.

Our next check is whether during desorption the local equilibrium concept applies, and whether the desorption can be described by eq. 5.4. In order to be able to do this, first the transport coefficient k was determined from the initial adsorption rate for $c=5$ g/m^3 . From eq. 5.1 a value of 2.86 10^{-6} m/s for k was obtained, corresponding to $\tau=0.24$ s. The adsorbed amount during desorption was then calculated with eq. 5.4 and the result is represented by the dashed line in fig. 5.7. The experimental desorption rate is much lower than that calculated according to mass transfer limitation. This implies that for PS/decalin not the mass transfer, but detachment of polymer molecules is rate limiting, in contrast to the PEO/water system. The time scale for the detachment process is initially of the order of seconds to minutes, because reversibility with respect to concentration changes between 5 and 500 g/m^3 occurs at these time-scales.

5.3.2 Effect of a non-solvent

In order to decrease the solvent quality we decided to add a non-solvent to solutions of PS in decalin. For two reasons *n*-alkanes are suitable non-solvents in our experiments. Firstly, they are chemically related to decalin, and therefore perfectly miscible with this solvent. Secondly, they are non-polar and hardly polarisable and therefore we do not expect a large effect on the adsorption energy of the polymer from the mixed solvent as compared to pure decalin. We chose *n*-hexadecane because of its low vapour pressure. In this way temperature fluctuations due to evaporation at the free solution/air interface in the flow cell are avoided.

The effect of *n*-hexadecane on the solvent quality can be characterised by an increase of the cloud point of PS solutions. In fig. 5.8 the cloud point T_c of PS solutions of concentration 500 g/m^3 is plotted as a function of the weight fraction w_{hex} of *n*-hexadecane in mixtures with decalin. Three molecular weights were used, as indicated. For $T > T_c$ a solution is clear, for $T < T_c$ it is cloudy by phase separation. As expected, the addition of the non-solvent *n*-hexadecane to decalin solutions of PS leads to flocculation of the polymer at a certain value of w_{hex}. Hence, the solvent quality is indeed decreased by *n*-hexadecane. According to polymer solution theory, the cloud point approaches the θ-temperature Θ for infinitely long chains. The extrapolation to infinite chain length should be made in a plot of $1/T_c$ as a function of $M^{-1/2}$[24]. The value of T_c for $M \rightarrow \infty$ (= Θ) thus obtained is indicated in fig. 5.8 by the dashed line. In pure decalin Θ is about 16 °C (fig. 5.8). Our experiments were carried out at ≈ 22 °C, where decalin is

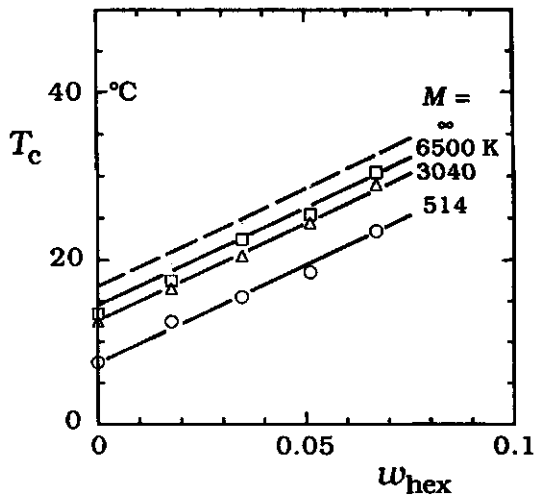

Figure 5.8 Cloud point T_c of PS in solvent/non-solvent mixtures of decalin and hexadecane as a function of the weight fraction w_{hex} of hexadecane, for different molar masses, as indicated. The dashed line is an extrapolation to infinite chain length and gives thus the Θ-point. Polymer concentration 500 g/m^3.

thus a slightly better than θ-solvent for PS.

The effect of *n*-hexadecane on the adsorption kinetics for M=3040 K shown in fig. 5.9 for three values of w_{hex}: 0, 0.035 and 0.051. The inset shows the same experiments on a longer time scale. The experiments were carried out at 22 °C, which is for w_{hex}=0 about 6 °C above Θ, for w_{hex}=0.035 about 2.5 °C below Θ, and for w_{hex}=0.051 about 6.5 °C below Θ. For the latter experiment it was even 2 °C below the cloud point of a ten times more concentrated solution of c=500 g/m^3. During the experiment at w_{hex} = 0.051 the solution was clear, but one day after we noted a blue haze, indicating incipient phase separation.

The initial slopes in fig. 5.9 are the same for all three experiments. Since the hydrodynamic conditions are hardly affected by the addition of *n*-hexadecane, the same must apply to the optical calibration, and thus dn/dc of the polymer. However, the final level in fig. 5.9 increases with w_{hex}. Since the optical calibration is not affected by the addition of *n*-hexadecane, the increase of the final level must reflect an increase of the final adsorbed amount Γ_f. The increase of Γ_f is in accordance with the expectation that *n*-hexadecane decreases the solvent quality. The inset shows that the two lower curves approach a constant level after some minutes, which indicates that the adsorbed layer is saturated. In contrast, the adsorbed amount for the upper curve corresponding to the unstable

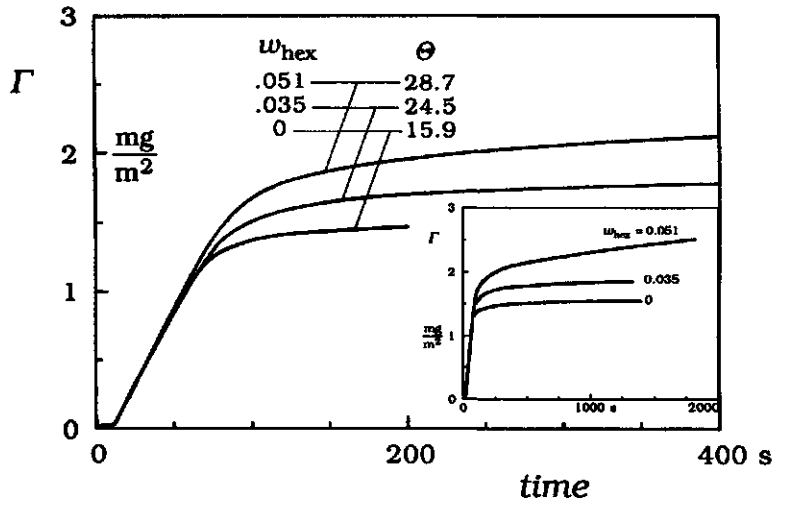

Figure 5.9 Adsorption kinetics of PS in different solvent/non-solvent mixtures of decalin and hexadecane. The weight fraction w_{hex} and the corresponding Θ-point of the solution are indicated. The inset shows the same experiments on a longer time-scale. $M = 3040$ K, $c = 50$ g/m^3 and $T \approx 22$ °C.

solution, is a continuously increasing function of time. Presumably, this increase reflects incipient phase separation at the interface.

We want to stress that in fig. 5.9 the increase of Γ_f goes along with a wider transport limited region, as indicated by the longer initial straight line. This is rather unexpected beforehand. The additional adsorption due to a decrease of the solvent quality could also have taken place at a lower rate, somewhere in the transition region towards saturation. Apparently, a decrease of the solvent quality affects mainly the fast part of the adsorption process.

Control experiments for another molecular weight (514 K) showed a similar extension of the transport limited region in the presence of *n*-hexadecane. Also the coincidence of curves $\Gamma(ct)$ for different concentrations was preserved in mixtures with *n*-hexadecane. From this we conclude that by the addition of *n*-hexadecane the attachment process remains essentially the same, but its influence on the adsorption rate is shifted to somewhat higher values of the adsorbed amount.

Final adsorbed amounts for $w_{hex} = 0.035$ are plotted in fig. 5.6 as a function of M for $c = 50$ (filled circles) and 500 g/m^3 (filled squares). The value of $w_{hex} = 0.035$ closely corresponds to θ-conditions in the experiment. The results of Vander Linden and Van Leemput for PS adsorption on silica were also obtained under θ-conditions (cyclohexane,

35 °C), but at a higher concentration (2000 g/m^3; open triangles). For a comparison of our results on oxidised silicon and theirs on dispersed silica we should therefore use our values at 500 g/m^3. Considering the fact that Γ_f is still lower than the equilibrium level and the completely different techniques used, the results compare quite favourably.

5.3.3 Effect of a displacer

In order to decrease the adsorption energy of PS we decided to use a displacer. Van der Beek et al.[14-17] showed that the effective segmental adsorption energy of a polymer can be varied in a quantitative manner by the use of mixed solvents, one of which is a displacer of the polymer. As the displacing solvent ethyl acetate was chosen, which is a strong displacer of PS[17]. Consequently, only small amounts are needed to decrease the adsorption energy. Therefore we do not expect a large influence of ethyl acetate on the hydrodynamic conditions and the optical calibration.

In fig. 5.10 the effect of the weight fraction w_{eth} of ethyl acetate in decalin solutions on the final adsorbed amount of PS is given for M=20000 K. As expected, the adsorbed amount decreases with increasing concentration of the displacer. The shape of the curve is in good agreement with experimental results of van der Beek[16] and with equilibrium calculations using the Scheutjens-Fleer theory[14]. An extrapolation of the

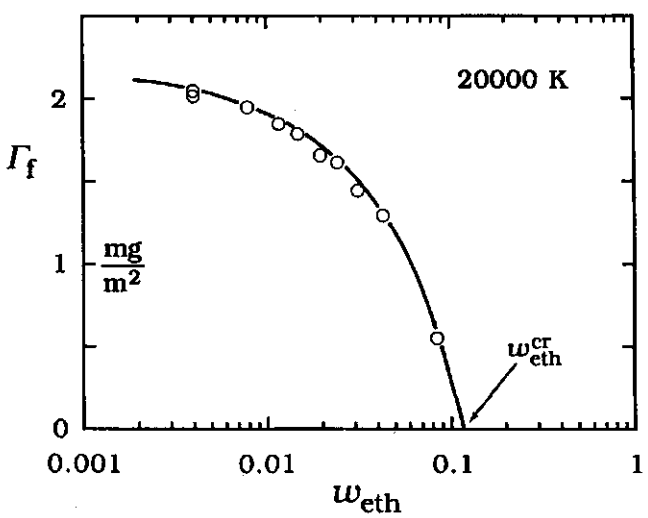

Figure 5.10 Final adsorbed amount of PS in solvent mixtures of decalin and ethyl acetate as a function of the weight fraction w_{eth} of ethyl acetate. From the intercept with the abscissa the critical ethyl acetate fraction w_{eth}^{cr} is determined to be 0.11. Polymer concentration 50 g/m^3.

experimental data to zero adsorbed amount gives the so-called critical displacer concentration w_{eth}^{cr} of ethyl acetate. We find w_{eth}^{cr} = 0.11. Unfortunately it is not possible to calculate quantitatively from this the segmental adsorption energy χ_s (PS/decalin), since the adsorption energy of ethyl acetate from decalin and the solvency parameters are not known. Van der Beek found for χ_s (PS /cyclohexane) a value of 1.9[16]. We expect that χ_s (PS/decalin) is more or less the same, since these solvents are chemically quite similar, and the interaction with the silica surface is very weak for both.[1]

Figure 5.11 shows the effect of ethyl acetate on the adsorption kinetics for M=20000 K for four weight fractions of ethyl acetate. Before t=0 solvent of the same decalin/ethyl acetate composition was injected into the cell. At t=0 the injection of polymer solution starts. The initial slope is the same in all solvents, regardless of the concentration ethyl acetate. As discussed already for *n*-hexadecane, this implies that the addition of ethyl acetate does not affect the optical calibration, and thus dn/dc of the polymer. This, in turn, is an indication that ethyl acetate is not (strongly) associated to PS, since that would probably lead to a change in the optical properties. In the final adsorbed amount Γ_f a peculiar irregularity occurs: the first addition of ethyl acetate leads to a considerable increase in Γ_f as compared to pure decalin. Each further increase of w_{eth} leads to a decrease in Γ_f, which can be explained by a decrease of the adsorption energy. We do not have an explanation for the increase of Γ_f upon first addition of ethyl acetate.

As to the kinetics, an important observation can be made. The displacer mainly affects the extension of the transport limited region. For w_{eth} = 0.008 the adsorption rate is transport limited up to $\Gamma \approx 1.5$ mg/m^2, whereas for w_{eth} = 0.085 the adsorption rate is close to zero already at $\Gamma \approx 0.5$ mg/m^2. The region of transition from mass transfer limitation to

---

[1] A remarkable difference exists between w_{eth}^{cr} in decalin and in carbon tetrachloride. We find in decalin w_{eth}^{cr} = 0.11, whereas Van der Beek et al. give for CCl_4 w_{eth}^{cr} = 0.017 [17]. According to displacement theory, for not too low values of χ_s (polymer/ solvent) any differences in w^{cr} between two solvents are entirely due to the solvency parameters between solvent and polymer or displacer, respectively [14]. Using this theory we calculated that approximately χ(ethyl acetate/decalin) - χ(ethyl acetate/carbon tetrachloride) $\cong$ - 2. A similar effect of the solvent on w^{cr} of strong displacers was reported by Kawaguchi [25]. Kawaguchi found for w^{cr} of acetone displacing PS from silica a value of 0.11 in cyclohexane, and 0.017 in carbon tetrachloride. For dioxane an even larger difference was found. We conclude that solvency effects between strong displacers and the solvent may have a large effect on the critical displacer concentration.

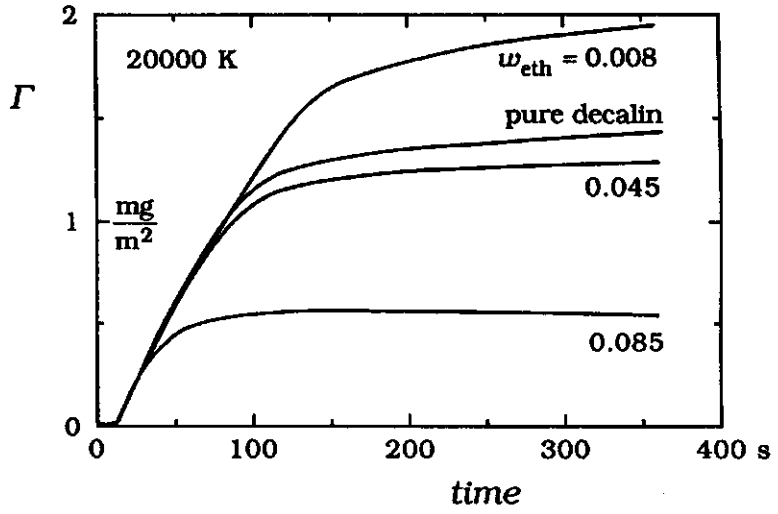

Figure 5.11 Effect of a low molecular weight, strong displacer on the adsorption kinetics of PS. The weight fraction w_{eth} of the displacer ethyl acetate in solvent mixtures of ethyl acetate and decalin is indicated. Polymer concentration 50 g/m^3.

saturation is more or less congruent for all curves. Since attachment is rate-limiting in this part of the curve, the results suggest that the rate of the attachment step is mainly determined by the distance to saturation, and not so much by the amount already adsorbed.

5.3.4 Polystyrene with a polar end group

In this section we consider the effect of a polar end group on the adsorption of a low molar mass polystyrene (M = 17 K). The polymer chain contains now at one end a single iminium ion end-group. In fig. 5.12.a the adsorbed amount of such an end-capped polymer (PS-X) is plotted as a function of time and the results are compared with those for normal polystyrene (PS). First we compare the adsorption of PS-X and PS for c=5 g/m^3. For PS the adsorbed amount reaches after a short time a stable saturation value of about 0.9 mg/m^2. For PS-X, the adsorbed amount at the end of the experiment is much higher, around 1.5 mg/m^2. This is not yet a saturation value, since Γ continues to increase slowly. Probably, the reason for the enhanced adsorption is the strong binding of the iminium ion end group to the silica. More molecules can be accommodated in the adsorbed layer because of the end-on attachment. The extra adsorption due to the end group proceeds at a rate which is initially mainly governed by mass transfer from the bulk solution (compare initial sections in fig. 5.12.b), and later on by a much slower adsorption process. The effect of

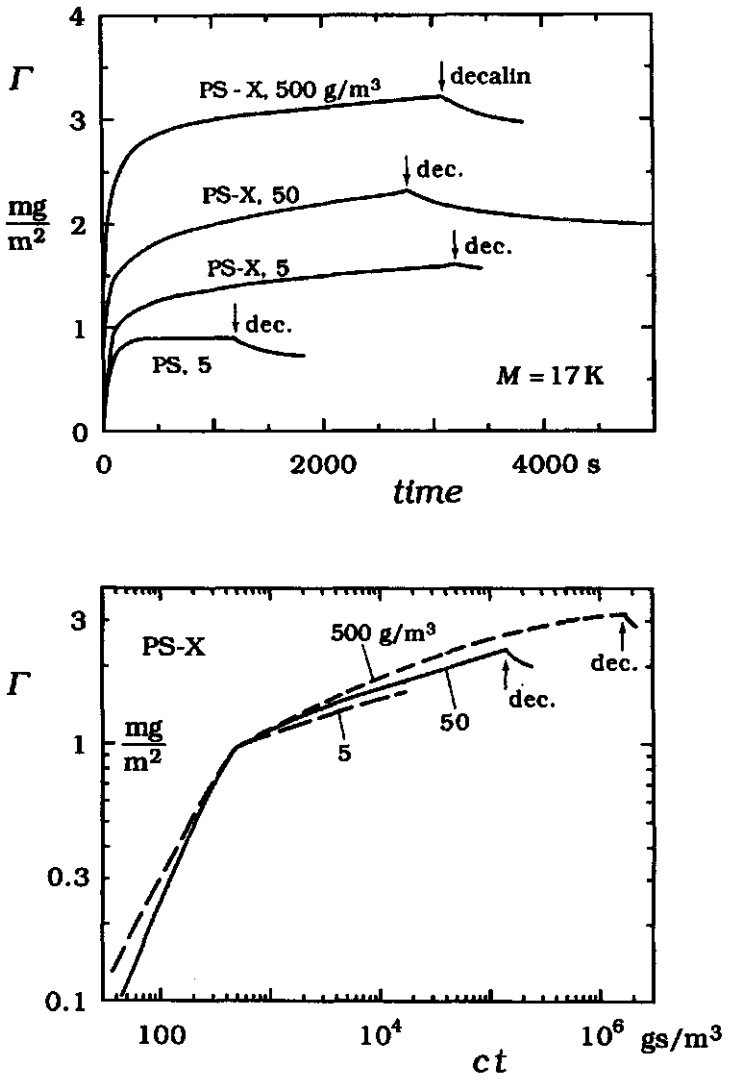

Figure 5.12.a and **b** Comparison of the adsorption kinetics of polystyrene with alkane and iminium-ion end group (PS, and PS-X, respectively), and effect of the concentration c on the adsorption of PS-X. In (a) the experiments are given as $\Gamma(t)$, whereas in (b) the same curves for PS-X are replotted as $\Gamma(ct)$, now double logarithmically. The curves in (a) suggest that the saturated value of Γ is strongly concentration dependent. However, figure (b) shows that the adsorption proceeds in the same direction for different concentrations (see also text).

the iminium ion end group is comparable to that of an increase of the chain length (cf. fig. 5.3).

The two experiments at a higher concentration are included in fig. 5.12.a for a misleading purpose. In the plateau region $d\Gamma/dt$ is low and not so much different for the three concentrations of PS-X. From this it might be concluded that the levelling-off corresponds to near-saturation, and that

thus the adsorption isotherm $\Gamma(c)$ strongly increases with c. This is, in our opinion, a false conclusion. In order to explain this, we replotted in fig. 5.12.b the curves of PS-X, but now Γ is given as a function of the product ct of concentration and time, on a double logarithmic scale. These curves for the three concentrations more or less coincide, like the curves $\Gamma(ct)$ in fig. 5.4 for PS of molar mass 3040 K. This implies that also the adsorption rate of PS-X can be described by a combination of mass transfer and an attachment step with a rate proportional to the concentration, as discussed in section 5.3.1. The results in fig. 5.12.b suggest that the adsorption for different concentrations proceeds in the same direction along a kind of master curve, at a rate proportional to c. Nevertheless, the final adsorbed amount in fig. 5.12.a is strongly concentration dependent, since the end points of the experiments lie far apart on the concentration time scale of the master curve. It could well be that the equilibrium values of Γ are hardly dependent on concentration, as predicted by polymer adsorption theory. We conclude that the concentration dependence of Γ_f in fig. 5.12.a is kinetically determined, and that the observed values of Γ_f of PS-X may be far below equilibrium values, especially for the two lower concentrations.

5.4 Discussion

A picture of the adsorption process should take into account the following experimental findings:

(i) The adsorption rate is proportional to solution concentration for every Γ (fig. 5.4 and 5.12.b). Nowhere an effect of the age of the adsorbed layer on $d\Gamma/dt$ is observed.

(ii) The duration of the region of the adsorption curve where $d\Gamma/dt$ equals the maximum mass transfer rate increases with increasing chain length (fig. 5.3), with decreasing solvent quality (fig. 5.9), and with increasing adsorption energy (fig. 5.11).

(iii) The dependence of the final value of the adsorbed amount on chain length, solvent quality and adsorption energy is at least qualitatively in agreement with equilibrium polymer adsorption theory.

Check of local equilibrium

The rounded shape of the adsorption curve $\Gamma(t)$ at higher coverage was in section 5.3.1.2 attributed to the influence on the adsorption rate of the attachment of a chain to the surface. However, since the final adsorbed amounts are in qualitative agreement with equilibrium, and because the

maximum mass transfer is to a large extent rate limiting, the question arises whether the adsorption curves $\Gamma(t)$ can be described using the local equilibrium concept discussed in chapter 4. Therefore, we first check the applicability of this concept.

According to the concept of local equilibrium the adsorption rate is mass transfer limited and, for a stagnation point flow, described by eq. 5.1. The concept amounts to the assumption that in eq. 5.1 the surface concentration c_s is determined by equilibrium between the adsorbed layer and directly adjacent solution, and can thus be described by the adsorption isotherm of the polymer. The bulk concentration c_b is that of the solution which is injected, and only at saturation, when there is full equilibrium between the bulk solution and the surface, c_b equals c_s. As long as c_s is smaller than c_b there is a flux of polymer to the surface, and the adsorption increases. Due to the high affinity of a polymer adsorption isotherm c_s is very low until close to saturation, and thus negligibly small as compared to c_b. Consequently, according to eq. 5.1 the adsorption rate should be constant and equal to kc_b until close to saturation, and then it falls abruptly to zero at saturation. Polymer adsorption isotherms calculated with the theory of Scheutjens and Fleer are under nearly all conditions of the high affinity type, except for very short chains consisting of only a few tens of segments or for χ_s near its critical value. Therefore, on the basis of theory we expect a constant adsorption rate until close to saturation. This is in contrast with our experimental adsorption curves for PS, which under all conditions have a clearly rounded shape.

The existence of local equilibrium can be tested using experimental results only by comparing adsorption isotherms obtained under static and dynamic circumstances. For the 'static' isotherm we use values of Γ_f obtained at different concentrations. The 'dynamic' isotherm is calculated from an adsorption curve $\Gamma(t)$ assuming local equilibrium during adsorption. Hence, during adsorption Γ should be determined by c_s according to the isotherm of the polymer, and we call $\Gamma(c_s)$ the 'dynamic' adsorption isotherm.

The concentration c_s during adsorption can be obtained from eq. 5.1, which describes the flux J $(=d\Gamma/dt)$ of polymer to the surface. The transport coefficient k in this equation can be determined from the initial adsorption rate according to $k = (d\Gamma/dt)_0 / c_b$ (see section 5.3.1.1). Substituting this expression for k in eq. 5.1 we obtain

$$c_s = c_b\left\{1 - \frac{d\Gamma/dt}{(d\Gamma/dt)_0}\right\} \qquad (5.6)$$

With eq. 5.6 c_s can be determined from an adsorption curve $\Gamma(t)$ at any moment during adsorption, and from this a dynamic adsorption isotherm $\Gamma(c_s)$ is obtained.

A 'static' and calculated 'dynamic' adsorption isotherm are given in fig. 5.13 for M = 3040 K. The static isotherm $\Gamma_f(c)$ is of the high affinity type, as expected for a high molar mass polymer. The dynamic isotherm $\Gamma(c_s)$ has a rounded shape and gives lower values of Γ. If there had been local equilibrium during adsorption, both isotherms would have been identical. However, this is clearly not the case, and thus there is no local equilibrium during adsorption. This is the same conclusion as we reached before on the basis of theoretical adsorption isotherms.

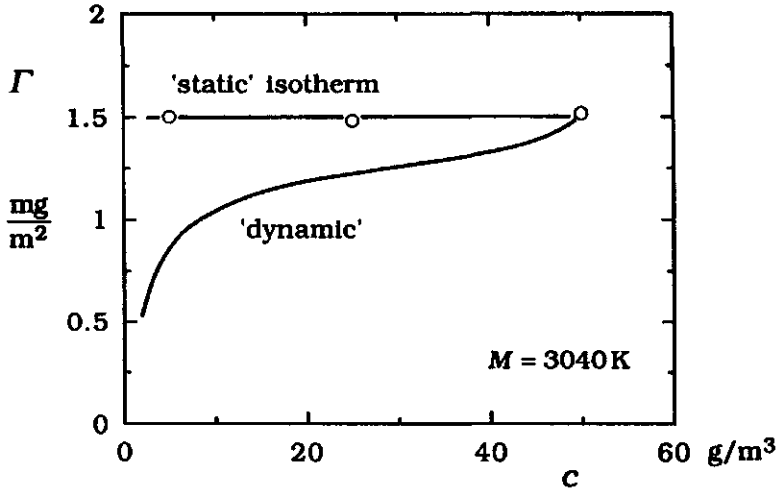

Figure 5.13 Experimental check of the existence of local equilibrium during adsorption of PS by comparison of a 'static' and 'dynamic' adsorption isotherm. The static isotherm is given by the final adsorbed amount at different concentrations. The dynamic isotherm is calculated from a curve $\Gamma(t)$ under the assumption of local equilibrium. Since both isotherms do not coincide, there is no local equilibrium.

Attachment of a chain to the surface

Since local equilibrium cannot explain the rounded shape of the curve $\Gamma(t)$, we now elaborate the idea that the attachment of a chain to the surface is rate-limiting at higher coverage, as discussed in 5.3.1.2. According to the analysis in 5.3.1.2, from the observed adsorption rate an attachment rate constant $K(\Gamma)$ can be extracted, which only depends on

the adsorbed amount and not on mass transfer conditions.

A strong argument in favour of the idea of an attachment step is the finding that the adsorption rate is at any Γ proportional to the solution concentration, and thus to the rate at which collisions occur between free chains and the surface with adsorbed layer. We imagine that these collisions occur by thermal motions, and that they lead to adsorption with a certain probability between zero and unity, depending on conditions. As long as successful collisions occur at a rate high enough to keep the surface concentration c_s of free molecules low as compared to the bulk concentration c_b, the mass transfer is entirely rate limiting in the adsorption process. When successful collisions occur less frequently, $d\Gamma/dt$ decreases and a finite concentration c_s develops. The mass transfer rate becomes then smaller due to the decreasing concentration gradient between surface and bulk solution. The question is now, by which factors the adsorption probability during a collision is determined, or, equivalently, which factors determine $K(\Gamma)$.

Most of the experimental results suggest that the adsorption of PS is not too far from equilibrium. In a saturated layer the dependencies of the final adsorbed amount Γ_f on M, χ and χ_s are in qualitative agreement with predictions of equilibrium theory, suggesting that Γ_f is determined by equilibrium, and thus by energetic and entropic factors. Moreover, the duration of the initial adsorption region is directly affected by two energetic factors, namely solvent quality and adsorption energy. We therefore consider it to be plausible that the adsorption probability during initial adsorption and also at higher coverage can be described using energetic and entropic arguments.

Before we do this, we first briefly recall the factors that in equilibrium contribute to the free energy of exchange of a polymer chain in solution against solvent molecules at the interface. The free energy of exchange is composed of the following terms:

- adsorption energy, expressed by χ_s. Usually χ_s is of the order of one or a few kT per segment. Since long chains may be attached by hundreds or even thousands of segments, the adsorption energy per chain may be very high.
- mixing energy, expressed by χ. For athermal solvents (χ=0) this term is zero. For $\chi > 0$ demixing is energetically favoured.
- loss of conformational entropy of the polymer chain, due to reduced orientational freedom at the surface.

- mixing entropy; the demixing due to the segregation of a concentrated surface phase from a dilute, homogeneous polymer solution leads to an entropy loss. Alternatively, this can be seen as an osmotic pressure in the adsorbed layer.

Usually, polymer adsorption is favoured by the energetic terms, and opposed by the entropic factors. In equilibrium their sum is zero.

Now we discuss the attachment of a free chain in terms of energetic and entropic arguments. For a polymer molecule approaching a bare surface there is no barrier to actually reach the surface. The formation of new polymer-surface contacts, the unfolding of the coil, and the concomitant formation of a concentrated surface phase are practically simultaneous processes. We therefore expect that the free energy decreases continuously during adsorption on a bare surface. As a result, each collision between a free chain and a bare surface leads to adsorption, and the adsorption probability equals unity.

For adsorption on a surface covered already with a polymer layer a balance between repulsive and attractive forces during a collision determines whether or not adsorption occurs. On approach of a chain towards a surface with an adsorbed layer a repulsive osmotic pressure builds up due to overlap and penetration by the incoming molecule. This may be accompanied by entropy loss due to chain deformation. On the other side of the balance is the gain in adsorption energy due to the formation of new polymer surface contacts. If during the collision this gain of adsorption energy is not high enough, then the chain is quickly expelled by the force of the entropic terms. If the initial contact is successful, then the newly adsorbed chain will try to attain an equilibrium conformation with more segments adsorbed. This process involves partial displacement of surrounding adsorbed molecules. As will be shown in the next chapter, displacement of short polystyrene chains by longer ones is a slow process. We therefore suggest that the time needed to reach conformational equilibrium in an adsorbed polystyrene layer may be rather long.

During a collision of a free chain with a surface, the gain in adsorption energy is proportional to the number of surface contacts made by the incoming chain, and the adsorption energy per contact. New contacts can be made by occupying free sites, or by displacing adsorbed segments of surrounding molecules. If displacement is a slow process, this displacement is less important. An increase of the segmental adsorption χ_s leads to stronger attraction and thus to a higher adsorption probability.

Consequently $d\Gamma/dt$ increases. This is consistent with the experimentally observed increased duration of the mass transfer limited region with increasing χ_s. We can also imagine that the gain in adsorption energy increases with chain length, since for long chains more free sites are available than for shorter ones. Consequently, the adsorption probability and $d\Gamma/dt$ increase with chain length. Again, this is consistent with the experimental results for different molar masses.

The effect of a gain in adsorption energy is opposed by the repulsive barrier formed by the adsorbed layer. This barrier mainly consists of two contributions: demixing of polymer and solvent, resulting in entropy loss and energy gain, and chain deformation, leading to entropy loss. With decreasing solvent quality, the energy gain increases, so that the barrier becomes less repulsive, and an incoming chain obtains more opportunities to form surface contacts. Therefore the adsorption probability during a collision increases with decreasing solvent quality. Accordingly, $d\Gamma/dt$ should increase. In experiments, indeed an increased duration of the mass transfer limited region is observed upon a decrease of the solvent quality.

In general, we would expect that with increasing adsorbed amount the repulsive barrier formed by the adsorbed layer increases, and that the gain in adsorption energy upon initial contact decreases. As a result, the adsorption probability, and thus $d\Gamma/dt$ should decrease with increasing coverage. This is indeed observed under all conditions for all molar masses. The decrease in $d\Gamma/dt$ can be quantitatively described by the attachment rate constant $K(\Gamma)$. Figure 5.5 shows for M = 3040 K that $K(\Gamma)$ decreases strongly from 10^{-5} m/s at low coverage (0.5 mg/m^2) to 10^{-9} m/s at 1.5 mg/m^2, which is probably close to saturation. The decrease in $K(\Gamma)$ with increasing Γ reflects the decreasing adsorption probability. Unfortunately, we are not yet able to establish a direct, quantitative relation between $K(\Gamma)$ and the adsorption probability.

Comparison with other results

As already pointed out in section 5.1 systematic studies on the kinetics of adsorption of polystyrene have not been published before. Therefore, a comparison is hardly possible and we only discuss results of Lee and Fuller[26], which seem to be in agreement with the presence of an attachment step as found in this chapter.

Lee and Fuller[26] studied the effect of flow on the adsorption and desorption kinetics of polystyrene. The authors observed that for high M (>4000 K) both $d\Gamma/dt$ and Γ_f decrease with increasing shear rate $\dot{\gamma}$. The

inhibiting effect increases with chain length and for M = 20000 K it starts at $\dot{\gamma} \approx 400\ s^{-1}$. The concentration ($\approx 1000\ g/m^3$) was high enough to ensure that transport could nowhere be rate limiting. These results suggest that the flow field reduces the adsorption probability during a collision with the surface. For adsorbed layers formed in rest ($\dot{\gamma} = 0$) during 24 h, a considerable, flow-induced desorption occurred, but at much higher values of $\dot{\gamma}$ ($> 5000\ s^{-1}$) than needed for flow inhibited adsorption. From this it was concluded that initially a polystyrene molecule adsorbs by a few segment-surface contacts, and that in an equilibrated layer much more segments are adsorbed. Our view of the adsorption process points in the same direction.

5.5 Conclusions

The kinetics of adsorption and desorption of polystyrene from decalin solutions onto silica were studied by reflectometry in a stagnation point flow. It was found that for all molar masses studied (3 K < M < 20000 K) the initial adsorption rate is entirely determined by mass transfer from the bulk solution. Between the initial mass transfer limited part of the adsorption curve and saturation the adsorption rate $d\Gamma/dt$ decreases gradually, due to the build-up of the adsorbed layer. For the whole adsorption curve, $d\Gamma/dt$ is proportional to the solution concentration. For the initial part this reflects the mass transfer limitation. At higher coverage it implies that the attachment of a chain to the surface affects the adsorption rate. By an analysis of the adsorption curve we were able to extract an attachment rate constant $K(\Gamma)$, that depends only on the adsorbed amount and not on mass transfer conditions. The chain length dependence of the final adsorbed amount indicates that decalin at 22 °C is (near to) a Θ-solvent for PS. This is confirmed by cloud point measurements, from which we determined that $\Theta \approx 16$ °C.

The influence of the addition of n-hexadecane (a non-solvent for PS) and ethyl acetate (a strong displacer of PS) on the final adsorbed amount shows that these additives decrease the solvent quality and adsorption energy, respectively.

Variation of the chain length, solvent quality, and adsorption energy mainly affects the extent of the mass transfer limited part of the adsorption curve; the shape and size of the transition region to saturation remain more or less the same. From this we infer that the rate of the attachment step is mainly determined by the distance to saturation and not so much by the value of the adsorbed amount. In our opinion these results are

consistent with the following picture of the attachment process. During a collision between a free molecule and the surface with adsorbed layer the adsorption probability depends on a balance between the gain in adsorption energy and the repulsive interaction with the adsorbed layer. The gain in adsorption energy during a collision decreases when a displacer is added, and increases with chain length since long chains can make more contacts. By a decrease of the solvent quality the repulsion by the adsorbed layer is reduced.

Desorption into a flow of pure solvent was only observed for low molar masses. The desorption rate was considerably lower than the one predicted for mass transfer limited desorption assuming local equilibrium near the surface. This result indicates that the equilibration is slow.

It was found that a strongly adsorbing end group enhances adsorption. Most of the extra adsorption due to the end group takes place at a rate which is limited by the attachment to the surface.

As consequence of the finding that up to saturation the adsorption rate of polystyrene is proportional to solution concentration, the time needed to attain equilibrium is *inversely* proportional to concentration. For low c the equilibration time thus becomes extraordinary long. In order to obtain an adsorption isotherm it is therefore advisable to determine the adsorbed amount after a fixed value of the product ct of concentration and time, and not after a fixed time.

5.6 References

(1) Stromberg, R.R.; Passaglia, E.; Tutas, D.J. *Journal of Research of the National Bureau of Standards-A. Physics and Chemistry* **1963**, *67A*, 431.

(2) Stromberg, R.R.; Tutas, D.J.; Passaglia, E. *J. Phys. Chem.* **1965**, *69*, 3955.

(3) Stromberg, R.R.; Smith, L.E. *J. Phys. Chem.* **1967**, *71*, 2470.

(4) Kawaguchi, M.; Takahashi, A. *J. Polym. Sci., Polym. Phys. Ed.* **1980**, *18*, 943.

(5) Kawaguchi, M.; Hayakawa, K.; Takahashi, A. *Macromolecules* **1983**, *16*, 631.

(6) Kawaguchi, M.; Hattori, S.-i.; Takahashi, A. *Macromolecules* **1987**, *20*, 178.

(7) Kawaguchi, M.; Anada, S.; Nishikawa, K.; Kurata, N. *Macromolecules* **1992**, *25*, 1588.

(8) Takahashi, A.; Kawaguchi, M.; Hirota, H.; Kato, T. *Macromolecules* **1980**, *13*, 884.
(9) Vander Linden, C. "*Adsorption du Polystyrene sur la silice*"; Université libre de Bruxelles, **1976**, thesis
(10) Frantz, P.; Leonhardt, D.C.; Granick, S. *Macromolecules* **1991**, *24*, 1868.
(11) Loulergue, J.C.; Lévy, Y.; Allain, C. *Macromolecules* **1985**, *18*, 306.
(12) Zhang, Y.; Levy, Y.; Loulergue, J.C. *Surface Sci.* **1987**, *184*, 214.
(13) Grant, W.H.; Smith, L.E.; Stromberg, R.R. *Faraday Discuss. Chem. Soc.* **1975**, *59*, 209.
(14) Cohen Stuart, M.A.; Fleer, G.J.; Scheutjens, J.M.H.M. *J. Colloid Interface Sci.* **1984**, *97*, 515.
(15) Cohen Stuart, M.A.; Fleer, G.J.; Scheutjens, J.M.H.M. *J. Colloid Interface Sci.* **1984**, *97*, 526.
(16) Van der Beek, G.P.; Cohen Stuart, M.A.; Fleer, G.J.; Hofman, J.E. *Langmuir* **1989**, *5*, 1180.
(17) Van der Beek, G.P.; Cohen Stuart, M.A.; Fleer, G.J.; Hofman, J.E. *Macromolecles* **1991**, *24*, 6600.
(18) "*Polymer Handbook*"; Brandrup, J.; Immergut, E.H., Ed.; John Wiley and Sons: New York, **1989**, 3rd ed.; p. VII-441.
(19) Weill, G.; des Cloizeaux, J. *J. Phys. Fr.* **1979**, *40*, 99.
(20) Tsunashima, Y.; Nemoto, N.; Kurata, M. *Macromolecules* **1983**, *16*, 1184.
(21) Tsunashima, Y.; Nemoto, N. *Macromolecules* **1983**, *16*, 1941.
(22) Vander Linden, C.; Van Leemput, R. *J. Colloid Interface Sci.* **1978**, *67*, 48.
(23) Chin, S.; Hoagland, D.A. *Macromolecules* **1991**, *24*, 1876.
(24) Flory, P.J. In " *Principles of Polymer Chemistry*"; Cornell University Press: Ithaca, **1953**.
(25) Kawaguchi, M.; Chikazawa, M.; Takahashi, A. *Macromolecules* **1989**, *22*, 2195.
(26) Lee, J.-J.; Fuller, G.G. *J. Colloid Interface Sci.* **1985**, *103*, 569.

6 EXCHANGE KINETICS OF POLYMERS DIFFERING IN LENGTH ONLY

6.1 Introduction

In the previous chapters the role of the adsorbing chain was emphasised: transport through solution and attachment to the interface. Hardly any information was obtained on subsequent reorganisations in the adsorbed polymer layer. In polymer exchange, there is not only adsorption, but also desorption. The desorption is the result of a competition between chains in the adsorbed layer, and can therefore possibly be used as a probe of the dynamics of the adsorbed polymer layer.

For polymers the adsorption energy per molecule is usually very high due to the great number of segment-surface contacts. It is therefore extremely unlikely that desorption proceeds by simultaneous release of all segments. More probable is a segment-by-segment displacement process. The competition at a segmental level might be seen as an elementary step in the exchange process. We expect that the rate of this step depends on the interactions between polymer, surface and solvent. The displacement rate might also depend on the rate of conformational changes in the adsorbed layer, and thus on the stiffness of the polymer chain.

The rate of conformational changes could also be reduced by topological constraints. Examples of such constraints are the intertwining of chains, or the pinning of a molecule to the surface by a loop of another chain. Disentanglement and thus desorption proceeds by slow diffusional motions of the adsorbed chain. Probably, the formation of entanglements proceeds also slowly. One may therefore expect that the number of entanglements increases with time, so that the desorption rate of a polymer decreases with the residence time on the surface. Granick and co-workers have obtained some evidence that such processes indeed play a role[1,2]. The effect of topological constraints on the exchange kinetics presumably strongly depends on the chain length of the polymer.

In this chapter, we are only concerned with exchange of chemically identical polymers. The exchange of polymers of a different chemical nature will be discussed in the next chapter.

The driving force for the exchange between chemically identical polymers from dilute solutions is the (small) increase in translational entropy in solution when short chains are replaced by longer ones. In equilibrium longer chains are therefore preferentially adsorbed over shorter ones. According to the results of the Scheutjens-Fleer theory complete

preferential adsorption occurs as soon as the chains differ in length by a factor of about two or more[3].

Experimentally the exchange between chemically identical polymers is difficult to assess. Exchange between chains of equal length does not lead to any change at all in the adsorbed layer or solution. Here, the only method seems the use of labelled polymers. However, the label may itself influence the adsorption. Exchange between polymers of different length leads to a different composition of the surface and the solution that might be measurable without using labelled material. For example, the adsorbed amount Γ may increase if a layer of short chains is completely displaced by longer ones.

As yet there are only few experimental studies on polymer exchange kinetics. Using radioactively labelled polymers Pefferkorn et al.[4,5] studied the exchange between chains of equal length. For polyacrylamide (M=1200 K; here we define 1 K as 1 kg/mole) it was found that the exchange is indeed very slow, and still incomplete after 15 hours[4]. For polystyrene (M=360 K) adsorbed on silica from carbon tetrachloride solution again a slow exchange was observed[5].

Granick and co-workers[2,6,7] have studied the exchange between protonated and deuterated samples of one and the same polymer. These could be distinguished by their infrared absorption spectra. Exchange of poly(methyl methacrylate) (M=60 K) proceeded extremely slowly, at a rate of about 1 % of the mass adsorbed per hour[6]. For polystyrene (M=550 K) adsorbed on silica from cyclohexane[2] and carbon tetrachloride[7], it was found that the age of the pre-adsorbed polystyrene layer strongly affects the exchange kinetics. Effects of ageing times up to tens of hours were observed. This is an indication that after the initial adsorption process slow rearrangements take place, possibly leading to entanglements.

Kawaguchi et al. studied displacement of adsorbed polystyrene of low molar mass (102 K and 422 K) by longer chains (775 K) using ellipsometry[8]. After introduction of the higher molecular weight the adsorbed amount rapidly increased, but the final level for individual adsorption of M=775 K was not yet attained after 50 hours. In view of the small chain length difference the final situation might well reflect equilibrium, because the adsorption preference is possibly not complete. Alternatively, a kinetic barrier might be present.

It therefore seems that exchange between chemically identical polymers is often a slow process. Some results indicate the formation of entanglements on the time scale of hours. However the exchange

mechanism and factors influencing it are so far hardly understood.

The approach in this chapter is the following. The same polymers are used as in the previous chapters: poly(ethylene oxide) (PEO) and polystyrene (PS). Also, the same techniques are applied: reflectometry in a stagnation point flow, and, for one experiment, the streaming potential technique.

We will focus on the displacement of low (≈ 10 K) by high molecular weight samples (> 100 K). Due to this large chain length difference the adsorbed amount Γ increases considerably upon exchange, and reflectometry measurements can monitor the exchange accurately. The experimental results will be compared to a prediction based on the assumption of local equilibrium near the surface and mass transfer limited adsorption. For PEO these concepts were found to be applicable. For PS the local equilibrium cannot fully explain the results, and therefore a series of additional experiments were performed for this polymer.

6.2 Exchange according to local equilibrium

In section 4.2 the concept of local equilibrium was introduced to predict polymer adsorption and desorption rates in cases where the equilibration of the adsorbed polymer layer is faster than the mass transfer through solution. In the present section we apply this concept to the exchange of polymers.

In order to be able to explain the kinetics of polymer exchange, we first discuss an equilibrium adsorption isotherm from a solution containing a bimodal mixture of chain lengths. Throughout this chapter we will denote the shorter and longer chains of the mixture by 1 and 2, respectively. A theoretical adsorption isotherm for a solution of a mixture of chains of length $r_1 = 100$ and $r_2 = 1000$ segments is given in fig. 6.1. The total adsorbed amount Γ_t (full curve), and the contributions of 1 (dotted) and 2 (dashed) to Γ_t are given as a function of the concentration c_2 for a fixed value of $c_1 = 1$ ppm. Note the logarithmic scaling of the abscissa. The isotherm was calculated with the theory of Scheutjens and Fleer[9], extended to polymer mixtures.

The isotherm can be divided in three regions of surface composition: 1 only ($c_2 < 10^{-50}$ ppm), 1 and 2 ($10^{-50} < c_2 < 10^{-30}$ ppm), and exclusively 2 ($c_2 > 10^{-30}$ ppm). The region of mixed surface composition is situated at extraordinary low values of c_2. This reflects the strong preferential adsorption of longer chains. In practice, the preference is so high, that mixed layers only exist if insufficiently long chains are available. For

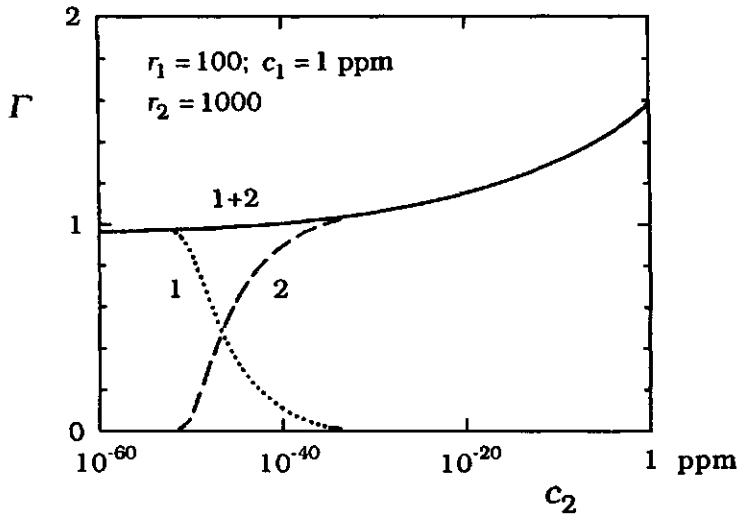

Figure 6.1 Theoretical adsorption isotherm from a solution containing a bimodal mixture of chain lengths. The chain lengths r_1 and r_2 are indicated and the concentration of 1 has a fixed value of 1 ppm. The isotherm was calculated with the theory of Scheutjens and Fleer. The adsorbed amount Γ is given in equivalent monolayers. The bulk volume fraction as given by the theoretical model was converted to ppm (= g/m^3) using a specific volume of 10^{-6} m^3/g. Segmental adsorption energy χ_s = 1.0, solvency parameter χ = 0.5, cubic lattice.

example, this may be the case when during adsorption the supply of 2 to the surface is limited by mass transfer from the bulk solution.

The region of mixed surface composition presents another important characteristic. The total adsorbed amount Γ_t is approximately constant, and about equal to Γ_1 in the absence of 2 ($c_2 < 10^{-50}$ ppm). In other words, during exchange according to equilibrium, adsorption of 2 is accompanied by an equal (mass) desorption of 1.

In order to arrive at a kinetic picture we now consider the mass transfer during exchange. As was extensively discussed in chapter 4, the steady-state flux J of polymer is proportional to the concentration difference $c^b - c^s$, where c^b and c^s are the polymer concentrations in the bulk solution and surface region, respectively:

$$J = k(c^b - c^s) \tag{6.1}$$

In this equation, k is a transport coefficient that depends on the hydrodynamics of the flow system and on the diffusion coefficient of the polymer. For stagnation point and capillary flow k is given by eqs. 5.1 and 4.1, respectively.

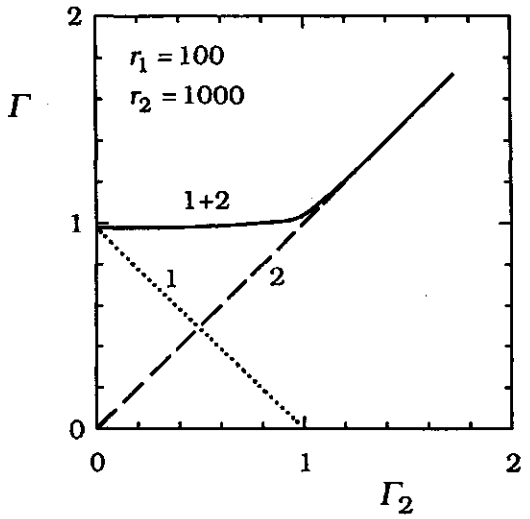

Figure 6.2 Equilibrium composition of mixed adsorbed layers, and exchange kinetics according to the local equilibrium concept. The adsorbed amounts Γ_1, Γ_2 and $\Gamma_t = \Gamma_1 + \Gamma_2$ are plotted as a function of Γ_2 according to the isotherm of fig. 6.1. For explanation, see text.

As an example, we discuss the exchange kinetics according to the adsorption isotherm in fig. 6.1. Imagine the following experiment. First an adsorbed layer of 1 is equilibrated with a solution of concentration c_1 = 1 ppm ($c_2 < 10^{-50}$ ppm in fig. 6.1). Since c_1 is uniform throughout the solution, we have $c_1^b = c_1^s = c_1$. Next, a solution of a mixture of 1+2 is injected, where the value of c_1^b is the same as before (i.e., 1 ppm) in order to avoid desorption of 1 by dilution. For the solution concentration c_2^b we choose also 1 ppm, which is the highest value in the isotherm of fig. 6.1.

According to eq. 6.1 the adsorption rate of 2 equals $k(c_2^b - c_2^s)$. The value of c_2^b remains constant at 1 ppm during the experiment, since continuously fresh solution is injected. We now assume that during adsorption of 2 the concentration c_2^s is determined by a local equilibrium near the surface between free and adsorbed molecules, which is described by the adsorption isotherm of the polymer. Hence, c_2^s equals c_2 according to the isotherm of fig. 6.1. Inspection of fig. 6.1 shows that $c_2^s << c_2^b$ for Γ nearly up to its final value for c_2^s = 1 ppm, at which value of c_2^s there is full equilibrium between the adsorbed layer and the bulk solution. Ignoring c_2^s during adsorption, we directly obtain $J \approx d\Gamma_2 / dt \approx kc_2^b$. The adsorption rate of 2 is constant nearly up to saturation, and it equals the *maximum* mass transfer rate from the solution. The adsorption rate of 2 is not influenced by the adsorption of 1.

The picture is shown in a different way in fig. 6.2. In this figure the isotherm values Γ_1, Γ_2 and $\Gamma_1 + \Gamma_2$ of fig. 6.1 are replotted, but now as a function of Γ_2 instead of c_2. The graph can be interpreted both in terms of equilibrium and in terms of kinetics. According to the equilibrium picture it shows the equilibrium surface composition of 1 and 2. In the range of mixed composition, the total adsorbed amount is constant (full curve).

The kinetic representation is as follows. According to the mass transfer limit we have $d\Gamma_2/dt = kc_2^b$. Since this adsorption rate is constant nearly up to saturation, integration immediately yields $\Gamma_2 = kc_2^b t$. Thus, replacing Γ_2 by $kc_2^b t$ transforms the abscissa into a (scaled) time-axis. The full curve then represents the total adsorbed amount during exchange of 1 by 2, which is constant in time. The dotted and dashed curves give the adsorbed amounts of 1 (nearly linearly decreasing in time) and 2 (linearly increasing), respectively. Diagrams like figure 6.2 will be used for the interpretation of experimental results.

6.3 Experimental

Materials

Aqueous solutions of PEO and decalin solutions of PS were prepared as described in chapters 3-4 and 5, respectively. For PS one experiment was performed in a mixture of decalin and toluene (93.5/6.5 w/w), and another in pure carbon tetrachloride. Toluene (Baker analysed) and carbon tetrachloride (Merck p.A.) were used without further purification.

For reflectometry the adsorbing surface was a strip cut from an oxidised silicon wafer. For streaming potential measurements it was the inside wall of a glass capillary.

Methods

A reflectometer as described in chapter 5 was used. For experiments with PS in decalin solutions all settings and the calibration were exactly the same as given in chapter 5. For the experiment with a toluene/decalin mixture the adsorbed amount was calculated using the same sensitivity factor as in pure decalin.

For the solvent carbon tetrachloride a separate calibration was performed, analoguously to that in chapter 5 for adsorption from decalin solutions. For this experiment a silicon wafer with an oxide film thickness of 128 nm was used. The angle of incidence on the wafer was 60°. The refractive index increment dn/dc for PS in carbon tetrachloride equals 0.156 cm^3/g at 633 nm[10]. Using this value of dn/dc the sensitivity

factor A_s as defined in eq. 2.9 was calculated. A value of 0.0217 m^2/mg was found.

For the experiments with PEO in water a wafer with oxide film thickness of 100 nm was used. The angle of incidence was 70°. The value of dn/dc for PEO in water equals 0.136 cm^3/g (chapter 3). Using this value of dn/dc we calculated A_s = 0.0232 m^2/mg in this case.

The streaming potential experiment for PEO was performed under exactly the same conditions as those described in chapter 4.

6.4 Results

6.4.1 Poly(ethylene oxide)

In fig. 6.3 an example of the exchange kinetics of PEO is given. The adsorbed amount as a function of time is plotted for injection of a solution of 1 or 2 only (dashed curves) and for a mixture of 1+2 (full curve). The molar masses of 1 and 2 were 7.1 K and 400 K, respectively. The difference $\Gamma_{1+2} - \Gamma_2$ is presented as the dotted curve.

At $t=0$ the injection of polymer solution starts. The adsorbed amount remains zero for a few seconds, due to the dead volume between valve and surface. For the individual adsorption of 1 and 2 (dashed curves) the adsorption rate is constant nearly up to saturation. As discussed

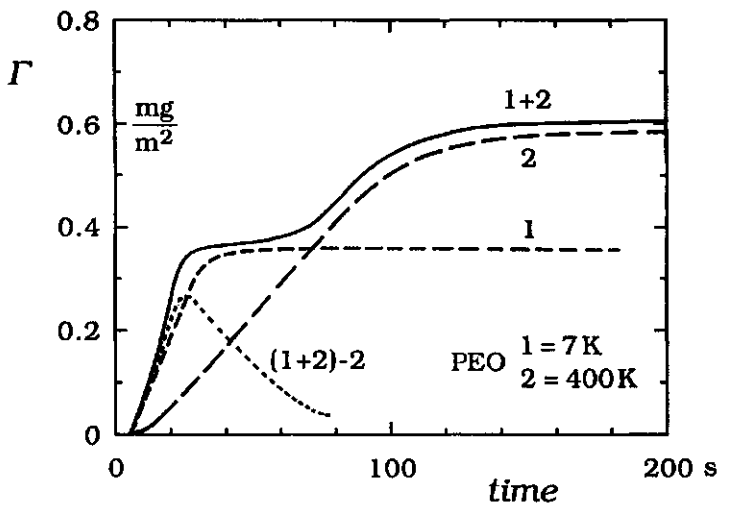

Figure 6.3 Exchange kinetics of PEO for adsorption from aqueous solution on silica. Experimental results are given for adsorption from a solution of 1+2 (full curve), and 1 or 2 individually (dashed). The dotted curve is the difference of the curves 1+2 and 2. The notation "1+2" is an abbreviation for "simultaneous addition of 1 and 2". Concentrations: c_1^b = 5.0, c_2^b = 10 g/m^3.

extensively in chapter 3 this rate is entirely determined by the *maximum* mass transfer kc_b from the bulk solution towards the surface.

For discussion of the curve for injection of 1+2 we can distinguish three regions: initial ($t<30$ s), middle ($30<t<70$ s) and final ($t>30$ s). In the initial part $d\Gamma/dt$ for the mixture of 1+2 practically equals the sum of the individual adsorption rates of 1 and 2. This implies that 1 and 2 adsorb independently at a rate limited by mass transfer from the bulk solution.

In the middle section Γ remains at a constant level that corresponds to the saturated value for adsorption of 1. In the final region the curves $\Gamma(t)$ for injection of 1+2 and 2 nearly coincide. From this we infer that no molecules 1 are left at the surface. Furthermore we conclude that the adsorption of 2 from the mixture 1+2 follows from the beginning onwards the dashed curve for individual adsorption of 2. This means that the adsorption of 2 from a solution of 1+2 is limited by the maximum mass transfer, and that there is no effect of adsorbed 1 on the adsorption rate of 2.

The above analysis implies that the adsorption of 1 in the experiment 1+2 is given by the difference $\Gamma_{1+2} - \Gamma_2$ (dotted curve). From fig. 6.3 it becomes apparent that in the middle section of the mixture experiment molecules 1 are exchanged by 2 at constant total mass adsorbed.

We may compare fig. 6.3 for $t>30$ s with fig. 6.2 in which exchange according to local equilibrium is plotted. In all respects the exchange kinetics of PEO is in agreement with the theoretical prediction. The adsorption of 2 is limited by the maximum mass transfer from solution, and during exchange of 1 by 2 the total adsorbed amount Γ_t remains constant at the value for individual adsorption of 1.

In the above experiment the molar mass of the displaced chain 1 is rather low, 7.1 K. It would be interesting to know whether for a longer chain the exchange kinetics is still the same. However, with increasing length of 1 the difference between the saturated values of Γ_1 and Γ_2 soon becomes too small for an accurate measurement. For long chains the hydrodynamic thickness δ_h is a more suitable quantity, since its value at saturation strongly depends on chain length at high molar mass (see chapter 4). For uncharged polymers like PEO δ_h can be obtained from the streaming potential.

The result $\delta_h(t)$ of a streaming potential experiment is plotted in fig. 6.4 for injection of a solution of 1+2. The molar masses of 1 and 2 were 100 K and 847 K, respectively. For 1 and 2 this is a factor of about 10 and 2, respectively, higher than in the reflectometry experiment of fig. 6.3. The

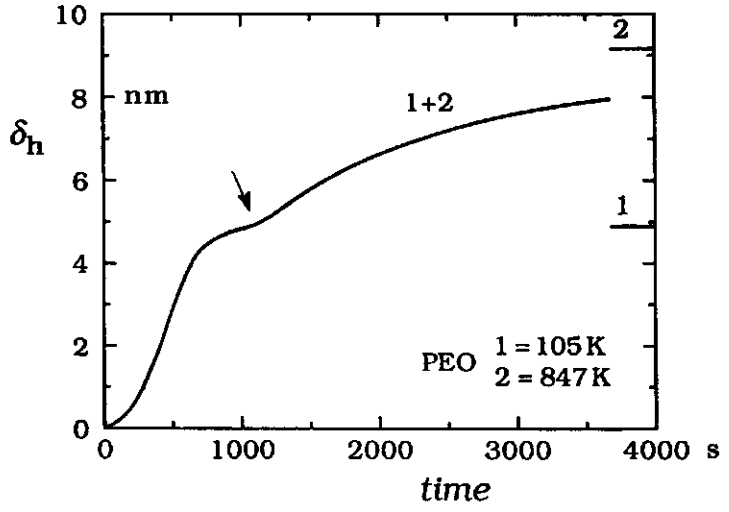

Figure 6.4 Exchange kinetics of high molar mass PEO in a streaming potential experiment. Along the ordinate the hydrodynamic thickness δ_h is plotted. To the right the saturated levels of 1 and 2 individually are indicated. Concentrations: $c_1^b = c_2^b = 0.50$ g/m^3.

saturated levels of 1 and 2 individually are indicated to the right.

The overall shape of the curve $\delta_h(t)$ resembles that of $\Gamma(t)$ for 1+2 in fig. 6.3. The arrow in fig. 6.4 points to a part of the curve where δ_h is at a nearly constant level that corresponds to saturation of 1. Probably, in this part 1 is exchanged by 2 at constant total mass adsorbed. The rate of transport, and, hence, the surface composition in the capillary is not uniform along its length, so that the streaming potential yields an average value of δ_h. This tends to smoothen the curve, so that a clear and well-defined plateau during exchange is not observed. Unfortunately $\delta_h(t)$ cannot be analysed quantitatively like $\Gamma(t)$, since δ_h is not an additive quantity. Nevertheless, qualitatively the exchange kinetics of high and low molar mass PEO look the same.

6.4.2 Polystyrene

6.4.2.1 Overshoot adsorption

An example of the exchange kinetics of PS is plotted in fig. 6.5 in the same way as in fig. 6.3 for PEO. In this case the molar masses of 1 and 2 are 9.2 K and 3040 K, respectively.

In the initial and final parts of fig. 6.5 the results for injection of 1+2 are similar for PS and PEO. For both polymers, the initial adsorption rate of 1+2 is limited by mass transfer from solution. The saturated value of Γ for

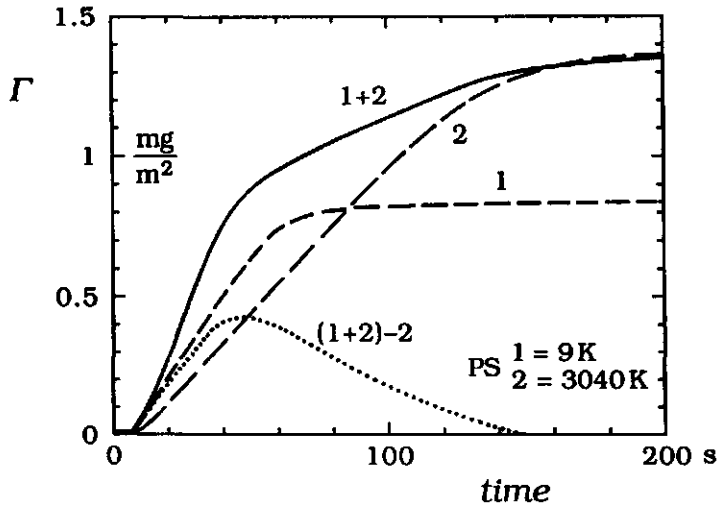

Figure 6.5 Exchange kinetics for adsorption of PS from decalin solutions on silica. The set-up of the experiment is the same as in fig. 6.3. Concentrations: c_1^b = 5.0, c_2^b = 25 g/m^3.

injection of 1+2 closely corresponds to that of 2, suggesting that all molecules 1 that were initially adsorbed are eventually displaced by 2.

However, the two polymers behave remarkably different during exchange (i.e., in the middle part), which for PS takes place for $40 < t < 140$ s in this experiment. For PS the adsorbed amount increases continuously during exchange, whereas for PEO it is constant in the middle part. For this difference we can imagine two explanations. Firstly, the increase of Γ during exchange of PS indicates a temporary overshoot of component 1 at the surface. Possibly, desorption of 1 is a slow process. A second possibility could be that local equilibrium is maintained during exchange of PS, but that for some reason the equilibrium adsorption theory does not fit the behaviour of PS.

In order to distinguish unambiguously between these two possibilities we performed a series of experiments which are presented in fig. 6.6 and 6.7. The idea of these experiments is to determine the surface composition $\Gamma_1(\Gamma_2)$ (like the dotted line in fig. 6.2) under static, equilibrium conditions and under dynamic conditions, like in fig. 6.5. If there is local equilibrium under the dynamic conditions, the curves $\Gamma_1(\Gamma_2)$ obtained under static and dynamic circumstances should be identical.

Figure 6.6 shows two experiments in which the order of adsorption of 1 and 2 is reversed (full curves). The lower curve represents a sequence of injection of 2, then pure solvent, and then 1. Henceforth, this sequence is

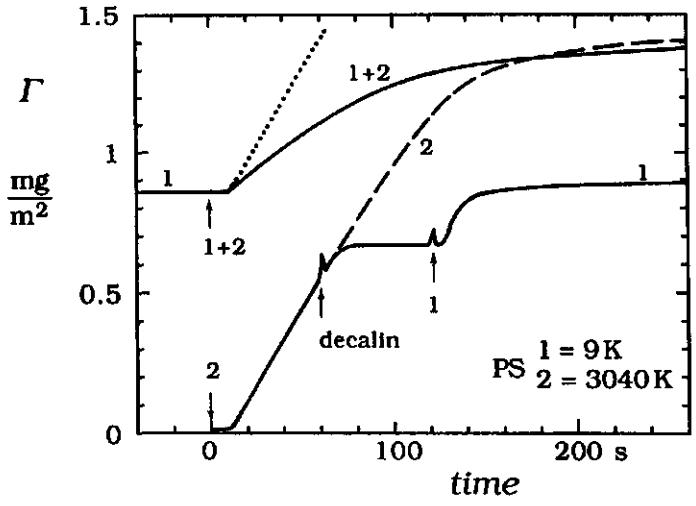

Figure 6.6 Sequential adsorption experiments with PS. The type of solution injected is indicated. The slope of the dotted line is drawn according to adsorption of 2 on a bare surface. Same molar masses and concentrations as for fig. 6.5. For explanation, see text.

denoted as 2,1. The upper curve is the result of injection of 1 followed by 1+2, which will be referred to as 1,1+2. For reference, we also plotted the result for continuous injection of 2 on an initially bare surface (dashed). The slope of the dotted line is drawn according to the adsorption rate of 2 on a bare surface.

We first discuss the sequence 2,1 (lower solid curve). From $t=0$ to 60 s a solution of 2 was injected. Then pure solvent was pumped into the cell, in order to prevent further adsorption, and to obtain an undersaturated layer of 2. Due to the high adsorption energy of long chains of PS no detectable desorption occurs in solvent flow. This is confirmed by control experiments in which the solvent flow was maintained over 1000 s.

At $t=120$ s the injection of 1 started, and the adsorbed amount quickly attains a higher, stable level. Desorption of 2 during injection of 1 is improbable, since the long chains remain attached to the surface by many segments in spite of the adsorption of shorter chains. Thus the adsorbed amount of 2 during injection of 1 is constant and equals the value of Γ ($= \Gamma_2$) during injection of solvent ($60 < t < 120$ s). The adsorbed amount of 1 is the additional adsorption upon injection of 1. For the example of fig. 6.6 $\Gamma_2 = 0.7$ mg/m^2 and $\Gamma_1 = 0.2$ mg/m^2.

This result gives one point for a curve of the surface composition $\Gamma_1(\Gamma_2)$, analogous to the dotted curve in the theoretical plot of fig. 6.2. More points were obtained by repeating the experiment with different times of injection

of 2. Each point of this curve reflects a static surface composition.

Next, we consider the sequence 1,1+2 (upper full curve). For $t<0$ the surface is saturated with 1. For $t>0$ a solution of 1+2 is injected and Γ increases due to adsorption of 2. The concentration of 1 in the mixture is the same as injected for $t<0$. Therefore the chemical potential of 1 in solution is constant, and any desorption of 1 must be the result of displacement by 2. Near saturation the curves for the injection of 1+2 and of only 2 coincide. We conclude that in this final stage component 1 is completely removed from the surface, and that the adsorption of 2 from 1+2 follows the curve for adsorption of 2 on a bare surface (dashed).

Just after the start of injection of 1+2 the observed adsorption rate (upper solid curve) is lower than that of 2 only (dotted line). The difference is due to desorption of 1. From a comparison of the adsorption rates of 1+2 and 2 we determined that the exchange ratio $d\Gamma_1/d\Gamma_2$ equals -0.55. For PEO, the adsorbed amount is constant during exchange. Hence $d\Gamma_1/d\Gamma_2 = -1$ for PEO. Since for PS the rates $d\Gamma_{1+2}/dt$ (slope of the upper full curve) and $d\Gamma_2/dt$ (slope of the dashed curve) remain more or less constant till close to saturation, also the exchange ratio $d\Gamma_1/d\Gamma_2$ is about constant till close to saturation.

As explained before, it is a reasonable assumption that at any moment during injection of 1+2 the contribution of 2 to the total adsorbed amount is given by that for individual adsorption of 2 (dashed). Consequently, Γ_1 equals the difference $\Gamma_{1+2} - \Gamma_2$. Since during injection of 1+2 the adsorbed amount of 1 decreases from its saturated value to zero, a complete curve of the surface composition $\Gamma_1(\Gamma_2)$ can be obtained from the upper two curves in fig. 6.6. This result might be considered as the surface composition under dynamic conditions.

In fig. 6.7 the composition $\Gamma_1(\Gamma_2)$ of an adsorbed PS layer under static conditions (circles "2,1") is compared to that under dynamic circumstances (full curve "1,1+2"). For comparison, the result for PEO of a sequence 1,1+2 is also included. The dotted lines are drawn according to exchange of 1 by 2 at constant total mass adsorbed. These lines correspond to the theoretically predicted equilibrium composition (compare the dotted curve in fig. 6.2).

A mixed adsorbed layer of PS under static conditions (lower PS-curve "2,1") has a composition that is close to the theoretical prediction for equilibrium. Only for $\Gamma_2 > 0.5$ mg/m^2 the value of Γ_1 is slightly higher than expected on the basis of fig. 6.2. Hence, the equilibrium composition is approximately attained if first 2 is adsorbed and then 1.

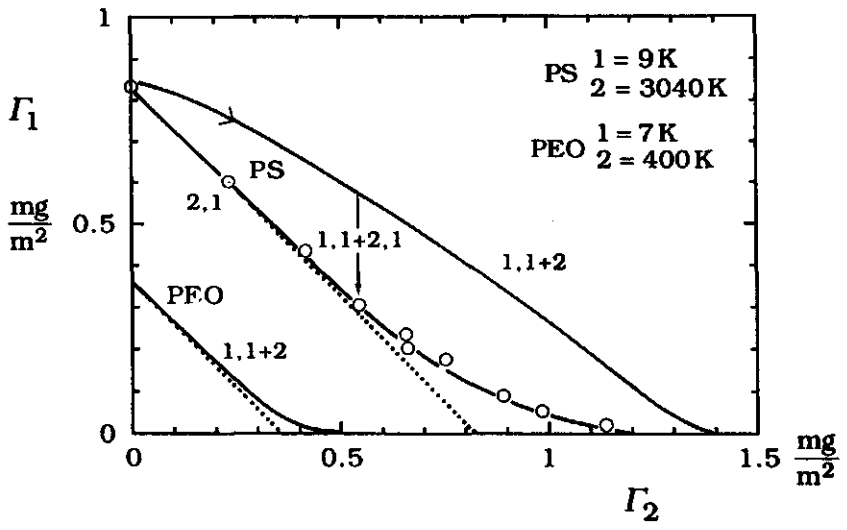

Figure 6.7 Overshoot adsorption of PS during exchange. The graph shows the composition $\Gamma_1(\Gamma_2)$ of the adsorbed layer under static (2,1) and dynamic conditions (1,1+2). Here "2,1" stands for "first 2, then 1". The composition is derived from sequential adsorption experiments like in fig. 6.6. For comparison, a result for PEO in water is also included. The dotted lines are drawn according to exchange of 1 by 2 at constant total mass adsorbed. The vertical arrow represents relaxation experiments of the type 1,1+2,1 as given in fig. 6.8. Molar masses and concentrations of PS and PEO the same as in fig. 6.5 and 6.3, respectively.

For adsorption in the reverse order (full curves "1,1+2") the adsorbed amount of 1 is for PS higher, and for PEO about equal to what is expected for equilibrium. For PS this implies an overshoot adsorption of component 1 during exchange. For PEO such an overshoot is not observed.

The existence of an overshoot gives rise to the question at what time scale an adsorbed PS layer relaxes towards an equilibrium situation. This question can be examined in an experiment in which the sequence 1,1+2 is interrupted before the surface is saturated with 2. If the injection of solution is switched back from 1+2 to 1, the adsorbed amount of 2 will remain constant, and the observed change in the total adsorbed amount (due to desorption of 1) reflects the relaxation process. Such an experiment is indicated in fig. 6.7 by the vertical arrow, and the sequence of injected solutions is referred to as 1,1+2,1. We discuss this type of experiments in the next section.

6.4.2.2 Relaxation experiments

The results of three relaxation experiments are shown in fig. 6.8 as three

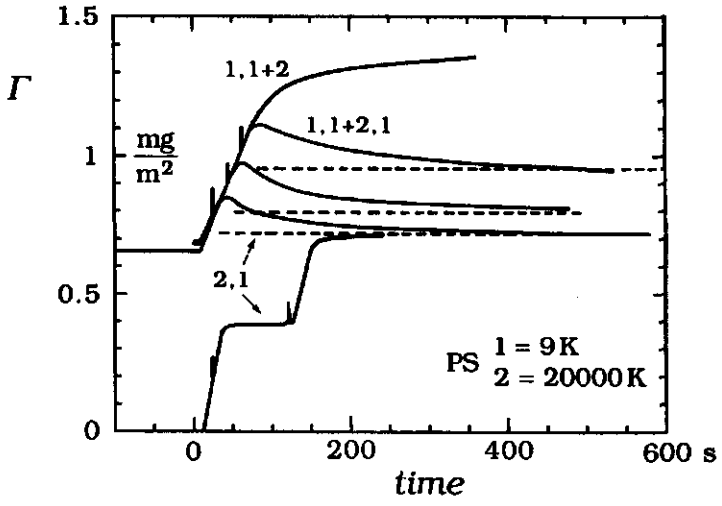

Figure 6.8 Desorption of PS by relaxation of the adsorbed layer. In these experiments the flow is switched back from the injection of 1+2 to 1 at the point indicated by a vertical tic. Following this a desorption of 1 occurs. The dotted horizontal lines represent the final value of experiments 2,1 with injection time of 2 corresponding to that of 1+2 in the relaxation experiments 1,1+2,1. Concentrations: $c_1^b = 5.0$, $c_2^b = 50$ g/m^3.

curves labelled 1,1+2,1. For comparison, also the result for continuous injection of 1+2 is included, in an analoguous experiment as described in fig. 6.6. The meaning of the dotted lines and the curve for injection of 2,1 will be explained later.

Before the relaxation experiments ($t < 0$) the surface is saturated with 1. Between $t=0$ and the vertical tic indicated on the curve a solution of 1+2 is injected. The three experiments shown have different times of injection of 1+2, and thus different amounts of 2 adsorbed. After the switch from injection of 1+2 to 1, the adsorbed amount continues to increase during a few seconds because there are still molecules 2 coming from the dead volume between valve and surface. As soon as the dead volume has passed, the adsorbed amount starts to decrease. After some 5 to 10 minutes a constant value is reached. The amount desorbed during injection of 1 is about 0.2 mg/m^2 for each experiment.

The question may be posed whether the decrease in Γ is indeed due to relaxation of the adsorbed layer. In our opinion desorption of 2 is very unlikely: even in pure solvent flow such a desorption is not found. For component 1, the chemical potential in solution is constant throughout the experiment, so that desorption of 1 by dilution does not occur. The only remaining explanation is indeed that the decrease in Γ is the result of

desorption of 1 by relaxation of (i.e., rearrangement within) the adsorbed layer, whereby the overshoot discussed in the previous figures disappears gradually.

In order to check whether at the end of the experiments the adsorbed layer is fully relaxed, and thus equilibrated, sequential adsorption experiments of the type 2,1 were performed. The injection time of 2 was chosen equal to that of 1+2, so that the adsorbed amount of 2 is the same for corresponding experiments 2,1 and 1,1+2,1. The total adsorbed amount after a sequence 2,1 is indicated by the horizontal dotted lines. The value of Γ at the end of the relaxation curves is in very good agreement with the equilibrium adsorbed amount obtained from a sequence 2,1. Thus, the adsorbed layer is then fully relaxed; the relaxation time is of the order of a few minutes. This result corroborates our conclusion that the decrease in Γ is due to desorption of 1 by relaxation of the adsorbed layer.

For the experiments of fig. 6.8 the adsorption rate of 2 is quite high as compared to the rate of desorption by relaxation. Therefore, we expect that the relaxation during injection of 1+2 is small. However, it is likely that the result depends on the time scale of the adsorption of 2, and thus on $d\Gamma_2/dt$. According to mass transfer limitation (i.e., $d\Gamma_2/dt = kc_2^b$) the adsorption rate of 2 can be varied by adjusting the concentration of 2 in solution. We expect that by variation of c_2^b the extent of relaxation during injection of 1+2 is affected, so that the shape of the curve 1,1+2 will change. As a consequence also the amount desorbed during subsequent injection of 1 is influenced.

Experimental results at four concentrations c_2^b in the range 5 - 200 g/m^3 are given in fig. 6.9.a and b for sequential injection of 1,1+2 (left) and 1,1+2,1 (right), respectively. The horizontal dotted lines in fig. 6.9.a refer to the point where the switch from injection of 1+2 to 1 was made in the experiments of fig. 6.9.b. For comparison, we included in fig. 6.9.a also the adsorption of 2 only on an initially bare surface (dashed).

Before $t=0$ in fig. 6.9.a, the surface was equilibrated with 1 ($\Gamma_1 \approx 0.65$ mg/m^2) and at $t=0$ the injection of a solution of 1+2 started. In order to be able to compare results, the adsorbed amount Γ is plotted as a function of $k_2 c_2^b t$. Here k_2 is the transport coefficient of 2, which we determined from the initial adsorption rate on a bare surface of 2 only, according to the mass transfer limitation $(d\Gamma_2/dt)_0 = k_2 c_2^b$. As a result of this scaling the initial slope for adsorption of 2 only is unity (dashed). Also, curves coincide as long as $d\Gamma/dt \propto c_2^b$. The results in fig. 6.9.a are plotted in the same way as the theoretical prediction for exchange according to local equilibrium in

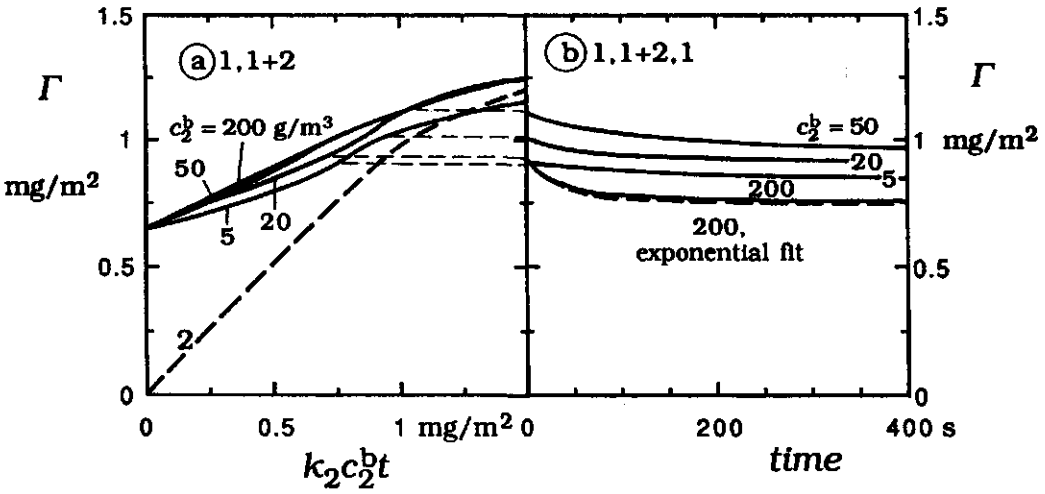

Figure 6.9 Desorption by relaxation for different concentrations of 2 (as indicated). Results are given for experiments of the type 1,1+2 (a) and 1,1+2,1 (b). In (a) Γ is plotted as a function of $k_2c_2^bt$ during injection of 1+2 on a layer which was initially saturated with 1. For comparison, also the result for adsorption of 2 only on an initially bare surface is included (dashed). Figure 6.9.b gives $\Gamma(t)$ during injection of 1 after a sequence 1,1+2. The concentration c_2^b of 2 during injection of 1+2 is indicated. The horizontal dashed lines connect the curves in (b) to their starting points on the curves in (a). Molar masses and concentration c_1^b are the same as for fig. 6.8; $k_2 = 3.04 \times 10^{-7}$ m/s. See also text.

fig. 6.2 (with $\Gamma_2 \approx k_2c_2^bt$).

For all four concentrations in fig. 6.9.a the initial rate $d\Gamma_{1+2}/dt$ is lower than the adsorption rate of 2 only (dashed). This implies that during adsorption of 2 there is also desorption of 1. Furthermore, for all curves 1,1+2 the adsorption increases initially, in contrast with the prediction of constant total adsorbed amount for exchange according to local equilibrium (solid curve in fig. 6.2). This means that in all cases there is an overshoot adsorption of 1 during exchange. However, for c_2^b decreasing from 50 to 5 g/m³ the shape of the curves becomes gradually more convex with respect to the abscissa axis, which indicates that with decreasing value of c_2^b (= decreasing adsorption rate) the overshoot of 1 during exchange gets less. The adsorbed layer is more relaxed during adsorption of 2 at lower concentration, probably due to the longer time available.

For c_2^b equal to 50 and 200 g/m³ the curves in fig. 6.9.a nearly coincide, which implies that the overshoot adsorption is the same for both experiments. However, at c_2^b = 200 g/m³ the time available for relaxation is only 25% of that at c_2^b = 50 g/m³, due to the higher adsorption rate. Probably, for both experiments the injection time of 1+2 is so small that relaxation during adsorption of 2 is negligible. However, there is still

desorption of component 1, as we inferred above from a comparison of the initial slopes for injection of 1+2 and 2 only. At saturation (not shown in fig. 6.9.a), for c_2^b in the range 20 - 200 g/m^3, the curves $\Gamma(t)$ for injection of 1,1+2 and only 2 coincide, like in fig. 6.6 the upper solid curve "1+2" and dashed one "2". As before, we conclude from this that at saturation component 1 is completely desorbed.

Figure 6.9.b shows $\Gamma(t)$ during injection of 1 after an initial sequence 1,1+2. The value of c_2^b during injection of 1+2 is indicated. The injection time of 1+2 was not varied systematically, so that the amount of 2 adsorbed is different for each experiment. The time along the abscissa axis is corrected for the effect of dead volume between valve and surface.

As before, the observed decrease in Γ is due to desorption of 1 by relaxation of the adsorbed layer. The desorption rate and the total desorbed amount during injection of 1 decrease with decreasing value of c_2^b. This is due to the increasing time available for relaxation during the preceding injection of 1+2. The decrease in the desorption rate is most conspicuous for c_2^b = 5 and 20 g/m^3. This is in agreement with the results in fig. 6.9.a, which show for these concentrations a pronounced change in the shape of the curve, indicative of a more relaxed adsorbed layer.

In order to obtain a quantitative characterisation of the relaxation process, a single exponential function was fitted to the relaxation curve for c_2^b = 200 g/m^3. This experiment was chosen for the fit because the adsorption of 2 was fastest. We therefore expect that all molecules 2 are more or less in the same, initial state of relaxation. The fit provided a time constant of 45 s and is given in fig. 6.9.b by the dashed curve. The experimentally observed desorption appears to be slightly different from the single exponential function. This is not surprisingly, however, because we do not have any *a priori* reason or model to expect an exponential behaviour.

In our opinion the results in fig. 6.9.a/b may be interpreted in terms of two different time scales for the exchange: (i) fast desorption of 1 *during* adsorption of 2, and (ii) slow desorption of 1 due to relaxation of adsorbed chains 2. During injection of 1+2, and at a high adsorption rate of 2 (c_2^b > 50 g/m^3 in fig. 6.9.a) the desorption of 1 and the overshoot adsorption are entirely determined by the fast process (i). In that case a variation of the adsorption rate by changing c_2^b has no influence on the overshoot adsorption (the curves for 50 and 200 g/m^3 in fig. 6.9.a coincide), since the desorption rate of 1 according to process (i) is proportional to the adsorption rate of 2. As noted in the discussion of fig. 6.9.a, at high

concentration c_2^b complete desorption of 1 is possible during adsorption of 2. This implies that all molecules 1 can leave the surface by the fast process (i).

At lower adsorption rates (for $c_2^b < 50$ g/m^3) there is also desorption by the (slow) relaxation process (ii). This leads to a smaller overshoot adsorption during injection of 1+2 (in fig. 6.9.a the curves for 5 and 20 g/m^3 have a more concave shape towards the abscissa axis than at higher concentration). The desorption observed in fig. 6.9.b reflects this slow relaxation process (ii).

6.4.2.3 Effect of chain length

In fig. 6.10 the exchange of PS of molar mass 3 K by 28 K is plotted analogously to the exchange of 9 K by 3040 K in fig. 6.7. In both figures we compare the composition $\Gamma_1(\Gamma_2)$ of an adsorbed PS layer under static and dynamic conditions (open circles "2,1" and full curve "1,1+2", respectively). The dotted line is drawn according to exchange at constant total mass adsorbed.

For the sequential adsorption 28 K, 3 K the total adsorbed amount is constant for $\Gamma_2 < 0.2$ mg/m^2, and it gradually increases for higher values of Γ_2. As explained in the discussion of fig. 6.7 this type of sequential experiments is supposed to give a static, equilibrium composition $\Gamma_1(\Gamma_2)$. However, the theoretical calculations in section 6.2 showed that in equilibrium the value of Γ_t should remain constant if the composition of a

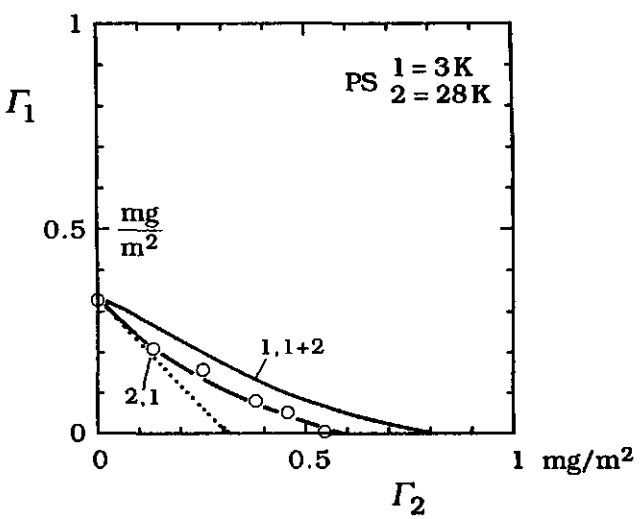

Figure 6.10 Exchange of low molar mass PS. The results are plotted in the same way as in fig. 6.7. Concentrations: $c_1^b = c_2^b = 10$ g/m^3.

mixed adsorbed layer changes (solid curve fig. 6.2). The discrepancy between experiment (increase of Γ_t) and theory (Γ_t constant) is probably a consequence of the low molecular weight of the samples. Theoretical calculations for short chains confirm this view.

The adsorbed amount obtained for adsorption under dynamic conditions (upper curve "1,1+2" in fig. 6.10) is everywhere somewhat higher than that under static circumstances ("2,1"). This implies that under dynamic conditions there is continuously a small overshoot of 3 K on the surface. Qualitatively, this is the same result as for displacement of 9 K by 3040 K (fig. 6.7); quantitatively the difference between the curves is less.

6.4.2.4 Effect of solvent

The dynamics of an adsorbed polystyrene layer may depend on the interactions between the polymer, the solvent and the surface, and thus on the type of solvent. Below we compare the exchange kinetics in decalin to that in two other solvents: a mixture of toluene and decalin, and carbon tetrachloride (CCl_4). These solvents were chosen because they have an effect on the solvency and adsorption energy of the polymer.

Decalin at 16 °C is a Θ-solvent for PS (chapter 5), whereas toluene and CCl_4 are good solvents. The segmental adsorption energy of PS on silica is in decalin about 2 kT (chapter 5) and in carbon tetrachloride around 1 kT[11]. Toluene is a weak displacer for PS adsorption on silica[11]. Qualitatively, the poor solvent quality and high adsorption energy in decalin can be explained from the fact that decalin is apolar and hardly polarisable and, consequently, has only little interaction with PS and the surface. Due to these weak interactions, the effective intramolecular interaction in PS, and the effective binding of the polymer to the surface are relatively strong.

In fig. 6.11 the adsorption of 1+2 from decalin is compared to that from a 92.5/7.5 (w/w) mixture of decalin and toluene. We discuss three effects of the addition of toluene. Firstly, the initial adsorption rate slightly increases upon the addition of toluene. Probably, this increase reflects a higher mass transfer rate. The reduction of the viscosity due to toluene causes an increase of the flow rate, and, hence, the mass transfer. Also the diffusion coefficient of the polymer might be affected.

Secondly, we infer from the results a decrease of the saturated adsorbed amount of 1 and 2 when toluene is added. As discussed before, the value of Γ at the first kink in the curve closely corresponds to saturation of 1. In the solvent mixture the kink occurs at a considerably lower value of Γ than

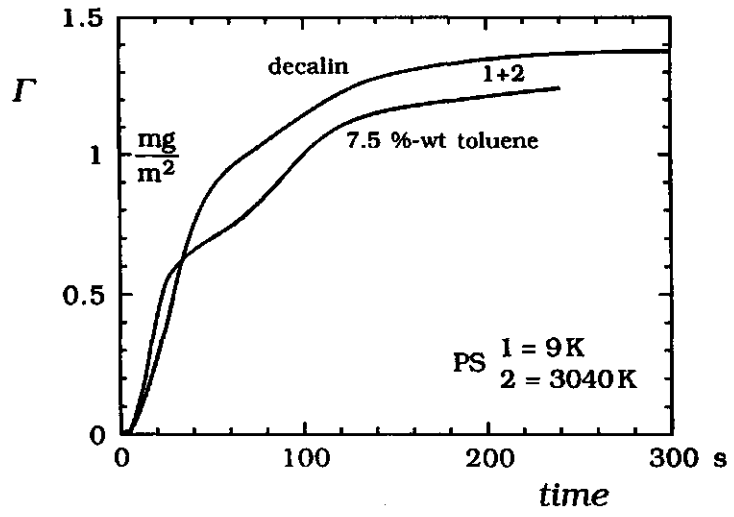

Figure 6.11 Effect of toluene on the exchange kinetics of PS. Concentrations: c_1^b = 5.0, c_2^b = 25 g/m^3.

in decalin (≈0.6 and ≈0.9 mg/m^2, respectively). The adsorbed amount at the end of the experiment corresponds to saturation of 2. This value is only slightly lower in the toluene/decalin mixture than in decalin (≈ 1.25 as compared to 1.4 mg/m^2). We explain the influence of toluene on the saturated adsorbed amount of 1 and 2 by a decrease of the adsorption energy, and an increase of the solvency. Both effects lead to lower adsorption levels.

Thirdly, toluene addition has an effect on the exchange kinetics. During exchange in decalin ($50 < t < 140$ s) the adsorbed amount increases linearly with time, whereas during exchange in the toluene/decalin mixture ($30 < t < 120$ s) the curve $\Gamma(t)$ has a convex shape with respect to the abscissa axis. The change in the shape of the curve indicates that the overshoot adsorption in the toluene/decalin mixture is smaller than in decalin. This must reflect a more rapid relaxation of the adsorbed layer.

The exchange kinetics in carbon tetrachloride and decalin are compared in fig. 6.12. The graph shows $\Gamma(t)$ during injection of a solution of 1+2. In order to obtain a comparable mass transfer rate in both solvents, differences in hydrodynamic conditions and in diffusion coefficients were compensated by adjusting the polymer concentrations (for values of c, see legend).

Along the same lines as in the discussion of fig. 6.11 we infer from the results in fig. 6.12 that the saturated adsorbed amounts of 1 and 2 in

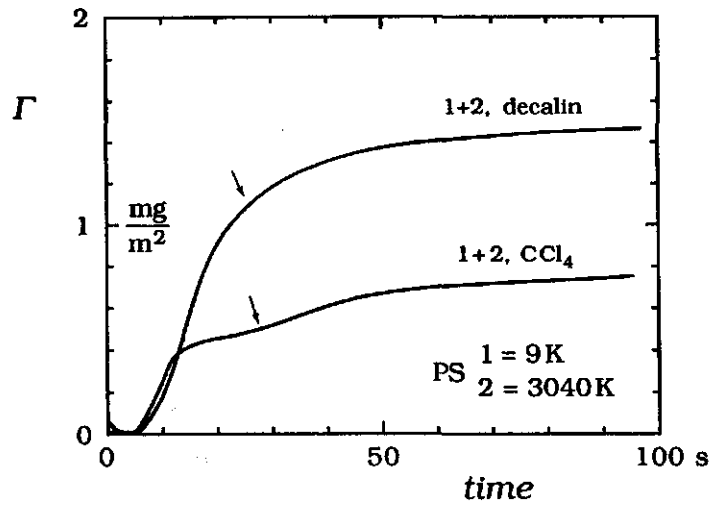

Figure 6.12 Comparison of the exchange kinetics of PS from decalin and carbon tetrachloride (CCl_4) solutions. In decalin c_1^b = 20, c_2^b = 100 g/m^3. In carbon tetrachloride c_1^b = 5.0, c_2^b = 20 g/m^3.

carbon tetrachloride are considerably lower than in decalin. The most likely explanation is again the lower segmental adsorption energy and the better solvency in CCl_4 as compared to decalin.

During exchange (indicated by an arrow) the shape of the curve is convex with respect to the abscissa axis for CCl_4, and slightly concave for decalin. Again, this indicates that the overshoot adsorption is less in CCl_4 than in decalin.

The above examples show an interesting parallel. An increase of the solvency and a decrease of the adsorption energy is in both examples accompanied by a decrease of the overshoot adsorption during exchange. This suggests strongly that the dynamics of an adsorbed layer depend on the interactions between polymer, solvent and surface, with a faster relaxation for better solvents and weaker affinity.

6.5 Discussion

In order to arrive at a picture of the exchange mechanism this section starts with a discussion of the observed behaviour of PEO and PS. The qualitative picture arising from this will be visualised in a series of cartoons of the adsorbed layer during exchange. Finally, a comparison with some other results is made.

Several exchange experiments with PS demonstrate that *desorption* is at least partly a slow process. For example, an overshoot adsorption with

respect to full equilibrium occurs when the surface is first saturated with the shorter chains that are subsequently displaced by longer ones (fig. 6.7). Moreover, this overshoot relaxes only slowly (fig. 6.8).

We could imagine that desorption is slow if the displaced chain would remain attached to the surface by a strongly adsorbing end-group. However, according to the manufacturer the polystyrene used had a vinyl hexane end-group. Such a group has probably a lower adsorption energy than the styrene segments. Therefore, strong attachment by an end-group is unlikely.

Slow desorption could also be explained if there were topological constraints within the adsorbed layer (e.g., entangled chains, or molecules pinned to the surface by loops of other chains). Polymer molecules can only release themselves from such constraints (and thus desorb) by slow diffusional motions out of the adsorbed layer. However, in the discussion of fig. 6.9.a/b we pointed out that at a high adsorption rate of the long chains *rapid* and *complete* desorption of the short chains occurs. In our opinion such rapid and complete desorption would not be possible if the short chains were trapped by topological restraints. Therefore, topological constraints provide also an unsatisfactory explanation for the observed slow relaxation of the adsorbed layer.

Another mechanism explaining slow relaxation would be that the spreading of an adsorbed chain is a slow process. We could imagine that upon attachment of a long chain to the surface quickly some short molecules are desorbed, but that further desorption is much slower because reconformation of an already adsorbed chain towards a relatively flat equilibrium structure is slow. In this picture the relaxation rate depends on the rate of reconformation of an adsorbed polymer chain. We can conceive at least four factors on which this rate depends.

Firstly, the rate of reconformations at the surface may be related to that in solution, and thus it would depend on the flexibility of the polymer. Possibly, this factor could explain the different behaviour of PEO and PS. Since PEO is much more flexible than PS due to the presence of bulky side groups in the latter polymer, conformational changes are much faster for PEO than for PS. This would explain that adsorbed PEO layers are essentially fully relaxed during exchange (fig. 6.3), whereas for PS on a similar time scale and with comparable chain lengths an overshoot adsorption occurs (fig. 6.5), indicative of slow relaxation of the adsorbed layer.

A second factor affecting the rate of conformational changes is the

intramolecular interaction, which stabilises the chain conformation. For PS, especially π-orbital overlap between styrene units of different segments may play a role. These interactions depend on the solvent present, and are partly reflected in the solvent quality parameter χ. Thirdly, reconformations are slowed down by the binding of the chain to the surface. The strength of the bond is characterised by the value of the segmental adsorption energy parameter χ_s. A fourth factor which might slow down the rate of reconformations is the presence of surrounding adsorbed molecules.

Accordingly the rate of reconformation of adsorbed polymers should depend on χ and on χ_s. Since the value of both parameters depends on the solvent, an effect of the solvent on the exchange kinetics is expected.

Indeed, for PS experimentally such an influence of the solvent on the overshoot adsorption during exchange is found (figs. 6.11 and 6.12). As discussed, the relaxation is slower in decalin than in a mixture of decalin and toluene or in pure carbon tetrachloride. This difference is accompanied with a higher adsorption energy and a poorer solvent quality in decalin. Both factors favour a stable conformation of the adsorbed chain in decalin, and thus a slow relaxation in this solvent, in agreement with the experiment.

A molecular picture which describes the main results in this chapter is presented in fig. 6.13. In the upper graph $\Gamma(t)$ during sequential injection 1,1+2 is plotted schematically for two limiting cases: no relaxation (curve *a*) and full relaxation (curve *b*) in the adsorbed layer during exchange. Curve *a* corresponds to exchange of PS at a high adsorption rate (corresponding to c_2^b = 50 or 200 g/m^3 in fig. 6.9.a). Curve *b* represents the exchange kinetics of PEO (fig. 6.3), and the theoretical prediction with the local equilibrium concept (fig. 6.2). An intermediate position between *a* and *b* was found for PS in decalin at low adsorption rates (corresponding to c_2^b = 5 or 20 g/m^3 in fig. 6.9.a), or for PS in decalin/toluene mixtures, and in carbon tetrachloride (figs. 6.11 and 6.12, respectively).

The open circles numbered I - IV on curves *a* and *b* refer to the cartoons of the adsorbed layer below. In these cartoons the surface is represented one-dimensionally by a solid line, and the adjacent solution by a two-dimensional square lattice. A lattice site is occupied by one segment of a polymer chain 1 or 2 (open and closed circles, respectively), or by solvent (not indicated).

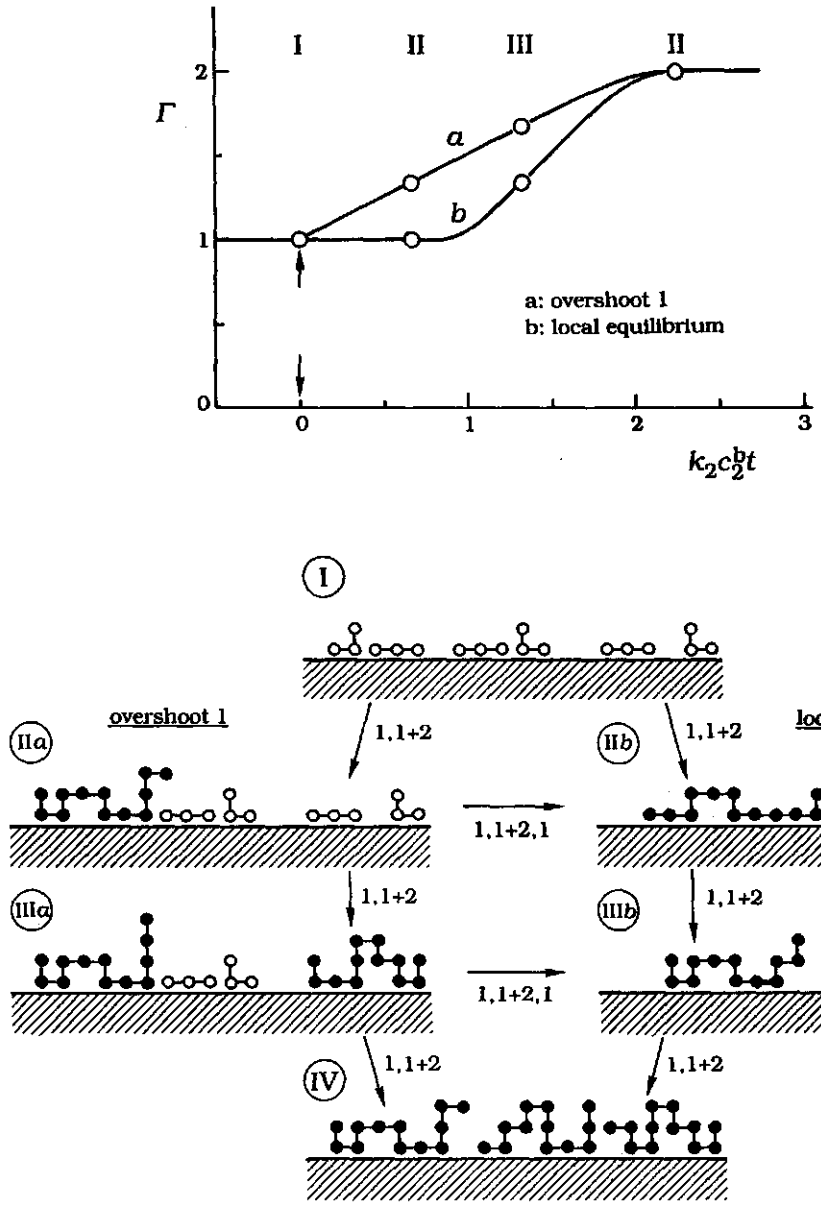

Figure 6.13 Pictorial representation of the adsorbed layer during exchange. The open circles in the upper graph (labelled I, II*a*, II*b*, etc.) refer to the cartoons below. Route *a* (top curve, left-hand side cartoons) represents the overshoot situation, route *b* (bottom curve, right-hand side cartoons) the situation according to the local equilibrium concept. For further explanation, see text.

Picture I shows a (highly schematised) saturated adsorbed layer of 1 with six molecules on the surface. The relatively short chains have a rather flat conformation due to the favourable adsorption energy. In each subsequent step (I → II, etc.) one molecule 2 adsorbs. The essential difference between route *a* and *b* is the following. In *a* the conformation of adsorbed molecules is nearly frozen on the time scale of the experiment, whereas in *b* the chains are fully relaxed and in an equilibrium conformation. First, route *b* is discussed and then *a*.

In picture II*b* the adsorption and complete unfolding of a molecule 2 has led to desorption of four short chains, so that the total adsorbed amount remains constant. Upon adsorption of the next two long chains (III*b* and IV), complete unfolding is no longer possible, since the surface layer is already too highly occupied. Longer loops and tails are formed by *all* molecules on the surface, including those previously adsorbed in a flat conformation.

In route *a* there is an overshoot adsorption of 1 during exchange. In each step one molecule 2 (12 segments) adsorbs at the expense of two molecules 1 (3 segments each), so that the total adsorbed amount increases, and an overshoot adsorption occurs in state II*a* and III*a*. The exchange ratio $d\Gamma_1 / d\Gamma_2$ equals -0.5, which is about the same as in the experimental results (see the discussion of fig. 6.6). In route *a* the unfolding of an adsorbed chain of 2 is slow as compared to the rate of arrival of new ones, so that the conformation of 2 remains more or less constant till saturation in IV. However, when in II*a* or III*a* the supply of new long chains is stopped, then the adsorbed layer slowly relaxes towards the equilibrium situation in II*b* and III*b*, respectively. This is indicated by the horizontal arrows 1,1+2,1 and corresponds to the relaxation experiments presented in fig. 6.8 and 6.9.b. Relaxation thus seems to be determined by unfolding of molecules 2.

Comparison with other results

In chapter 5 we found that at higher coverage the adsorption rate of PS decreases by the build-up of an adsorbed layer. Particularly, we concluded that the adsorption probability of a polystyrene chain depends on its gain in adsorption energy during collision with the surface. At high coverage, part of this gain may be due to displacement of adsorbed segments of other molecules, a process comparable to the relaxation observed in this chapter. The mere fact that at higher coverage the adsorption rate is decreased by such an attachment step is an indication that the

competition between polystyrene chains is slow on a segmental level, in agreement with the slow relaxation observed in this chapter.

Also in chapter 5, it was observed that desorption of low molecular weight PS into pure solvent is much slower than expected on the basis of local equilibrium. This is another indication that adsorbed PS slowly equilibrates. For PEO this desorption follows the equilibrium picture (chapter 4), in agreement with the absence of an overshoot in this chapter.

Frantz and Granick studied the exchange kinetics of PS adsorbed from cyclohexane on silica at 30 °C[2]. They found a considerable effect of the age of the pre-adsorbed protonated PS layer on the displacement rate by deuterated PS of the same molar mass (550 K). The displacement rate gradually decreased with ageing times up to tens of hours. This was interpreted to be the result of slow reconformations in the pre-adsorbed layer, possibly reflecting the formation of entanglements. In comparison with their experiments our results were obtained for very young layers. Qualitatively, there is agreement on the idea of slow reconformations within an adsorbed PS layer. However, no further comparison is possible, since the design of the experiments is rather different.

6.6 Conclusions

In this chapter we studied the exchange kinetics between polymers that differ in chain length only.

A theoretical prediction of the exchange kinetics was made by using the local equilibrium concept that was developed in chapter 4 for adsorption and desorption. According to this concept, near the surface free and adsorbed chains are in equilibrium, and the adsorption rate is fully determined by mass transfer from the bulk solution. Using an isotherm calculated with the theory of Scheutjens and Fleer, it was found that the exchange in this model takes place at a *constant* total adsorbed amount, which is approximately equal to the value for individual adsorption of the displaced chain. The rate of the exchange is limited by the adsorption of the displacer, and is equal to the *maximum* mass transfer rate from solution. The adsorption rate of the displacer is in this picture not affected by the presence of an adsorbed layer of shorter chains.

For aqueous solutions of poly(ethylene oxide) the exchange kinetics on silica is in full agreement with these local equilibrium predictions. In chapter 4 we reached the same conclusion for the kinetics of PEO adsorption, and for desorption into a flow of pure solvent. All our results for PEO indicate that an adsorbed layer of this polymer rapidly equilibrates

with the adjacent solution.

For polystyrene adsorbed from decalin on silica the equilibration at the surface is much slower than for PEO. During exchange of PS we observed an overshoot adsorption of the displaced component. The overshoot may desorb either by rapid exchange against newly adsorbing molecules, or by slow relaxation of the adsorbed layer. The time constant for the latter process is about one minute for displacement of PS of molar mass 9.2 K by a sample of 20000 K.

In addition to decalin, also a toluene/decalin mixture and carbon tetrachloride were used as solvents for PS. In these solvents the overshoot during exchange is smaller than in decalin, indicating that the relaxation process is faster.

Slow reconformation (spreading) of adsorbed chains is probably the cause for the overshoot adsorption during exchange of PS. The rate of conformational changes depends on the type of polymer, on the intramolecular interactions and on the binding to the surface. In this picture, PEO equilibrates more rapidly than PS, since it is much more flexible. The solvent effect on the exchange kinetics of PS could be explained by faster relaxation in better solvents and for weaker interaction with the surface.

6.7 References

(1) Johnson, H.E.; Granick, S. *Science* **1992**, *255*, 966.

(2) Frantz, P.; Granick, S. *Phys. Rev. Lett.* **1991**, *66*, 899.

(3) Scheutjens, J.M.H.M.; Fleer, G.J. In "*The effects of polymers on dispersion properties*"; Tadros, T.F., Ed.; Academic Press: London, **1981**

(4) Pefferkorn, E.; Carroy, A.; Varoqui, R. *J. Polym. Sci., Polym. Phys. Ed.* **1985**, *23*, 1997.

(5) Pefferkorn, E.; Haouam, A.; Varoqui, R. *Macromolecules* **1989**, *22*, 2677.

(6) Johnson, H.E.; Granick, S. *Macromolecules* **1990**, *23*, 3367.

(7) Schneider, H.M.; Granick, S. *Macromolecules* **1992**, *25*, 5054.

(8) Kawaguchi, M.; Hattori, S.-i.; Takahashi, A. *Macromolecules* **1987**, *20*, 178.

(9) Scheutjens, J.M.H.M.; Fleer, G.J. *J. Phys. Chem.* **1979**, *83*, 1619.

(10) "*Polymer Handbook*"; Brandrup, J.; Immergut, E.H., Ed.; John Wiley and Sons: New York, **1989**, 3rd ed.; p. VII-441.

(11) Van der Beek, G.P.; Cohen Stuart, M.A.; Fleer, G.J.; Hofman, J.E. *Langmuir* **1989**, *5*, 1180.

7 EXCHANGE KINETICS OF CHEMICALLY DIFFERENT POLYMERS

7.1 Introduction

Segments of chemically different polymers usually have a different affinity for the surface, which leads to preferential adsorption of the polymer with the highest segmental adsorption energy. Under most conditions the preference on the basis of a different segmental adsorption energy is much stronger than that due to different chain lengths, so that the adsorption preference is determined by the type of polymer, irrespective of its chain length. A long polymer is easily displaced by a shorter one if the latter has a higher adsorption energy.

Displacement of a polymer molecule by simultaneous desorption of all segments of the chain is very unlikely due to the high adsorption energy per molecule. Therefore, a segment-by-segment process is more likely. If the adsorbing and desorbing segment are chemically the same (chapter 6), the adsorption energy remains constant upon exchange. Hence, in this case there is no driving force at the segmental level for exchange. For chemically different polymers the adsorption energy increases upon exchange, which constitutes a driving force at the segmental level. We might therefore expect faster exchange kinetics for chemically different polymers as compared to chains that differ in length only. In addition to differences in the adsorption energy, for chemically different polymers also differences in solvency might play a role.

Experimentally, the exchange kinetics between chemically different polymers has hardly been investigated. The displacement of polystyrene (PS) adsorbed on silica by poly(methyl methacrylate) (PMMA) in a dilute solution of trichloroethylene was studied as early as in 1966 by Thies[1]. Much later, in 1992, Johnson and Granick[2] investigated the same combination of polymers adsorbing on an oxidised silicon surface from the solvent carbon tetrachloride. In both studies it was found that, after addition of PMMA, PS desorbed rather slowly, over a time-scale of hours. A similar slow exchange kinetics was observed by Van der Beek et al.[3] for displacement of adsorbed poly(butyl methacrylate) (PBMA) by polytetrahydrofuran (PTHF) in carbon tetrachloride solution. These results indicate that slow exchange processes occur in the adsorbed layer. However, as yet no general conclusions on the nature of these processes can be drawn.

The experimental approach in this chapter is the same as before: the polymers adsorb in a stagnation point flow on an oxidised silicon surface, and after some time the second polymer is injected into the cell. The adsorption process is monitored by reflectometry. The exchange kinetics of three polymers was investigated: polystyrene (PS), poly(butyl methacrylate) (PBMA) and polytetrahydrofuran (PTHF). In all cases the solvent was decalin. Van der Beek et al.[4] determined for these polymers the segmental adsorption energy parameter χ_s for adsorption from cyclohexane onto silica, and found values of 2, 3.8 and 4.8 for PS, PBMA and PTHF, respectively. Since cyclohexane and decalin are chemically very similar we expect that in decalin the values of χ_s are approximately the same as in cyclohexane. Accordingly, for adsorption from decalin on silica PBMA is expected to displace adsorbed PS, and PTHF should displace both PS and PBMA.

By reflectometry one cannot distinguish directly between different polymers on the surface because the reflectometric signal contains contributions of all adsorbed species. However, for the polymers chosen in this study the exchange can be investigated because the sensitivity of the method is quite different for adsorption of PS, PBMA and PTHF, due to differences in the refractive index increment dn/dc of these polymers in decalin solutions. As a result, the reflectometric signal of a saturated adsorbed layer is very different for these polymers, and a large change in the signal is expected if an adsorbed layer of one of these polymers is displaced by another.

In order to study the effect of the adsorption energy of the polymers on the exchange kinetics we examine in this chapter for one of the polymer pairs (PS/PBMA) the effect of two displacers of low molar mass. By addition of a low molar mass displacer the effective segmental adsorption energy of the polymers decreases, the effect being relatively stronger for the displaced component (PS) than for the polymeric displacer (PBMA). Generally, we would expect that a decrease of the adsorption energy leads to an increase of the mobility of the adsorbed polymers, possibly resulting in faster exchange kinetics. In addition to the adsorption energy a low molar mass displacer will usually also influence the solvency of the polymers, which also might have an effect on the exchange kinetics.

The two low molar mass displacers chosen for this study are ethyl acetate and toluene, which are solvents for both PS and PBMA[5]. Ethyl acetate is a strong displacer, and toluene a weak one. In chapter 5 we determined for adsorption of PS from decalin on silica the critical weight

fraction w_{eth}^{cr} of ethyl acetate, and found $w_{eth}^{cr} \approx 0.11$. For PBMA the value of w_{eth}^{cr} is probably considerably higher. Van der Beek et al.[6] determined for displacement of PS that the critical volume fraction of toluene in cyclohexane equals 0.80. In decalin this value is expected to be about the same. Toluene cannot completely displace PBMA adsorbed on silica[4].

7.2 Experimental

Materials

Polystyrene and polytetrahydrofuran samples of narrow molar mass distribution were purchased from Polymer Laboratories. Analytical grade, rather polydisperse poly(butyl methacrylate) was obtained from Aldrich Chemical Company. All samples were used without further purification. Their molar masses and degree of polydispersity are listed in table 6.1. For PBMA, the molar mass distribution as determined by gel permeation chromatography is given by Van der Beek et al.[3].

The solvents decalin (Merck, for synthesis quality), ethyl acetate (Merck, P.A.) and toluene (Baker analysed) were purified before use by the method described in section 5.2.

As the substrate for adsorption, strips cut from an oxidised silicon wafer were used. These were cleaned in a gas flame, as described in section 3.3. The silica film thickness was about 105 nm for all strips used.

Methods

The refractive index increment dn/dc of the polymers in decalin solutions was determined interferometrically at 20 °C from the difference in the refractive index of pure solvent and a polymer solution with a concentration of about 2000 g/m^3, using white light. For PS a value for dn/dc of +0.135 cm^3/g was found, which is in reasonably good agreement

Table 6.1 Polymer samples

sample	M, kg/mole	M_w / M_n
PS 9	9.2	1.03
PS 1030	1030	1.05
PS 3040	3040	1.04
PS 20000	20000	1.3
PTHF 4	4	1.12
PTHF 690	690	1.25
PBMA	240 (= M_w)	2.5

with the value of +0.12 cm^3/g measured by Appelt and Meyerhoff[7] at 20 °C and 633 nm. For PTHF and PBMA we determined that dn/dc is -0.0096 and +0.0061 cm^3/g, respectively. However, for these polymers the measurement was probably rather inaccurate because of the small optical contrast, so that dn/dc may contain a large error.

The adsorption measurements were carried out with a reflectometer as described in chapter 5. In this chapter the output signal S of the reflectometer is given in an uncalibrated form as $\Delta S/S_0$, where S_0 is the initial value of S on a bare surface and $\Delta S = S - S_0$ is the change in S upon adsorption. According to eq. 2.8 the adsorbed amount Γ equals $(\Delta S/S_0)/A_s$, where A_s is the sensitivity factor for adsorption, defined by eq. 2.9. Using the values of dn/dc given above we calculated that for PS, PTHF and PBMA A_s equals +0.0196, -0.0014 and +0.00088 m^2/mg, respectively. In adsorbed layers containing only one type of polymer the adsorbed amount can be calculated directly from $\Gamma = (\Delta S/S_0)/A_s$, although with limited accuracy for PTHF and PBMA. In mixed adsorbed layers the signal $\Delta S/S_0$ contains contributions of different polymers that are measured with a different sensitivity. Separation of these contributions is not possible in a direct way, and therefore the adsorbed amount cannot be calculated unambiguously for mixed adsorbed layers.

7.3 Results

7.3.1 Exchange of PS by PTHF

An example of the adsorption of PS and PTHF on an initially bare silica surface, and of the exchange kinetics of PS by PTHF is given in fig. 7.1. First we discuss the individual adsorption of PS and PTHF, then the exchange.

At $t = 0$ a solution of PS 1030 was injected and $\Delta S/S_0$ increases due to adsorption of PS onto a bare surface. As discussed in chapter 5, the initial adsorption rate is determined by the maximum mass transfer of PS from the bulk solution to the surface. After some time (≈200 s) the adsorption rate decreases considerably due to the build-up of an adsorbed layer. We stopped the injection of PS at t = 750 s. The adsorbed layer is not yet completely saturated then. The final level of $\Delta S/S_0$ corresponds to an adsorbed amount Γ of 1.2 mg/m^2.

The adsorption of PTHF 690 on silica is represented by the dashed and dotted curves. The dashed curve gives $\Delta S/S_0$ during injection of PTHF. Due to adsorption $\Delta S/S_0$ *decreases* for PTHF because A_s has a negative value for this polymer. In order to show more detail we rescaled the

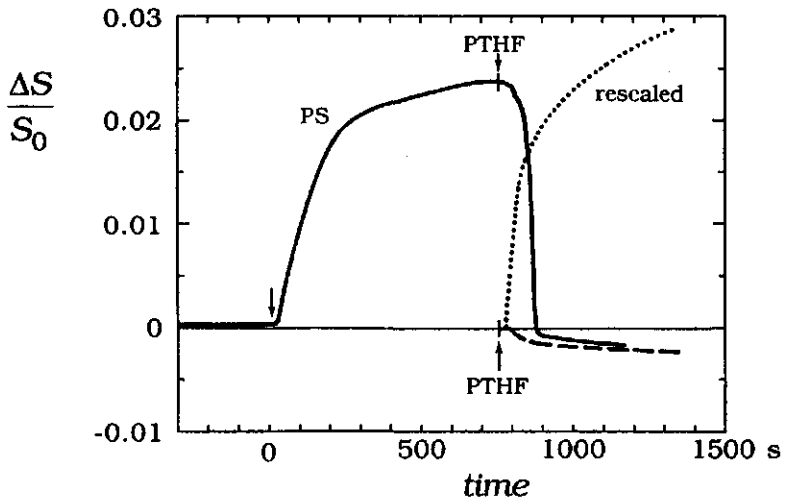

Figure 7.1 Example of the exchange kinetics of PS by PTHF. At t=0 the injection of a solution of PS on an initially bare surface starts. Then, at t=750 s the valve is switched to the injection of PTHF. For comparison, the adsorption of PTHF on a bare surface is given as $\Delta S/S_0$ (dashed) and by a dotted curve, which is corrected for the different sensitivity of the method for PS and PTHF (see text). Parameters: PS, M = 1030 K, c = 10 g/m^3; PTHF, M = 690 K, c = 10 g/m^3; S_0 = 0.99.

adsorption curve of PTHF by multiplication of $\Delta S/S_0$ with A_s(PS)/A_s(PTHF). The result is given as a dotted curve. Since Γ(PTHF) = $(\Delta S/S_0)/A_s$(PTHF), the adsorbed amount of PTHF can be obtained from the dotted curve by division through A_s(PS), which is the same factor as needed to calculate Γ from the adsorption curve of PS. Consequently, equal ordinate values in fig. 7.1 for the adsorption curves of PS (full) and PTHF (dotted) correspond to equal adsorbed amounts.

For PTHF the shape of the adsorption curve and the amount adsorbed is roughly comparable to that of PS. The initial rapid increase of the adsorption of PTHF is presumably due to mass transfer limited adsorption, like for PS. Since the change in the reflectivity of the surface is very small for adsorption of PTHF, the adsorption curve for this polymer might well be strongly affected by drift of the signal caused by, e.g., temperature fluctuations. Therefore a more detailed discussion of the adsorption curve of PTHF is not meaningful.

The exchange of PS by PTHF is represented in fig. 7.1 by the full curve for t > 750 s. At t = 750 s the valve was switched from the injection of PS to PTHF. During injection of PTHF $\Delta S/S_0$ decreases rapidly, and around t = 900 s it has attained a small, negative value, closely corresponding to that for individual adsorption of PTHF. This result strongly suggests that PS is

completely desorbed and replaced by PTHF. Since the desorption of PS occurs at the same time scale as the adsorption of PTHF on a bare silica surface (dotted curve), it is likely that the mass transfer of PTHF is the rate-limiting step in the exchange process. In order to check this we varied the adsorption rate of PTHF by adjusting its solution concentration.

For three concentrations of PTHF in the range 2.5-25 g/m^3, the exchange of PS by PTHF is given in fig. 7.2. The ratio $\Delta S/S_0$ is plotted as a function of the product *ct* of the concentration and the time of injection of PTHF. For comparison, also the result for adsorption of PTHF on a bare surface is included (dashed). For $t < 0$ a solution of PS 1030 was injected for about one hour with a different concentration in each experiment, as indicated. The final adsorption during injection of PS (i.e., $t < 0$ in fig. 7.2) increases with increasing concentration of PS. The adsorption level after one hour does not yet correspond to equilibrium, but is kinetically determined. As discussed in chapter 5, the adsorption rate of PS increases proportionally with the solution concentration, even at higher coverage where attachment to the surface is the rate-limiting step. As a result, the adsorbed amount after a fixed time (here about one hour) increases with concentration.

For the three exchange experiments in fig. 7.2 $\Delta S/S_0$ decreases during

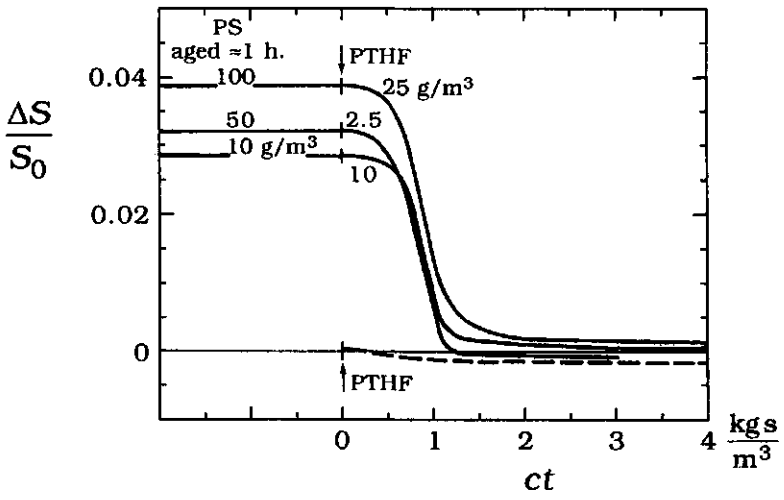

Figure 7.2 Effect of the concentration of PTHF on the exchange kinetics of PS by PTHF. Initially ($t < 0$), a solution of PS (M = 1030 K) at a concentration as indicated was injected for about one hour. At $t = 0$ the injection of PTHF (M = 690 K, concentration as indicated) starts. The signal $\Delta S/S_0$ is plotted as a function of the product *ct* of the concentration and the time of injection of PTHF. For comparison, the dashed curve gives the result for adsorption of PTHF on an initially bare surface.

injection of PTHF to a value close to that for adsorption of PTHF on silica, which strongly suggests that in all three cases PS is completely displaced by PTHF. The three displacement curves more or less coincide, which implies that the exchange rate is proportional to the solution concentration of PTHF, and, hence, to the adsorption rate of the displacer. We conclude that the desorption rate of PS is fully determined by the adsorption rate of PTHF which is limited by the maximum mass transfer from solution; there is no detectable barrier for PS desorption.

In the examples given above PS was displaced by a high molar mass sample of PTHF (690 K). In figure 7.3 we examine the exchange kinetics of low and high molar mass PS (9 K and 3040 K, respectively) by short chains of PTHF (M = 4 K). For comparison, the adsorption of PTHF 4 on a bare surface is given in the same way as in fig. 7.1 by a dashed and dotted curve. The final level of $\Delta S/S_0$ for PTHF 4 corresponds to an adsorbed amount of only 0.25 mg/m^2.

The result in fig. 7.3 for displacement of PS by PTHF 4 is very similar to that in fig. 7.1 for displacement by PTHF 690, which implies that the displacement rate of PS by low molar mass PTHF is also mass transfer limited. In fig. 7.3, the displacement of PS 3040 lags about 10 s behind that of PS 9, which implies that a somewhat higher coverage with PTHF 4 is needed to displace the long chains of PS as compared to the short ones.

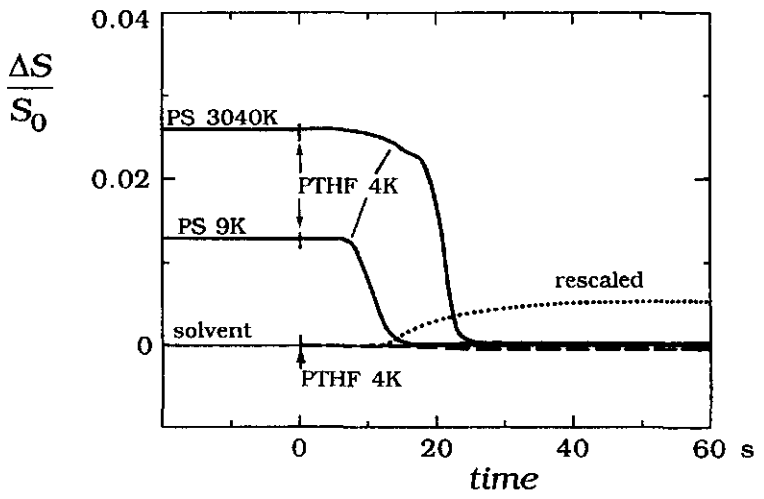

Figure 7.3 Effect of the chain length of PS on the kinetics of displacement by low molar mass PTHF. For comparison, we also included the result for adsorption of PTHF on an initially bare surface (dashed and dotted; the meaning of these curves is the same as in fig. 7.1). Concentrations: PS (9K) 5 g/m^3, PS (3040K) 50 g/m^3, PTHF (4K) 10 g/m^3.

However, both for PS 9 and PS 3040 the displacement is complete before the surface is saturated with PTHF 4. The only combination of chain lengths we did not investigate was the displacement of low molar mass PS by high molar mass PTHF. We see no reason to suppose that the result would be different. We therefore generalise our previous conclusion: for *any* combination of chain lengths the exchange kinetics of PS by PTHF is determined by the mass transfer limited adsorption of PTHF. The surface processes are faster than the transport through solution, and therefore they have no influence on the exchange rate. Note in fig. 7.3 that PTHF 4 is still preferentially adsorbed over PS 3040, although the molar mass of PTHF is about 750 times lower than that of PS. This example clearly shows that the adsorption preference is mainly determined by a difference in the segmental adsorption energy of the polymers ($\chi_s \approx 2.0$ and 4.8 for PS and PTHF, respectively), and much less by a difference in the chain length.

7.3.2 Exchange of PBMA by PTHF

In this section we discuss first the adsorption of PBMA and then the exchange of PBMA by PTHF. In fig. 7.4 an example is given of the kinetics of adsorption of PBMA on an initially bare surface. The lower curve is for the pure solvent decalin, the upper curve is for a mixture of decalin and ethyl acetate. The results for the mixture will be discussed in section 7.3.3.2. For PBMA in decalin the adsorption rate is constant till it abruptly

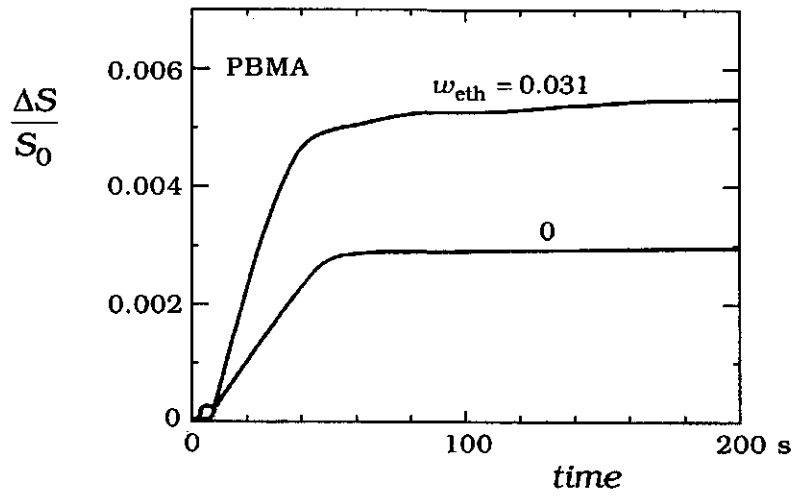

Figure 7.4 Adsorption kinetics of PBMA in decalin and a mixture of decalin and ethyl acetate. The weight fraction w_{eth} of ethyl acetate is indicated. The effect of ethyl acetate is to a large extent optical (see sec. 7.3.3.2). Polymer concentration 25 g/m^3.

falls to zero around t = 50 s, and then it remains zero during ongoing injection of PBMA. Presumably, the initial adsorption rate is again determined by mass transfer from the bulk solution. For the highly polydisperse sample of PBMA which was used, we did not expect such a sharp transition between initial adsorption and saturation. Instead, for polydisperse polymers we would expect a rounded shape of the adsorption curve due to the exchange of shorter by longer chains. An explanation for the observed behaviour could be that there is no exchange on the time-scale of our experiment. This would imply that the exchange process between PBMA chains of different length is slow.

The final level of $\Delta S / S_0$ in decalin corresponds to an adsorbed amount Γ of 3.4 mg/m^2, which is quite high for an adsorbed layer of an uncharged homopolymer. However, this value is subject to a considerable error, due to the low optical contrast between PBMA and decalin, which makes an accurate determination of dn/dc impossible.

The exchange kinetics of PBMA by high molar mass PTHF (M = 690 K) is presented in fig. 7.5 for a young (3 min) and a strongly aged (20 h) adsorbed layer of PBMA. For the aged PBMA layer the reflectometric signal after 20 h was apparently affected by drift. We therefore used in fig. 7.5 rather arbitrarily the value of $\Delta S / S_0$ after 30 min injection of PS. After 30 min the adsorption rate was zero within experimental error, so that the

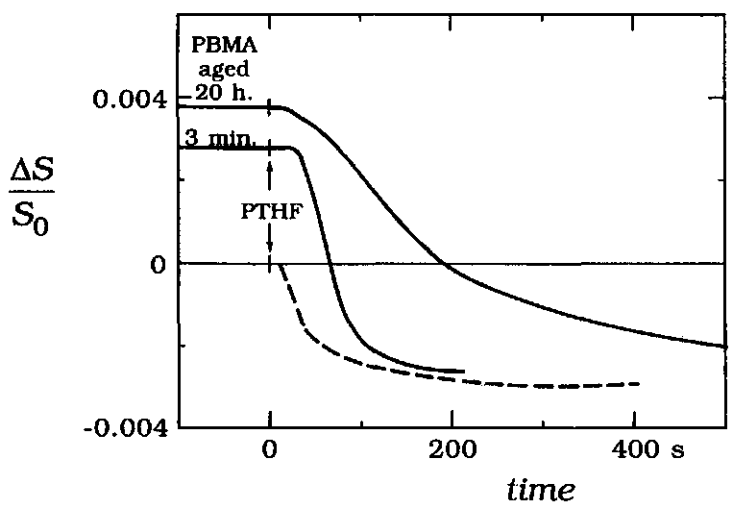

Figure 7.5 Kinetics of displacement of PBMA by PTHF in decalin solution for young and strongly aged adsorbed layers of PBMA, as indicated. For comparison, the dashed curve gives $\Delta S / S_0$ for adsorption of PTHF on an initially bare surface. Concentrations: PBMA 255 g/m^3, PTHF (690 K) 25 g/m^3.

value of $\Delta S/S_0$ used in fig. 7.5 probably is a reasonable indication for the adsorption after 20 h. For comparison, $\Delta S/S_0$ for adsorption of PTHF on an initially bare surface is given by a dashed curve.

During injection of PTHF on a young layer of PBMA (lower full curve) $\Delta S/S_0$ decreases rapidly to a value characteristic for a saturated adsorbed layer of PTHF only, which indicates that PBMA is completely exchanged by PTHF. The time-scale for exchange of PBMA by PTHF is the same as that for adsorption of PTHF on an initially bare surface. Hence, the exchange rate of PBMA by PTHF is again determined by the adsorption rate of the invading species, which, in turn, is controlled by mass transfer from the solution.

For the aged layer of PBMA (upper full curve) the exchange rate is slightly lower than for the young layer, but the exchange is still relatively fast with a time constant of a few minutes. Whether for this case the exchange is complete we cannot say due to the uncertainty in the adsorption level of PBMA before exchange. Nevertheless, it seems that ageing of the adsorbed PBMA layer does not have a large effect on the exchange kinetics of PBMA by PTHF.

7.3.3 Exchange of PS by PBMA

7.3.3.1 Decalin solutions

The exchange kinetics of PS by PBMA in decalin is given in fig. 7.6 for PS 9 and PS 3040 (upper full curves, as indicated). The horizontal, dashed line at the upper full curve indicates the adsorption level of PS just before injection of PBMA. In one experiment first PBMA was adsorbed and then PS 3040 added; this result is given by the lower full curve. The adsorption of PBMA on an initially bare surface is represented by a dashed curve.

During injection of PBMA on an adsorbed layer of PS 9 $\Delta S/S_0$ decreases and finally reaches a value close to that for adsorption of PBMA only, suggesting that ultimately all PS 9 is exchanged by PBMA. During exchange of PS 9 by PBMA the rate of decrease of $\Delta S/S_0$ decreases sharply around $t \approx 40$ s, which is approximately the time needed to form a saturated adsorbed layer of PBMA on an initially bare surface (dashed curve). Therefore, in the exchange experiment for PS 9 the adsorption of PBMA is probably more or less the same as that on an initially bare surface. For $t < 40$ s the decrease of $\Delta S/S_0$ in the exchange experiment is thus due to desorption of PS 9 during adsorption of PBMA. For $t > 40$ s in the exchange experiment the adsorbed amount of PBMA remains probably nearly constant and the decrease of $\Delta S/S_0$ is then caused by desorption of

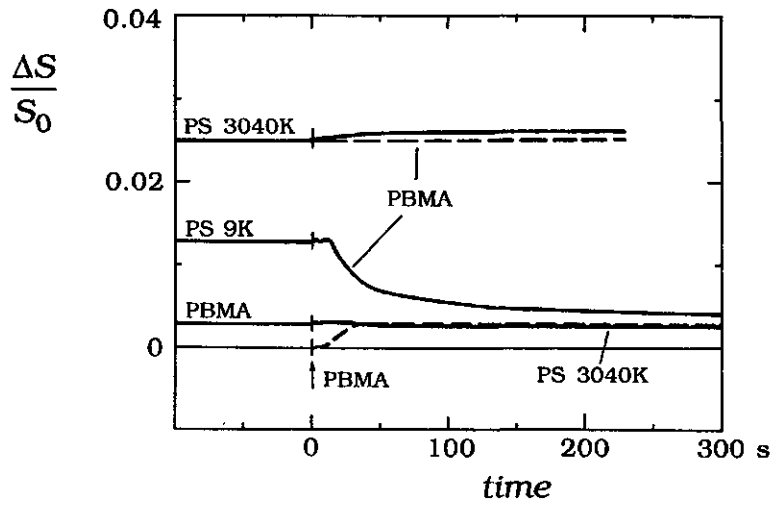

Figure 7.6 Kinetics of displacement of high and low molar mass PS by PBMA in decalin solutions. Initially ($t < 0$), a solution of PS is injected for about 2-3 minutes, and at $t = 0$ the injection of PBMA starts (upper full curves). The horizontal dashed line at the upper curve is the value of $\Delta S/S_0$ during injection of PS. In order to check whether the adsorption preference is reversed in the case of the high molar mass PS, also the result for injection in the reverse order is included: first PBMA, then PS 3040 K (lower full curve). The dashed curve is the result for adsorption of PBMA on an initially bare surface. Concentrations: PS (9K) 5 g/m^3, PS (3040 K) 50 g/m^3 and PBMA 50 g/m^3.

PS 9 only, presumably as the result of rearrangements within the adsorbed layer.

For exchange of high molar mass PS by PBMA (upper full curve) the result is quite different. During injection of PBMA $\Delta S/S_0$ increases slightly for $t < 40$ s and it remains constant after this time. The small increase of $\Delta S/S_0$ for $t < 40$ s suggests that adsorption of PBMA does occur. However, in this case the desorption of PS is small, if any. If it is assumed that the adsorption of PS 3040 is constant for $t < 40$ s, then the increase of $\Delta S/S_0$ corresponds to an adsorption of PBMA of about 20% of its saturated value on an initially bare surface. If there is some desorption of PS 3040 during adsorption of PBMA, than the adsorption of PBMA would be more than this 20%. For $t > 40$ s $\Delta S/S_0$ remains constant, which implies that there is no (measurable) desorption of PS on this time scale (about 4 min.). Probably, the exchange process of PS 3040 by PBMA is too slow to be observed in the experiment of fig. 7.6.

Since the segmental adsorption energy of PBMA is considerably higher than that of PS (χ_s = 3.8 and 2.0 for PBMA and PS, respectively), we would expect complete displacement of PS by PBMA, irrespective of the chain

length of PS. In order to make sure that the adsorption preference is not reversed in the case of high molar mass PS and PBMA we performed an exchange experiment in the reverse order: first PBMA was adsorbed and then PS 3040 was injected (lower full curve in fig. 7.6). During injection of PS 3040 on an adsorbed layer of PBMA $\Delta S/S_0$ remains constant, which implies that there is no exchange of PBMA by PS, nor any adsorption of PS. Therefore, it is very unlikely that the adsorption preference is reversed.

In order to try to enhance the exchange rate of high molar mass PS by PBMA we decided to decrease the adsorption energy of the polymers by addition of low molar mass displacers. The results are described in sections 7.3.3.2 and 7.3.3.3 for a strong and a weak displacer, respectively. If indeed the adsorption energy is a key factor, then an effect should be the same for both displacers.

7.3.3.2 Effect of a strong displacer

In this section we first discuss the effect of ethyl acetate on the individual adsorptions of PS and PBMA, and then its influence on the exchange kinetics of PS by PBMA.

The effect of ethyl acetate on the adsorption kinetics of PS was extensively discussed in section 5.3.3 and therefore here only the main aspects are repeated. Figure 7.7 is a plot of the adsorption of PS 20000 on silica from mixtures of decalin and ethyl acetate for a series of weight

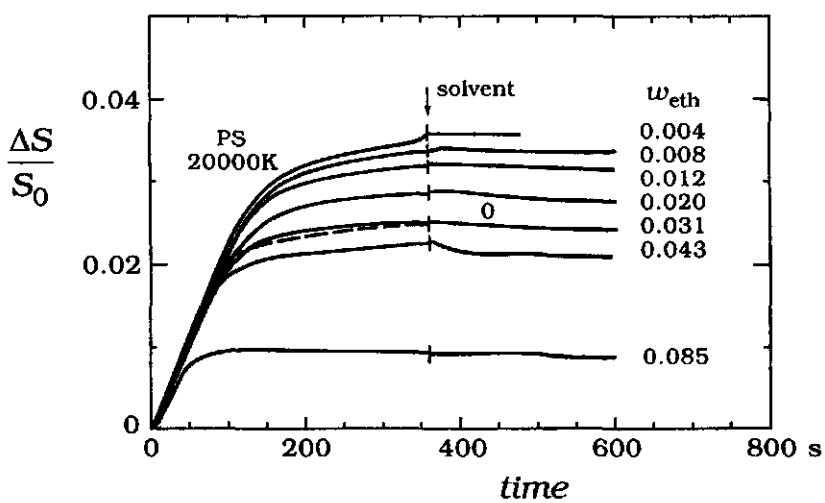

Figure 7.7 Adsorption of high molar mass PS in solvent mixtures of decalin and ethyl acetate. The weight fraction w_{eth} of ethyl acetate is indicated. The dashed curve gives the result for the adsorption from pure decalin.

fractions w_{eth} of ethyl acetate, as indicated. The result for adsorption from pure decalin (i.e., $w_{eth} = 0$) is given by the dashed curve. Part of these results are also given in fig. 5.11 of chapter 5.

For all curves in fig. 7.7 the initial adsorption rate is practically the same because for all experiments the concentration of ethyl acetate was so low that there is hardly any effect on the mass transfer conditions. The fact that the initial slopes coincide, implies that also the optical calibration is not affected by the addition of ethyl acetate. The final level of $\Delta S/S_0$ decreases regularly with increasing concentration of ethyl acetate, as is expected for a low molar mass displacer. In pure decalin in this respect an anomalous result is obtained for which we have no explanation. The final level of $\Delta S/S_0$ as a function of w_{eth} is given in fig. 7.8 by the open circles. (The meaning of the triangles in this graph will be discussed later). The shape of the curve in fig. 7.8 (open circles) is well-known for displacement of polymers by low molar mass displacers[6,8]. From the intercept with the abscissa we determined the critical weight fraction w_{eth}^{cr} of ethyl acetate needed for complete desorption of PS and found $w_{eth}^{cr} = 0.11$.

In fig. 7.4 we compare the adsorption kinetics of PBMA in decalin and a mixture of ethyl acetate and decalin ($w_{eth} = 0.031$). Due to ethyl acetate the initial slope $d(\Delta S/S_0)/dt$ and the final level of $\Delta S/S_0$ are a factor of about 2.5 and 1.9, respectively, higher than in decalin. Since for both

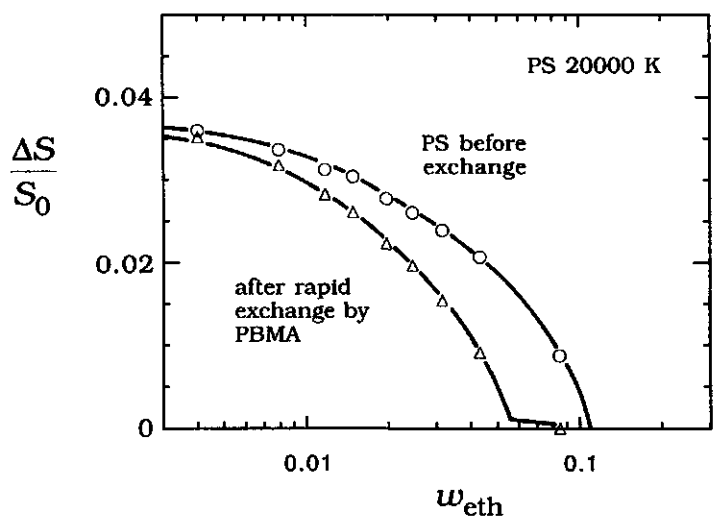

Figure 7.8 Effect of ethyl acetate on the final level of $\Delta S/S_0$ during injection of high molar mass PS (circles), and $\Delta S/S_0$ after rapid exchange of PS by PBMA (triangles). The circles represent $\Delta S/S_0$ at t = 360 s in fig. 7.7. The precise meaning of the triangles is given after the discussion of fig. 7.10.

experiments the mass transfer conditions were nearly the same, we expect that also the initial adsorption rates were more or less equal. The influence of ethyl acetate on the initial rate $d(\Delta S/S_0)/dt$ must then be an optical effect that corresponds to an increase of A_s by a factor 2.5. Although the effect of ethyl acetate on A_s for PBMA is large in a relative sense (factor 2.5), it is only small if absolute values of A_s are considered: A_s = +0.00088 and 0.0022 m^2/mg for w_{eth} = 0 and 0.031, respectively. Both values of A_s for PBMA are still much smaller than that of PS in decalin, for which A_s = +0.0196 m^2/mg. Possibly, the effect of ethyl acetate on A_s for PBMA is due to some association between PBMA and ethyl acetate. If the effect of ethyl acetate on the initial slope in fig. 7.4 is indeed entirely optical, then the final adsorbed amount of PBMA is about 25% lower for w_{eth} = 0.031 than in decalin. Possibly, this is caused by a decrease of the adsorption energy and an increase of the solvency of PBMA by the addition of ethyl acetate.

An example of the exchange of high molar mass PS (M = 20000 K) by PBMA in a mixture of decalin and ethyl acetate (w_{eth} = 0.031) is given in fig. 7.9 (full curve). For comparison, the dashed curve represents adsorption of PBMA on an initially bare surface. For $t < 0$ in the exchange experiment a sequence of a PS solution and the solvent mixture was

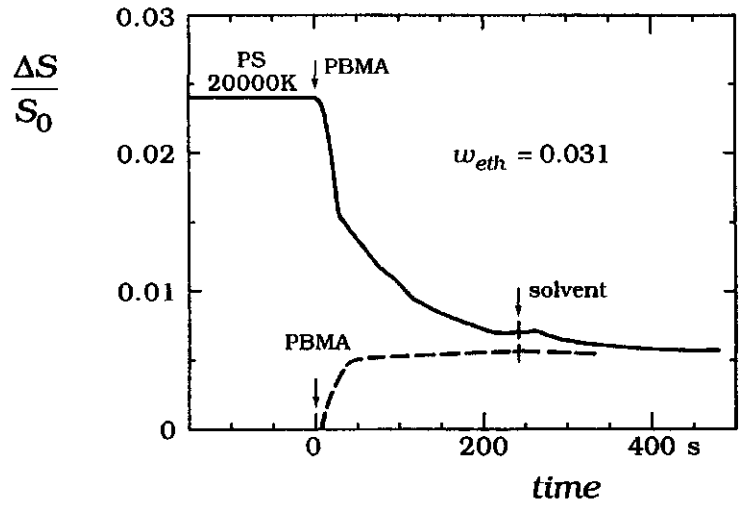

Figure 7.9 Kinetics of displacement of high molar mass PS by PBMA in a solvent mixture of decalin and ethyl acetate, as indicated. For $t < 0$ a sequence of PS and the solvent mixture is injected, as given in fig. 7.7. For comparison, the dashed curve gives the result for adsorption of PBMA on an initially bare surface. Concentration of PBMA equals 25 g/m^3.

injected, as given in fig. 7.7.

During injection of PBMA in the exchange experiment of fig. 7.9 $\Delta S/S_0$ decreases in a few minutes to a value characteristic for a saturated layer of PBMA only, indicating that PS is completely exchanged by PBMA. In a similar experiment in pure decalin (upper curve in fig. 7.6) no desorption of PS was observed. Thus, due to the addition of ethyl acetate the exchange rate of high molar mass PS by PBMA increases strongly. In fact, the curve for exchange of PS 20000 by PBMA for w_{eth} = 0.031 (fig. 7.9) resembles that of PS 9 by PBMA in pure decalin (fig. 7.6), suggesting that the exchange mechanism is the same. Accordingly, we distinguish in fig. 7.9 two stages in the displacement of PS 20000 by PBMA. Initially, for $t < 30$ s $\Delta S/S_0$ decreases due to desorption of PS during mass transfer limited adsorption of PBMA. Then, for $t > 30$ s the adsorption of PBMA is probably more or less constant, and the decrease of $\Delta S/S_0$ is due only to desorption of PS, presumably as the result of slow rearrangements in the adsorbed layer.

Exchange experiments of PS 20000 by PBMA were performed for a series of concentrations of ethyl acetate with w_{eth} increasing nearly up to its critical value of 0.11, above which there is no adsorption of PS. The result is plotted in fig. 7.10 in the same way as the exchange in fig. 7.9; the curve for w_{eth} = 0.031 is the same in both figures. The dashed curve in fig. 7.10 is for displacement of PS by PBMA in decalin (i.e., w_{eth} = 0). For $t < 0$ a sequence of PS and the solvent mixture was injected, as shown in fig. 7.7.

The rate of displacement of PS 20000 by PBMA increases gradually with increasing concentration of ethyl acetate. All curves in fig. 7.10 (except those for w_{eth} = 0 and 0.085) show a kink around t = 30 s, which is approximately the time needed to form a saturated adsorbed layer of PBMA on an initially bare surface (compare fig. 7.9). As before, we suggest that in the initial stage up to $t \approx 30$ s PS desorbs during mass transfer limited adsorption of PBMA. The decrease of $\Delta S/S_0$ in the initial stage increases with increasing concentration of ethyl acetate. Since PBMA gives only a small contribution to $\Delta S/S_0$, this means that the amount of PS desorbed in the initial stage increases with increasing value of w_{eth}. For w_{eth} = 0.085, PS is presumably already completely desorbed after a small adsorption of PBMA, giving rise to the minimum in the curve at t ≈ 20 s. After this minimum ($t > 20$ s), $\Delta S/S_0$ increases due to continuing adsorption of PBMA, and finally it reaches a stable value of about 0.004, characteristic for a saturated layer of PBMA only.

For $t > 30$ s (after the kink in the curves of fig. 7.10) the adsorption of

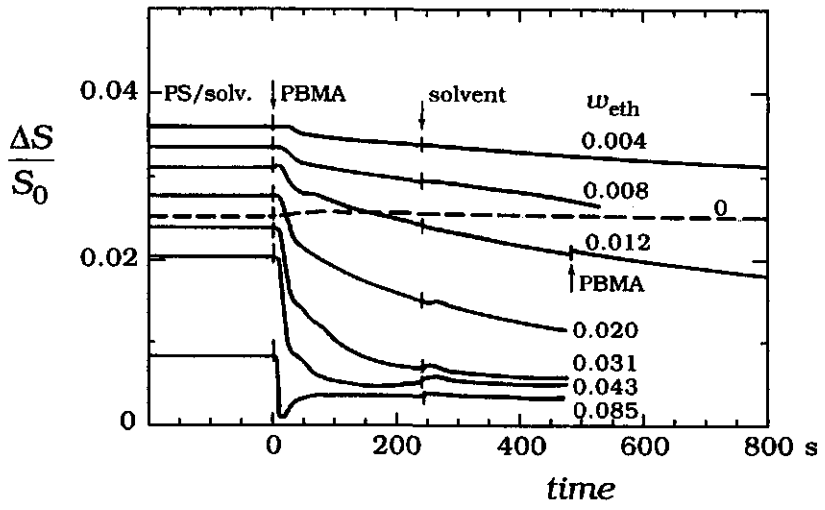

Figure 7.10 Effect of ethyl acetate on the exchange kinetics of high molar mass PS by PBMA in solvent mixtures of decalin and ethyl acetate. For $t < 0$ a sequence of PS and the solvent mixture is injected, as given in fig. 7.7. At $t = 0$ the injection of PBMA starts, followed by solvent again at $t = 240$ s. Up to the kink in the curves around $t = 30$ s PBMA adsorbs with concomitant desorption of PS. After the kink $\Delta S/S_0$ decreases due to desorption of PS by rearrangements in the adsorbed layer (see also text). The curve for $w_{eth} = 0$ (dashed) represents continuous injection of PBMA from $t = 0$ onwards. Concentration of PBMA equals 25 g/m^3.

PBMA is probably more or less constant and $\Delta S/S_0$ decreases due to desorption of PS. For all curves (except that for pure decalin), at $t = 240$ s we switched from the injection of PBMA to pure solvent. The rate of decrease of $\Delta S/S_0$ is hardly affected by the switch to pure solvent, which is a strong indication that for $t > 30$ s the desorption of PS is caused by a *surface process*. The desorption rate of PS for $t > 30$ s increases with increasing concentration of ethyl acetate, which implies that the surface process becomes faster with increasing value of w_{eth}.

In order to characterise the effect of ethyl acetate more quantitatively we analysed the curves in fig. 7.10 more precisely. The effect of ethyl acetate on the initial part of the exchange is examined in fig. 7.8, in which we compare $\Delta S/S_0$ at two points on the exchange curves of fig. 7.10: at $t = 0$, just before the exchange started (circles in fig. 7.8) and just before the kink ($t \approx 30$ s) (triangles in fig. 7.8). The triangles represent the adsorption of PS which is left after exchange during adsorption of PBMA. Consequently, the vertical difference between the two curves in fig. 7.8 corresponds to the amount of PS which is desorbed during adsorption of PBMA. With increasing concentration of ethyl acetate an increasing amount of PS

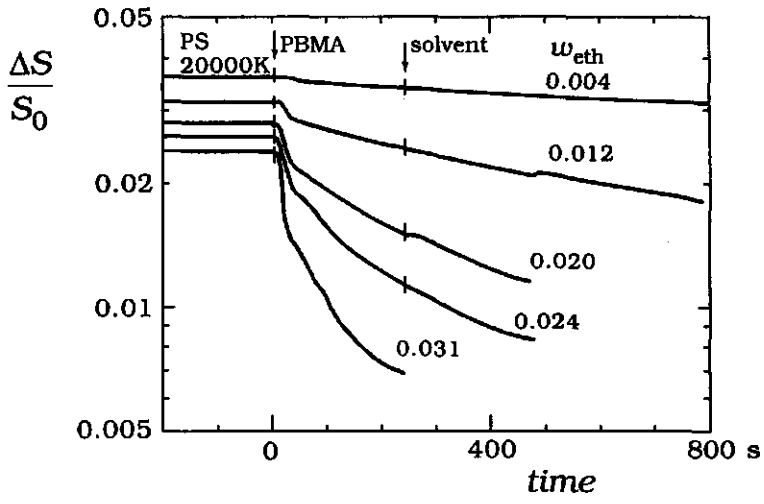

Figure 7.11 Check of exponential decrease of the adsorption of PS during displacement by PBMA in solvent mixtures of decalin and ethyl acetate. Results of fig. 7.10 are replotted, but now on a logarithmic scale for $\Delta S/S_0$. Here, we are only interested in the part of the curves after the kink around $t \approx 30$ s, in which part the decrease of $\Delta S/S_0$ is presumably due to desorption of PS by rearrangements in the adsorbed layer.

desorbs by this rapid exchange process. Probably this is due to the weaker binding of PS with increasing w_{eth}.

In order to check the effect of ethyl acetate on the surface process we replotted the results of fig. 7.10 on a logarithmic scale for $\Delta S/S_0$ (fig. 7.11). We are only concerned with the part of the curves after the kink around $t = 30$ s. If this part is linear on the semi-logarithmic scale, the adsorption of PS decays exponentially. For $w_{eth} = 0.004$ and 0.012 the curves are indeed nearly linear. For higher values of w_{eth} the slope of the curves decreases with time, so that the desorption is slower than exponential. We determined from the slope of the curves just after the kink (at $t = 30$ s) a time constant τ for the decrease of $\Delta S/S_0$ in time. This time constant is a measure for the rate of desorption of PS from a mixed adsorbed layer of PS and PBMA. Consequently, the value of τ is related to the rate of the rearrangements in such a mixed layer. In fig. 7.12 τ is plotted as a function of the weight fraction w_{eth} of ethyl acetate. With increasing concentration of ethyl acetate τ decreases sharply: it decreases from about 8 hours in pure decalin to about 100 s for $w_{eth} = 0.031$. Probably, this decrease is due to the weaker binding of PS with increasing concentration of ethyl acetate. It would be nice to relate w_{eth} to the (effective) segmental adsorption energy of PS. Unfortunately, this was not

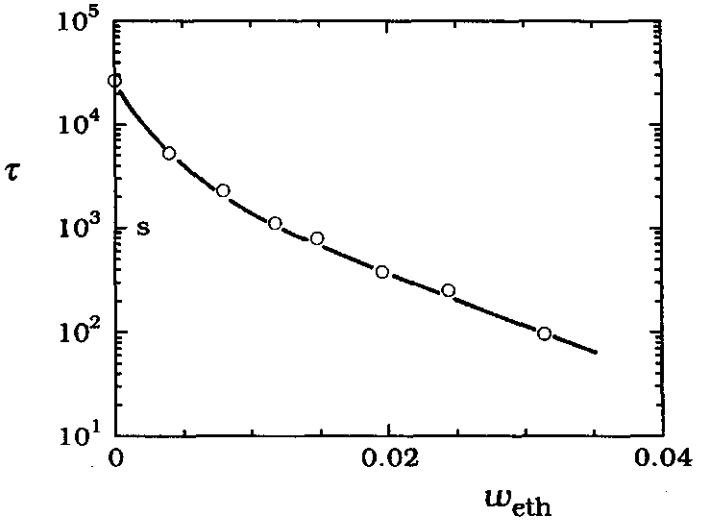

Figure 7.12 Effect of ethyl acetate on the time constant τ for the displacement of high molar mass PS by PBMA due to rearrangements in the adsorbed layer. The time constant τ was determined from the slope of the curves in fig. 7.11 just after the kink around $t \approx$ 30 s.

possible because we do not know the segmental adsorption energy and solvency parameters of ethyl acetate in this system (see also section 5.3.3).

7.3.3.3 Effect of a weak displacer

In this section we discuss the influence of the weak displacer toluene on the adsorption of PS and on the exchange kinetics of PS by PBMA. We would expect that toluene has an effect comparable to that of ethyl acetate, only it should occur at a much higher concentration because toluene is a weaker displacer than ethyl acetate.

In fig. 7.13 we plotted the final level of $\Delta S/S_0$ for adsorption of high molar mass PS (3040 K) as a function of the weight fraction w_{tol} of toluene in mixtures of toluene and decalin. These results may be compared with those for the strong displacer ethyl acetate, as given by the upper curve of fig. 7.8. However, there may be an important optical difference. Since in fig. 7.13 w_{tol} varies within a broad range (0.03 - 0.38), the question arises how the optical calibration depends on the solvent composition. The refractive index increment dn/dc of PS at 20 °C and 633 nm in decalin and toluene is 0.12 and 0.111 cm^3/g, respectively[5]. This difference in dn/dc in both solvents is rather small, and we expect therefore only a small effect of the solvent composition on the sensitivity factor A_s for the adsorption of PS. Consequently, the decay of $\Delta S/S_0$ in fig. 7.13 represents

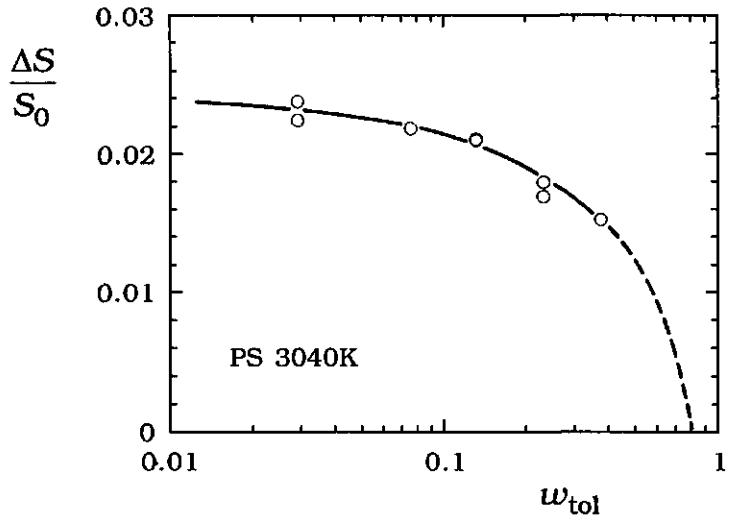

Figure 7.13 Effect of toluene on the final level of $\Delta S / S_0$ for adsorption of high molar mass PS in solvent mixtures of decalin and toluene. The value of $\Delta S / S_0$ after 4 minutes of injection of a solution of concentration 25 g/m^3 is given.

approximately the desorption of PS. The level of $\Delta S/S_0$ at low concentrations of toluene ($w_{tol} < 0.03$) corresponds to an adsorbed amount of 1.2 mg/m^2. With increasing concentration of toluene the adsorption of PS decreases, which can probably be explained by two factors: a decrease of the adsorption energy of styrene units, and an increase of the solvency for PS. We extrapolated the curve in fig. 7.13 to zero adsorption at $w_{tol} \approx 0.8$, which is the value of the critical point found by Van der Beek et al.[6] for PS on silica from mixtures of toluene and cyclohexane. Since cyclohexane and decalin are chemically very similar, this seems a reasonable approximation. If we compare the effect of toluene (fig. 7.13) and ethyl acetate (circles in fig. 7.8) on the adsorption of PS, it is found that the shape of the curves is more or less the same, and resembles the curves commonly found for displacement of polymers by low molar mass displacers[6,8]. The main difference is the shift of the desorption point towards higher weight fractions in toluene, which is related to the fact that toluene is a weaker displacer than ethyl acetate.

The displacement kinetics of PS 3040 by PBMA in three different mixtures of toluene and decalin is shown in fig. 7.14 in the same way as in fig. 7.13 for mixtures of ethyl acetate and decalin. Qualitatively, toluene and ethyl acetate have a similar effect on the exchange kinetics. For example, the shapes of the curves for w_{tol} = 0.13, 0.23 and 0.38 (fig. 7.14) are more or less the same as those for w_{eth} = 0.008, 0.020 and 0.031 (fig.

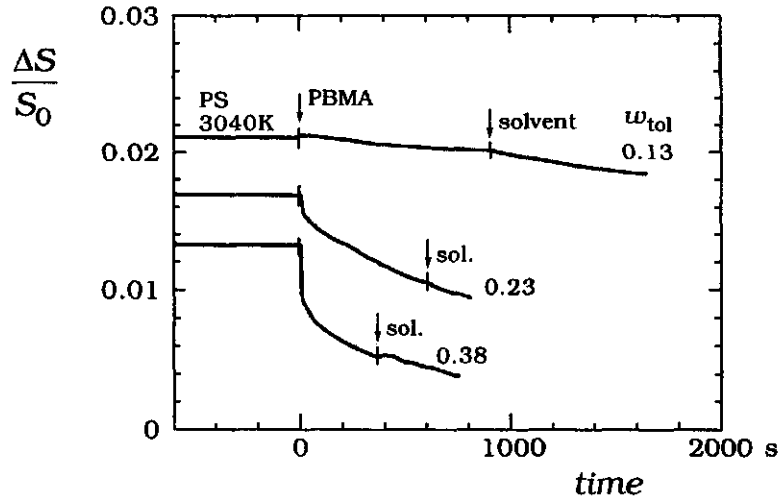

Figure 7.14 Effect of toluene on the exchange kinetics of high molar mass PS by PBMA in solvent mixtures of decalin and toluene, as indicated. Qualitatively, the effect of toluene in fig. 7.14 is comparable to that of ethyl acetate in fig. 7.10. Concentrations: PS (3040 K) 25 g/m^3 and PBMA 25 g/m^3.

7.10), respectively. Again, much higher values of w_{tol} are needed to obtain the same effect on the exchange kinetics as for ethyl acetate. It seems therefore likely that the effect of toluene and ethyl acetate on the exchange kinetics is determined by their effect on the adsorption energy of PS.

7.4 Discussion

A striking result of the present study is that the kinetics of exchange of both PS and PBMA by the displacer PTHF is much faster than that of PS by the displacer PBMA. A factor that might be important is the segmental adsorption energy. For PS, PBMA and PTHF adsorbing from decalin onto silica, χ_s is about 2.0, 3.8 and 4.8, respectively (see section 7.1). Since displacement of one and the same polymer (PS) is sometimes slow (in case of PBMA) and sometimes rapid (for PTHF), it is unlikely that the exchange kinetics are determined by the value of χ_s of the displaced component only. The difference $\Delta\chi_s$ between the segmental adsorption energies of the polymeric displacer and the displaced component is a measure for the driving force for the exchange, and this difference could determine the exchange rate. However, this is also unlikely: for the slow displacement of PS by PBMA $\Delta\chi_s$ = 1.8, and for the rapid displacements of PS and PBMA by PTHF $\Delta\chi_s$ = 1 and 2.8, respectively. Another possibility would be that χ_s of the polymeric displacer is rate-determining. The relatively high value

of χ_s for both displacers (3.8 for PBMA and 4.8 for PTHF) does not make this option very likely. Other effects than adsorption affinities (χ_s) must play a role.

We might expect that the exchange rate increases with increasing flexibility of the polymer chain. The experimental results support this view: the exchange rate is higher for the rather flexible displacer PTHF than for the stiffer displacer PBMA This effect of the chain flexibility was also suggested in the previous chapter, where only chain length differences were considered. For poly(ethylene oxide) (PEO), which is very flexible and chemically resembles PTHF, a mass-transfer-limited exchange was observed. The same conclusion seems to apply for displacement by PTHF in this chapter. For PS, which is less flexible than PEO, we found in chapter 6 indeed slower exchange kinetics than for PEO, while in this chapter the displacement of PS by the rather stiff PBMA was found to be relatively slow.

The exchange mechanism of adsorbed low molar mass PS (9 K) is qualitatively the same for the displacers PBMA (fig. 7.6) and high-molar-mass PS (20000 K) (chapter 6). In both cases we find some desorption of PS 9 during mass transfer limited adsorption of the polymeric displacer, followed by slower desorption of PS 9 due to rearrangements within the adsorbed layer. Even the time constant for the rearrangement process is about the same for both systems (of the order of one or a few minutes). Thus, high molar mass PS and PBMA behave more or less the same as polymeric displacers for PS 9.

For displacement of PS by PBMA in decalin solutions the desorption rate of PS strongly decreases with increasing chain length: for PS 9 the time constant is of the order of minutes (fig. 7.6), whereas it is about 8 h for PS 20000 (ω_{eth} = 0 in fig. 7.12). A strong effect of the chain length might be an indication that entanglements play a role. However, displacement of long chains of PS is much faster for exchange by PTHF (time scale of seconds) than by PBMA (hours). In our opinion the rate of disentanglement -and thus desorption- should not depend so strongly on the type of the displacing polymer, and therefore an effect of entanglements is unlikely here. Possibly, the slow exchange of PS 20000 by PBMA is related to the fact that the chain length of the displaced PS (M = 20000 K) is much higher than that of the displacer PBMA ($M \approx$ 240 K). We could imagine that an adsorbed molecule of PS surrounded by a number of chains of PBMA does not desorb even when the chains of PBMA are completely unfolded, because PBMA molecules are not long enough to reach to the centre of the

adsorbed PS chain. In order to come to a more detailed explanation, a systematic investigation of the effect of the chain length on the exchange kinetics would clearly be needed.

The exchange rate of high molar mass PS by PBMA in decalin strongly increases with increasing concentration of a low molar mass displacer (ethyl acetate, fig. 7.10, or toluene, fig. 7.14). Probably, this is due to the weaker binding of the polymers to the surface. We imagine that the decrease of the adsorption energy leads to a higher mobility of the adsorbed polymers, resulting in a faster exchange.

For the displacement of PBMA by PTHF in decalin solution, we find rapid exchange, which is completed in a few minutes and which is to a large extent limited by the mass transfer of the polymeric displacer PTHF (fig. 7.5). In contrast with this result, for the same polymers also adsorbing on oxidised silicon but now from a carbon tetrachloride solution, Van der Beek et al.[3] found much slower exchange which was incomplete even after many hours. We see no physical reason why the exchange would be so much slower in carbon tetrachloride solution than in decalin. Then, probably, undesired effects due to differences in the experimental setup or protocol must play a role. For example, the experiments of Van der Beek et al. were performed in a stagnant solution, which might give rise to effects of slow diffusion, while in our setup the adsorption takes place from a flowing solution. Also, different procedures were used in the preparation of the oxidised silicon surface. We cleaned the surface in a gas flame, whereas Van der Beek et al. used a "wet" method involving treatment with hydrogen peroxide and ammonia. According to Frantz and Granick[9] the surface preparation of silicon may indeed greatly influence the exchange kinetics. These authors observed rapid exchange between protonated PS and deuterated PS if the surface was cleaned with an oxygen plasma, whereas extremely slow exchange kinetics was found after "wet" cleaning with a mixture of sulphuric acid and hydrogen peroxide. It thus seems that "dry" methods (gas flame, oxygen plasma) produce a surface on which the exchange is rapid, and that "wet" preparations give slow exchange kinetics. We conclude that the different results of Van der Beek et al. as compared to ours are likely to be explained by the different surface preparations and different mass transfer conditions.

7.5 Conclusions

In this chapter we studied the exchange kinetics between three chemically different polymers: PS, PBMA and PTHF. Due to the widely different values

of the refractive index increment dn/dc for these polymers in decalin solution, the sensitivity of the reflectometric method is strongly different for adsorption of PS, PBMA and PTHF. This feature enables studying the exchange kinetics of these polymers.

The displacement rate of adsorbed PS by PTHF is entirely determined by the adsorption rate of PTHF. The latter is limited by the mass transfer from the solution. This conclusion applies to any combination of chain lengths of PS and PTHF.

Displacement of adsorbed PBMA by the displacer PTHF is also determined by the mass transfer limited adsorption rate of the displacer. The displacement rate of PBMA is hardly affected by ageing the adsorbed PBMA layer for about 20 hours.

The kinetics of exchange of PS by PBMA is determined by mass transfer through solution as well as by surface processes, and it was found to depend on the chain length of PS and the solvent composition. Under all conditions the adsorption rate of PBMA on a surface with an adsorbed PS layer is initially limited by mass transfer from the solution. For low molar mass PS (M = 9 K) in decalin, part of the adsorbed layer of PS desorbs during adsorption of PBMA, followed by a slower desorption of PS (over a time-scale of minutes) due to rearrangements (surface processes) in the adsorbed layer. For high molar mass PS in decalin, no desorption of PS occurs in the first stage, and slow desorption is found in the second process. The time constant for desorption in this second (rearrangement) stage was estimated to be about 8 hours for M = 20000 K.

With increasing concentration of a low-molar-mass displacer (ethyl acetate or toluene) the exchange kinetics of high molar mass PS by PBMA gradually becomes faster, resembling the exchange kinetics of low-molar-mass PS by PBMA in pure decalin. For the displacer ethyl acetate, the time constant for desorption of PS (M = 20000 K) due to surface processes decreases from about 8 hours in pure decalin to less than one minute near the critical displacer concentration for adsorption of PS. The addition of a low molar mass displacer causes a decrease of the segmental adsorption energy of the polymers, probably resulting in a higher mobility of the adsorbed chains and thus a higher rate of the displacement process in the adsorbed layer.

The exchange kinetics of PS by PBMA is much slower than that of PS by PTHF under comparable conditions. We suggest that the different exchange kinetics can be explained by an effect of the chain flexibility, which is higher for PTHF than for PBMA.

7.6 References

(1) Thies, C. *J. Phys. Chem.* **1966**, *70*, 3783.

(2) Johnson, H.E.; Granick, S. *Science* **1992**, *255*, 966.

(3) Van der Beek, G.P.; Cohen Stuart, M.A.; Fleer, G.J. *Macromolecules* **1991**, *24*, 3553.

(4) Van der Beek, G.P.; Cohen Stuart, M.A.; Fleer, G.J.; Hofman, J.E. *Macromolecules* **1991**, *24*, 6600.

(5) "*Polymer Handbook*"; Brandrup, J.; Immergut, E.H., Ed.; John Wiley and Sons: New York, **1989**, 3rd ed.

(6) Van der Beek, G.P.; Cohen Stuart, M.A.; Fleer, G.J.; Hofman, J.E. *Langmuir* **1989**, *5*, 1180.

(7) Appelt, B.; Meyerhoff, G. *Macromolecules* **1980**, *13*, 657.

(8) Cohen Stuart, M.A.; Fleer, G.J.; Scheutjens, J.M.H.M. *J. Colloid Interface Sci.* **1984**, *97*, 515.

(9) Frantz, P.; Granick, S. *Langmuir* **1992**, *8*, 1176.

Summary

The aim of the study in this thesis was to gain more insight in the kinetics of polymer adsorption. To this end some well-characterised polymers have been systematically investigated.

In the process of polymer adsorption one may distinguish three kinetic contributions: transport to the surface, attachment, and reconformation of the adsorbing and adsorbed chains. In order to assess the role of each of the three contributions it is necessary to measure the adsorption kinetics under well-defined hydrodynamic conditions. For such measurements the transport (convection and diffusion) can be calculated and therefore it becomes possible to study unambiguously the interfacial processes, i.e., attachment and reconformation.

For this study two experimental techniques were used that both fulfil the requirement that the adsorption occurs under well-defined hydrodynamic conditions: reflectometry in a stagnation point flow (chapters 2,3 and 5-7) and a streaming potential method (chapter 4). With both techniques it is possible to follow directly and continuously the build-up of an adsorbed layer. Reflectometry is a relatively new and simple optical technique for the measurement of adsorption on (optically flat) solid surfaces. In a reflectometer a linearly polarised light beam is reflected from the (adsorbing) surface, and the reflected beam is split into its parallel and perpendicular components. The intensity ratio between the two components is continuously measured. This ratio changes upon adsorption, and after calibration the adsorbed amount (mass/area) is obtained. For reflectometry there are only few restrictions on the choice of adsorbate, adsorbent and solvent.

The applicability in this study of the streaming potential method is limited to adsorption of uncharged polymers from aqueous solution. For that case, the streaming potential can be related to the hydrodynamic layer thickness of the adsorbed polymer layer. This thickness is mainly determined by loose ends of adsorbed chains, and it is sensitive to very small changes in the adsorbed amount of long chains near saturation. Such small changes occur for desorption of long chains into solvent, so that the streaming potential method is especially suitable for the measurement of the desorption kinetics.

In *chapter 1* the aim and scope of this study of this study are explained, and a general introduction to adsorption of polymers is given.

Chapter 2 deals with the measurement of adsorption by reflectometry.

Using the results of an optical model we discuss the possibilities of the method for measuring the adsorption from dilute solution on a thin film on top of a silicon substrate. For a wide variety of solvents and film materials, a sensitivity can be obtained of the order of 1-2% change in reflectivity per mg/m^2 adsorbed, which is quite enough for an accurate determination of the adsorbed amount. By choosing carefully the film thickness and angle of incidence of the light beam, it can be achieved that the reflected intensity varies proportionally with the adsorbed amount, independent of the concentration profile in the adsorbed layer. Under such conditions, the reflectometric signal can be simply converted into the adsorbed amount.

In *chapter 3* reflectometry is used to investigate the kinetics of adsorption of poly(ethylene oxide) (PEO) from water onto oxidised silicon. For the stagnation point flow the maximum rate of mass transfer of polymer to the surface is calculated. This rate is compared with the observed adsorption rate, and it is concluded that mass transfer is rate-limiting up to or nearly up to saturation, depending on the chain length. Only for long chains ($M > 100$ kg/mole) near saturation the adsorption rate is lowered by surface processes.

In *chapter 4* a model is discussed for the desorption rate of polymers into a flow of pure solvent. This model is based on the assumption that near the surface there is a rapid equilibration between free and adsorbed polymer, and that transport of free polymer away from the surface is rate-limiting for the desorption. Due to the shape of the (high affinity) isotherm, the equilibrium concentration of free chains even after a minute desorption is extremely low, so that the transport -and thus the desorption- proceeds slowly. Thus, in spite of the rapid local equilibration, the desorption is slow because of the slow mass transfer. For a logarithmic adsorption isotherm of the polymer (for which the adsorbed amount Γ increases linearly with the log of the concentration c in solution) an explicit expression for the adsorbed amount as a function of time is derived: the desorbed amount increases proportionally with $\log t$. The model predicts that the absolute value of the slope of the (kinetic) desorption curve $\Gamma(\log t)$ and the (static) adsorption isotherm $\Gamma(\log c)$ are the same.

Using the streaming potential method it is shown in chapter 4 that the above model gives an adequate description of the desorption kinetics in aqueous solutions of PEO on glass, even for high molar mass polymer (M = 847 kg/mole). Again, this shows that the equilibration of adsorbed layers of PEO is rapid as compared to the rate of mass transfer through solution.

Chapter 5 describes the adsorption kinetics of polystyrene (PS) from

decalin on oxidised silicon. On a bare surface the adsorption rate of PS is limited by mass transfer from solution, like for PEO. For PS, the adsorption rate decreases gradually with increasing coverage. This is due to a decreasing probability of attachment during a collision of a free chain with the (covered) surface. From experiments in which the chain length, the solvent quality and the adsorption energy were varied, the picture arises that the adsorption probability during a collision is the result of a balance between a gain in adsorption energy on the one hand, and repulsive interaction with the adsorbed layer on the other.

Exchange between polymers that differ in chain length only is the subject of *chapter 6*. Displacement of adsorbed short chains of PEO by longer ones in solution is limited only by transport of long chains to the surface. The adsorbed layer is continuously in equilibrium with the solution near the surface. The same conclusion was drawn from the desorption kinetics of this polymer in a flow of pure solvent (chapter 4). For PS also surface processes play a role. During exchange of short by long chains of PS there is a temporary overshoot of short chains in the adsorbed layer. This overshoot may desorb either during adsorption of long chains, or by relaxation of the adsorbed layer. By interrupting the transport of long chains to the surface, this relaxation could also be directly observed. The higher chain stiffness of PS as compared to PEO possibly explains the slower equilibration of adsorbed PS.

Finally, we present in *chapter 7* some results on the exchange kinetics between three chemically different polymers: polystyrene (PS), poly(butyl methacrylate) (PBMA) and polytetrahydrofuran (PTHF). Displacement of adsorbed layers of the rather stiff polymers PS and PBMA by the very flexible PTHF is limited only by transport of the displacing polymer from the bulk solution. For mutual exchange between the two stiff polymers, surface processes play an important role: the displacer PBMA adsorbs quickly, whereas PS desorbs slowly. Possibly, the slow exchange kinetics is caused by the low mobility of the adsorbed polymers. The displacement rate of PS by PBMA increases considerably after addition of a displacer of low molar mass. The faster exchange kinetics is probably due to the lower binding strength and, consequently higher mobility of the adsorbed polymers.

Kinetiek van Adsorptie, Desorptie en Uitwisseling van Polymeren

Samenvatting

Het doel van het in dit proefschrift beschreven onderzoek was het verkrijgen van meer inzicht in de kinetiek van polymeeradsorptie. Hiertoe is systematisch onderzoek verricht aan enkele goed gekarakteriseerde polymeren.

In het proces van polymeeradsorptie kunnen drie kinetische stappen worden onderscheiden: transport naar het oppervlak, aanhechting, en reconformatie van de adsorberende en reeds geadsorbeerde polymeerketens. Om de rol van ieder van deze drie bijdragen vast te kunnen stellen is het noodzakelijk de adsorptiekinetiek te meten onder goed omschreven hydrodynamische omstandigheden. Bij zulke metingen kan het massatransport (convectie en diffusie) berekend worden, waardoor het mogelijk is ondubbelzinnig het transport door de oplossing te onderscheiden van de oppervlakteprocessen (aanhechting en reconformatie).

Bij dit onderzoek zijn twee experimentele technieken gebruikt, die beide voldoen aan de eis dat de adsorptie plaatsvindt onder goed omschreven hydrodynamische omstandigheden: reflectometrie in stagnatiepuntstroming (hoofdstukken 2, 3 en 5-7) en een stromingspotentiaalmethode (hoofdstuk 4). Met deze twee technieken kan de opbouw van een geadsorbeerde laag direct en continu gevolgd worden. Reflectometrie is een relatief nieuwe en eenvoudige optische techniek voor meting van adsorptie aan (optisch vlakke) vaste oppervlakken. In een reflectometer wordt een lineair gepolariseerde lichtbundel na reflectie op het (adsorberende) oppervlak gesplitst in zijn parallelle en looodrechte componenten. De intensiteitsverhouding tussen deze twee componenten wordt continu gemeten. Uit de verandering van deze verhouding door adsorptie kan na ijking de geadsorbeerde hoeveelheid (massa/oppervlak) worden verkregen. Reflectometrie kent weinig beperkingen wat betreft de keuze van adsorbaat, adsorbens en oplosmiddel.

De toepasbaarheid in dit onderzoek van de stromingspotentiaalmethode beperkt zich tot adsorptie van ongeladen polymeren uit waterige oplossing. Voor dat geval kan uit de stromingspotentiaal de hydrodynamische laagdikte van de geadsorbeerde polymeerlaag gevonden worden. Deze dikte wordt hoofdzakelijk bepaald door losse einden van geadsorbeerde ketens,

en zij is gevoelig voor zeer kleine veranderingen in de geadsorbeerde hoeveelheid van lange ketens nabij verzadiging. Zulke kleine veranderingen treden op bij desorptie van lange ketens in oplosmiddel, zodat de stromingspotentiaalmethode bij uitstek geschikt is voor de meting van de desorptiekinetiek.

In *hoofdstuk 1* worden doel en opzet van het onderzoek uiteengezet, en er wordt een algemene inleiding gegeven over adsorptie van polymeren.

Hoofdstuk 2 gaat over de meting van adsorptie met reflectometrie. Aan de hand van berekeningen met een optisch model worden de mogelijkheden van de methode besproken voor de meting van adsorptie vanuit verdunde oplossing op een dunne film op een ondergrond van silicium. Voor een breed scala van oplosmiddelen en filmmaterialen kan met reflectometrie een gevoeligheid worden bereikt in de orde van 1-2% verandering in de reflectiviteit bij een adsorptie van 1 mg/m^2, hetgeen ruim voldoende is voor een nauwkeurige bepaling van de geadsorbeerde hoeveelheid. Door een zorgvuldige keuze van de filmdikte en de invalshoek van de lichtbundel kan worden bereikt dat de verandering in de reflectiviteit evenredig is met de geadsorbeerde hoeveelheid, onafhankelijk van het concentratieverloop in de geadsorbeerde laag. Onder zulke omstandigheden kan het reflectometrische signaal eenvoudig worden omgezet in de geadsorbeerde hoeveelheid.

In *hoofdstuk 3* wordt met reflectometrie de adsorptiekinetiek van polyethyleenoxide (PEO) vanuit water op geoxideerd silicium onderzocht. Voor de stagnatiepuntstroming wordt de maximale transportsnelheid van polymeer naar het oppervlak berekend. Deze snelheid wordt vergeleken met de waargenomen adsorptiesnelheid en hieruit wordt geconcludeerd dat massatransport snelheidsbepalend is tot aan of dicht onder verzadiging van de geadsorbeerde laag, afhankelijk van de ketenlengte. Alleen voor lange ketens (M > 100 kg/mol) nabij verzadiging is er een verlaging van de adsorptiesnelheid door oppervlakteprocessen.

In *hoofdstuk 4* wordt een model besproken voor de desorptiesnelheid van polymeer in een stroming van zuiver oplosmiddel. Dit model is gebaseerd op de aanname dat er nabij het oppervlak een snelle evenwichtsinstelling is tussen vrij en geadsorbeerd polymeer, en dat afvoer van vrij polymeer naar de bulkoplossing snelheidsbepalend is voor de desorptie. Door de vorm van de (hoge-affiniteits)isotherm is de evenwichtsconcentratie van vrij polymeer al na een geringe desorptie extreem laag, zodat de afvoer -en dus de desorptie- erg traag verloopt. Ondanks de snelle locale evenwichts-

instelling is de desorptie dus toch traag vanwege de langzame afvoer van polymeer. In geval van een logaritmische adsorptie-isotherm van het polymeer (waarbij de geadsorbeerde hoeveelheid Γ lineair toeneemt met de log van de concentratie c in de oplossing) wordt een expliciete uitdrukking voor de adsorptie als functie van de tijd afgeleid: de gedesorbeerde hoeveelheid neemt evenredig toe met $\log t$. Het model voorspelt dat de absolute waarde van de helling van de (kinetische) desorptiecurve $\Gamma(\log t)$ en de (statische) adsorptie-isotherm $\Gamma(\log c)$ gelijk zijn.

Met de stromingspotentiaalmethode wordt in hoofdstuk 4 aangetoond dat bovenstaand model een goede beschrijving geeft van de desorptiekinetiek in waterige oplossingen van PEO op glas, zelfs voor lange polymeerketens (M = 847 kg/mol). Dit betekent opnieuw dat de evenwichtsinstelling van geadsorbeerde lagen van PEO snel verloopt ten opzichte van het transport door de oplossing.

Hoofdstuk 5 gaat over de adsorptiekinetiek van polystyreen (PS) vanuit decaline op geoxideerd silicium. Op een kaal oppervlak is de adsorptiesnelheid van PS beperkt door aanvoer vanuit de oplossing, zoals bij PEO. Voor PS daalt de adsorptiesnelheid geleidelijk met toenemende bedekking door een verminderde kans op aanhechting tijdens een botsing van een vrije keten met het (bedekte) oppervlak. Uit experimenten waarin de ketenlengte, de oplosmiddelkwaliteit en de bindingssterkte werden gevarieerd, komt het beeld naar voren dat de aanhechtingskans het resultaat is van een balans tussen winst in adsorptie-energie enerzijds en repulsieve interactie met de geadsorbeerde laag anderzijds.

Uitwisseling tussen polymeerketens die alleen in lengte verschillen komt aan bod in *hoofdstuk 6*. Verdringing van geadsorbeerde korte ketens van PEO door langere wordt alleen beperkt door aanvoer van de lange ketens uit de bulkoplossing. De geadsorbeerde laag is voortdurend in evenwicht met de oplossing nabij het oppervlak, zoals ook al gevonden voor desorptie van dit polymeer in een stroming van zuiver oplosmiddel (hoofdstuk 4). Bij PS spelen ook oppervlakteprocessen een rol. Tijdens uitwisseling van korte door lange ketens van PS is er een tijdelijk overschot van korte ketens in de geadsorbeerde laag. Dit overschot kan desorberen ofwel tijdens adsorptie van lange ketens, ofwel als gevolg van relaxatie van de geadsorbeerde laag. Door de aanvoer van lange ketens te onderbreken kan deze relaxatie ook direct worden waargenomen. De grotere ketenstijfheid van PS in vergelijking met PEO verklaart mogelijk de tragere evenwichtsinstelling van geadsorbeerd PS.

Ten slotte wordt in *hoofdstuk 7* de uitwisselkinetiek besproken tussen

drie chemisch verschillende polymeren: polystyreen (PS), polybutylmethacrylaat (PBMA) en polytetrahydrofuraan (PTHF). Verdringing van geadsorbeerde lagen van de tamelijk stijve polymeren PS en PBMA door het zeer flexibele PTHF wordt alleen beperkt door aanvoer van het verdringende polymeer uit de bulkoplossing. Bij uitwisseling tussen de twee stijve polymeren onderling spelen oppervlakteprocessen een belangrijke rol: de verdringer PBMA adsorbeert snel, terwijl PS traag desorbeert. De trage kinetiek is mogelijk een gevolg van de geringe beweeglijkheid van de geadsorbeerde polymeren. De uitwisseling van PS door PBMA wordt aanzienlijk versneld door toevoeging van verdringers met een laag molgewicht. Dit is waarschijnlijk te wijten aan de verminderde bindingssterkte aan het oppervlak en de daardoor verhoogde beweeglijkheid van de geadsorbeerde polymeren.

Levensloop

Jacob Cornelis Dijt werd op 17 december 1963 geboren te Amsterdam en groeide op in Amstelveen, alwaar hij in 1982 aan de scholengemeenschap Casimir het diploma Gymnasium-B behaalde. In datzelfde jaar begon hij zijn studie Moleculaire Wetenschappen aan de Landbouwhogeschool Wageningen. In 1988 studeerde hij af aan de Landbouwuniversiteit Wageningen in de fysisch-chemische oriëntatie van Moleculaire Wetenschappen, met als hoofdvakken Fysische Chemie en Bodemhygiëne- en verontreiniging. Van september 1988 tot september 1992 was hij als Onderzoeker In Opleiding werkzaam bij de vakgroep Fysische en Kolloïdchemie van de Landbouwuniversiteit Wageningen. Gedurende deze periode is het in dit proefschrift beschreven onderzoek uitgevoerd. Vanaf 1 juli 1993 is hij in dienst bij PPG Industries Fiber Glass bv te Hoogezand.

Nawoord

Tot slot wil ik iedereen bedanken die heeft bijgedragen aan het welslagen van dit onderzoek of aan de uitermate plezierige tijd die ik op deze vakgroep heb gehad. Enkelen wil ik met name noemen.

De vele ideeën en grote belangstelling voor dit onderzoek van Martien Cohen Stuart vormden bijna dagelijks een bron van inspiratie en moed om door te zetten. Het schrijven van een wetenschappelijke tekst heb ik niet uit een boekje geleerd, maar van Gerard Fleer die steeds uiterst kritisch en nauwgezet mijn manuscripten van commentaar en zinvolle suggesties heeft voorzien.

De meetopstellingen voor dit onderzoek zijn grotendeels in eigen huis gebouwd. Henny van Beek, Louis Verhagen en Gerrit Buurman draaiden, vijlden en boorden apparaten die mooier en handiger waren dan ik kon bedenken. Van Henny heb ik geleerd dat je iets niet kunt bijvijlen omdat er alleen maar af gaat met vijlen. Van Dale's woordenboek zal moeten worden aangepast. De electronica voor de opstellingen werd op kundige wijze ontworpen door Ronald Wegh, waarbij Rob Vullings van de losse onderdelen een werkend geheel soldeerde. Geen experiment zonder glaswerk en chemicaliën. Willem van Manen, Ben Spee en Gea Lootsma zullen zich wel afvragen waar al die 100 ml potjes gebleven zijn. Ik heb ze nagelaten aan mijn huidige kamergenote. In de eerste jaren heeft Ans Hofman snel en efficiënt vele proeven voor mij uitgevoerd, waarvoor ik haar op deze plaats hartelijk bedank. Met veel plezier heb ik Maarten van der Wielen en Marijn Sipkema begeleid bij hun stage, respectievelijk afstudeervak. Bert Bouman speelde niet alleen voor Sinterklaas op 5 december, maar vooral ook op alle andere dagen van het jaar waarop hij met royale hand pennen en drop uitdeelde. Voor allerlei en voor gezellige praatjes ('mag ik even printen?') kon ik terecht bij mijn buren, het secretariaat: José Zeevat, Yvonne Toussaint en Wil Kleine.

Het woord 'vergaderen' heeft op deze vakgroep een iets andere, prettiger, betekenis dan gebruikelijk: vergaderingen zijn bijeenkomsten in een lokaliteit, beginnend op vrijdagmiddag om ongeveer zes uur, waarbij onder het genot van een biertje uiteenlopende zaken worden besproken. Van vergaderen is het een kleine stap naar goed bezochte promotiefeesten, verjaardagen, etentjes, roeiwedstrijden, en de Veluweloop. Het viel niet zwaar om naast het werk ook wat ontspanning bij deze vakgroep te vinden.

De bijdrage van Nynke Hoogeveen aan onderzoek en ontspanning zou ik niet kunnen schatten; zij is daarom van onschatbare waarde.

Jaap